Fires in Narrow Construction Cavities

Fire Dynamics and Material Fire Performance

Livkiss, Karlis

2020

[Link to publication](#)

Total number of authors:
1

Fires in Narrow Construction Cavities
Fire Dynamics and Material Fire Performance

KARLIS LIVKISS | DIVISION OF FIRE SAFETY ENGINEERING | LUND UNIVERSITY

Fires in Narrow Construction Cavities

Fire Dynamics and Material Fire Performance

Karlis Livkiss

LUND UNIVERSITY

Organization LUND UNIVERSITY	Document name DOCTORAL THESIS
Division of Fire Safety Engineering, Faculty of Engineering	Date of issue 28-02-2020
Karlis Livkiss	Sponsoring organization European Commission 7th framework program (Grant no. 316991) and Dansk Brand og Sikringsteknisk Institut DBI

Title
FIRES IN NARROW CONSTRUCTION CAVITIES

Abstract

There have recently been devastating fire incidents related to fire spread over ventilated façades. These incidents indicate gaps in our understanding of the fire behaviour of façades. This thesis takes a bottom-up approach to investigating fire behaviour in materials and elements associated with narrow cavities in modern constructions. Ventilated façade is a construction used as an example in this thesis, in which an air gap is introduced between the thermal insulation and the external cladding.

Experimental and numerical studies were conducted of flame heights and heat fluxes to the surfaces inside cavities. An experimental programme comprising more than 75 individual tests was done with cavity widths between 2 cm and 10 cm, as well as four different heat release rates from the burner. The study showed increasing flame heights and heat flux as the cavity width is reduced. In this experimental study, the flame height increased up to 2.2 times compared to those near one wall. FDS version 6.7.0 software was then used to assess its capability to replicate the experimental results. One of the identified limitations of FDS was the required small mesh cell size. Furthermore, the thermal response of stone wool and expanded polystyrene when exposed to fire conditions was studied. Four types of stone wool with densities of 37 to 154 kg/m^3 were investigated experimentally and numerically. Thermogravimetric analysis and micro combustion calorimetry were used to characterize the thermal decomposition of the stone wool's organic content. A numerical heat conduction model was developed and showed capability of reproducing the temperatures inside stone wool with relatively low density. Suggestions are provided for improving the model's performance for high density wools.

Key words
Fire, Ventilated Façade, Flame Heights, Stone Wool, Expanded polystyrene, Fire Dynamics Simulator

Classification system and/or index terms (if any)

Supplementary bibliographical information	Language English

ISSN and key title 1402-3504	ISBN 978-91-7895-394-3 (printed) 978-91-7895-395-0 (PDF)

Recipient's notes	Number of pages 133	Price
	Security classification Open	

I, the undersigned, being the copyright owner of the abstract of the above-mentioned dissertation, hereby grant to all reference sources permission to publish and disseminate the abstract of the above-mentioned dissertation.

Signature_____ Date 18 FEB 2020

Fires in Narrow Construction Cavities

Fire Dynamics and Material Fire Performance

Karlis Livkiss

LUND
UNIVERSITY

Veltīts maniem vecvecākiem - Aleksandram, Dagnijai, Mirzai un Žanim

Preface

This kappa is written to present the framework and the main conclusions of the research that I have carried out during my industrial doctoral education. It should be read as a summary of the appended research publications.

Some of the research presented in this document and the appended publications was carried out during the FIRETOOLS project (2013-2016), jointly funded by the European Commission and Danish Institute of Fire and Security Technology (DBI). The overall objective of the FIRETOOLS project was to advance predictive capabilities of fire behaviour of building content, construction products and fire separating elements, based on knowledge of the material's properties. I was one of five early-stage researchers selected to carry out this task with academic supervision from Lund University and industrial supervision from DBI. The project outcomes were summarized in reports and submitted to the European Commission. These reports are not included in this thesis. Additional research activities had been carried out after the completion of the FIRETOOLS project. It included further data analysis on the gathered experimental results and performing numerical simulations.

The work during the previous 7 years has resulted in the five appended research publications, forming the backbone of this thesis.

Karlis Livkiss

Copenhagen, 2020

Acknowledgements

You have provided me all the pieces of the puzzle for completing this thesis, and I only had the delightful task of putting them together.

x

Popular Science Summary

One of the pillars of fire safety in built environments is the choice of materials and constructions from the perspective of their fire behaviour. An example is building façade, which should be designed and constructed in a way not to allow fire spread from one building level to another. Nevertheless, devastating façade fires occur every year, often resulting in human casualties. Nowadays many new materials and design solutions are introduced in construction due to the growing environmental awareness and sustainability requirements. It is difficult to follow-up with the changes in the market and design practices to ensure acceptable fire safety levels. Yet it is also increasingly important to do so. The population growth and urbanization in world results in more and taller buildings being built and the potential consequences of fire incidents are rapidly rising. Building up the knowledge of the façade fire behaviour and the critical factors is therefore required.

This thesis is investigating the fire behaviour associated with narrow air gaps in ventilated façades. An air gap between the thermal insulation and the external cladding provides a path for fire spread horizontally along the façade. This thesis experimentally and numerically investigates flame characteristics inside a narrow space. More than 75 individual tests were performed in experimental series showing that narrower cavity results in elongated flames and more severe heat impact to the inner surfaces of the cavity. Numerical modelling was applied to assess todays capability to reproduce the experimental results. It was discovered that the numerical tools can in general reproduce the observed trends, yet underpredicting the flame heights and the heat exposure. Once fire enters the façade air gap, materials used inside the cavity are exposed, may ignite and contribute to the fire. Typically, these are thermal insulation materials. Therefore, as a part of the presented research, typical building insulation materials were studied when exposed to the heat. The heat transfer inside stone wool was investigated to provide a new insight in how the components of this product influence its temperature. Deformations of expanded polystyrene due to melting were also studied.

These results can be used for advancing the numerical simulations of the material and construction behaviour in fires. Numerical modelling, based upon this knowledge, will potentially offer a more flexible and effective way of assessing new designs and materials in the future.

List of Publications

Papers included in the thesis

The papers included in this thesis and the author's contributions to each paper are listed below.

Paper I   Livkiss K, Andres B, Johansson N, van Hees P. Uncertainties in modelling heat transfer in fire resistance tests: A case study of stone wool sandwich panels. Fire and Materials. 2017; 41:799–807. DOI: 10.1002/fam.2419

Paper II   Livkiss K, Andres B, Bhargava A, van Hees P. Characterization of Stone Wool Properties for Fire Safety Engineering Calculations. Journal of Fire Sciences. 2018 DOI: 10.1177/0734904118761818

Paper III Livkiss K, van Hees P. Development of a dynamic shrinkage/collapse measurement method for cellular polymer foams, Interflam - Nr Windsor, June 2016, pp. 991-1002

Paper IV   Livkiss K., Svensson S, Husted B, van Hees P. Flame Heights and Heat Transfer in Façade System Ventilation Cavities. Fire Technology. 2018; 1-25. DOI: 10.1007/s10694-018-0706-2

Paper V   Livkiss K., Husted B, Beji T, van Hees P, Numerical study of a fire-driven flow in a narrow cavity, Fire Safety Journal. 2019, 108: 102834 DOI: 10.1016/j.firesaf.2019.102834

Paper	Author's contribution
I	The author performed the Monte-Carlo simulations, did part of the literature research and data analysis. The author did most of writing of the paper. Overall, the author's contribution was 50%.
II	The author did part of the experimental work, performed most of the data analysis and wrote the paper. The author also contributed to the development of the numerical model. Overall, the author's contribution was 75%.
III	The author designed and performed the experiments, performed the data analysis and wrote the paper. Overall, the author's contribution was 90%.
IV	The author designed and performed the experiments, performed the data analysis and wrote the paper. Overall, the author's contribution was 90%.
V	The author performed the literature review, modelling work, data analysis and wrote the paper. Overall, the author's contribution was 90%.

List of publications not included in the thesis

Publications that are co-authored by the author, but which are not included in this thesis, are presented below.

Peer-reviewed papers

Andres B, Livkiss K, Hidalgo J, van Hees P, Bisby L, Johansson N, Bhargava A, Response of Stone Wool Insulated Building Barriers under Severe Heating Exposures, Journal of Fire Sciences. 2018 DOI: 10.1177/0734904118783942

Non peer-reviewed international conference papers

Wilkens K, Livkiss K, van Hees P. Experimental and numerical investigation on fire behaviour of foam/fabric composites, Fire and Materials – San Francisco, February 2017

van Hees P, Wahlqvist J, Andres B, Wilkens K, Bhargava A, Livkiss K. Analysis of fire barriers with respect to fires with combustible gases and liquids, Fire and Materials – San Francisco, February 2017

Livkiss K, B. Andres B, Johansson N, van Hees P. Uncertainties in material thermal modelling of fire resistance tests (poster), 2nd European Symposium of Fire Safety Science – Nicosia, June 2015

van Hees P, Andersson B, Guay F, Lauridsen D, Bhargava A, Livkiss K, Andres Valiente B, Vermina Lundstrom F, Wilkens K. Simulation of fire technical properties of products and construction barriers to support efficient product development in industry, Interflam - Nr Windsor, June 2013, pp. 589-59

Nomenclature

Symbols

a – smallest fuel bed dimension (m)

A – pre exponential constant (-)

A_{sl} – area of slug (Chapter 4) (m²)

b – largest fuel bed dimension (m)

c – specific heat capacity (J/kg/K)

C – empirical coefficientdepending on the orientation of surface

D – diameter, e.g. Diameter of the fuel bed (m)

E – activation energy (MJ/mol)

F – heating rate (equation 1) (K/s)

g – gravitational acceleration constant (9.81m/s²)

h – convective heat transfer coefficient (W/m²/K)

ΔH – heat of combustion (kJ/kg)

k – thermal conductivity (W/mK)

l – specimen or material thickness (m)

L – flame height (m)

m – mass (kg)

N – non dimensional group (-)

Nu – Nusselt number (-)

dn – mesh cell size (m)

Pr – Prandtl number (-)

$\dot{Q}$ – heat release rate (kW)

q – heat flux (kW)

R – gas constant (8.314 J/molK)

Re – Reynolds number (-)

s - number of data points in the interval

T – temperature (K or °C)

t – time (s)

u – velocity (m/s)

x – distance (m)

y – distance (m)

Y – amount of combustible content, or energy amount (-)

z – distance (m)

α – absorbtivity (-)

Δ - change or difference

ε – emisivity (-)

κ – von Kármán constant (-) (=0.41)

μ – dynamic viscosity (kg/ms)

ρ – density (kg/m^3)

σ – Stefan-Boltzmann constant (=5.6704 × 10–8 W/(m^2·K^4))

ϕ – configuration factor

Subscripts

a - abmbient conditions (typically room conditions)

c – convective

exp – exposure

g – gas, typically 'hot gas'

gen – generation

i – time or measurement step

in – in going

inc – incident

m – material (specimen)

max – maximum

min – minimum

mod – modified

OC – organic content

out – outgoing

p – in constant pressure

r – radiation

s – surface

sl – slug

SW – stone wool

t – turbulent

w – wall surface

x – direction x

y – direction y

z – direction z

0 – initial values

τ – tangential

Terminology

Accuracy – closeness of the agreement between the result of a model prediction and the measured value, or the closeness of the agreement between the measurement and the true value of the measured parameter

Boundary layer – layer of fluid in the vicinity of a bounding surface and having a temperature and/or flow velocity gradient over the thickness

Element (building element, construction element, separating element) – integral part of a built environment. It includes floors, walls, beams, columns, doors, and penetrations, but does not include contents

Composite-scale – physical scale investigated in this research, consisting of several layers of material

Exposed surface – surface of a test specimen subjected to the heating conditions in a fire test

Fire behaviour – change in, or maintenance of, the physical and/or chemical properties of an item and/or building element exposed to fire

Model or Simulation – calculation method that describes a system or process related to fire development, including fire dynamics and the effects of fire

Micro-scale – physical scale of a material, which is small enough to neglect the heat transfer inside the material, typically a few mg. Examples of micro-scale test methods include TGA and MCC

Fire performance – response of a material, product or building element in a fire

Fire plume – buoyant gas stream and any materials transported within it, above a fire

Fire resistance – ability of a test specimen to withstand fire or give protection from it for a period of time

Heat flux – amount of thermal energy emitted, transmitted or received per unit area and per unit of time

Heat release – thermal energy produced by combustion

Heat transfer – exchange of thermal energy within a physical system or between physical systems, depending on the temperature and pressure, by dissipating heat

Incident heat flux – heat flux received by (or falling on) the surface of a test specimen

Material-scale – physical scale investigated in this research, consisting only of a single material and typically with heat flow in one direction

Mechanical response or mechanical behaviour – measure of fire-induced changes to the deflection, stiffness and load-bearing capacity of building elements and the development of openings (e.g. cracks) in building elements during fire exposure as a result of the shrinkage or expansion of materials, spalling, or delamination

Pyrolysis – chemical decomposition of a substance by the action of heat

Reaction to fire – response of a test specimen when it is exposed to fire under specified conditions in a fire test

Real-scale fire test – fire test that simulates a given application, taking into account the real scale, the real way the item is installed and used, and the environment

Separating element – physical barrier intended to resist the passage of fire from one side of the barrier to the other side

Small-scale fire test – fire test performed on a test specimen with dimensions of a couple of cm

Test specimen or test sample – item subjected to a procedure of assessment or measurement. In a fire test, the item may be a material, product, component, element of construction, or any combination of these. It may also be a sensor that is used to simulate the behaviour of a product.

Thermal decomposition – process whereby the action of heat or elevated temperature on an item causes changes to the chemical composition

Thermal degradation – process whereby the action of heat or elevated temperature on an item causes a deterioration of one or more properties

Thermal insulation (criterion in a fire resistance test) – defined as the ability of a separating element, when exposed to fire on one side, to restrict the transmission of heat

Thermal response – temperature profile within an object resulting from an applied heat flux

Table of Contents

1 Introduction

The challenge in fire safety engineering is to ensure acceptable fire safety levels, hence reducing the number of fire casualties and injuries, and to reduce the property and environmental losses created by fire incidents [1]. Understanding the behaviour of materials and structures, and controlling which ones are used in built environments is an integral part of achieving this goal. Other parts include understanding evacuation, the performance of active systems, firefighting and rescue operations.

Prescriptive fire safety guidance is largely based on experience of building fires with significant negative consequences. Such fire incidents are relatively infrequent, hence the amount of gathered knowledge is limited and sparse. One example is the data provided by the German fire service, which reported 125 façade fires in Germany between 2011 and 2018 [2]. Some of the most important façade fires involving aluminium composite claddings between 2010 and 2017 are presented by Guillaume et al. [3] in a list of 13 fire events. In a position paper published in late 2019 by the International Association of Fire Safety Science IAFSS, work on universal data collection, improved exchange of data and learnings from real fires were listed as necessary research activities during the next decade [4]. The evaluation of new building systems, on the other hand, is based on the physical testing of relatively small-scale mock-ups, or sometimes even only on the materials used to build the system. How to bridge the gap between material behaviour in laboratory scale tests and in complete full-scale systems is not clear – arguably, it is based on past incident observations, sparse large-scale test results or simply on engineering assessments combined with embedded large safety factors. It can be argued that this approach can sometimes lead to overdesign and being too restrictive or, in other occasions, it can be incapable of identifying risks associated with new construction materials, products and systems.

Physical fire testing is not a feasible way to evaluate a wide range of possible fire scenarios due to economical, environmental and safety considerations. Mathematical modelling could provide a good alternative to testing. The word *modelling* will be used in this thesis to refer to predictive methodology that uses physical laws and mathematical correlations to calculate the construction response to heat exposure.

Modelling requires fewer material resources, could be faster, more environmentally friendly and more considerate of human health. Therefore, it could provide a way to assess the performance of systems in more different scenarios and provide input for system changes that improve performance.

Professionals who perform standard fire tests in their daily working life may have the ability to predict the influence of small modifications to a system's fire performance. Nevertheless, an important asset in modelling is the ability to quantify these influences.

The model development process is complex and a stepwise approach could be taken to perform it. Some goals are more easily achieved and should be done first. For example, a relatively simple goal would be predicting system fire behaviour in a well-understood scenario, with a precision that would allow only the ranking or categorizing the systems in groups. Once this goal is achieved, modelling could be used to effectively develop products and systems that fulfil standard fire classification requirements. In the existing testing framework, manufacturers are obliged to show the performance of their products or systems in expensive physical fire tests, with a probability of failure. System performance prediction would allow the system to be optimized during the development process, thereby reducing the probability of failure and decreasing time to market. It would also be possible to assess acceptable changes to the system's design, without the need to redo the test. The development of modelling could first of all benefit small companies that are not experienced in fire testing. Allowing the new and small companies to develop more effectively would support diversity in the building system market.

A more distant long-term goal would be to extend system performance modelling beyond the standard fire test scenarios, dimensions and classification groups. Current practice involves evaluating the system performance in one specific fire scenario, with the assumption that this fire scenario (e.g. ISO 834 standard fire resistance exposure, SBI tests or SP 105 façade testing) is representative for the evaluation of the system's or product's required fire performance during its lifetime. The validity of this assumption is continuously scrutinized as the understanding of compartment fires, external fires and fires in structural elements develops. An example of this point included development of concept of travelling fires [5]. Furthermore, in current testing practice, investigating systems in their full physical size is not feasible. Fire resistance test specimens typically have maximum dimensions of 3 × 3 m, and do not include connections to other construction system parts. Tested façades are in the order of a couple of metres, e.g. the SP 105 method uses a 4 × 6 m test sample [6]. Since testing all possible scenarios and full-size constructions is not feasible (and is not expected to become more feasible in the future), modelling

capabilities may provide a way to investigate real-life system fire behaviour. As a result, perspective prediction tools would contribute expanding the knowledge domain of fire behaviour.

Predicting fire behaviour of materials and systems is facing many challenges. Nowadays behaviour of very few materials in simple experimental arrangements can be predicted. Examples include predictions of the burning rate and heat release rate of polymer materials in a cone calorimeter test setup [7]. Nevertheless, the prediction accuracy collapses as the system or fire scenario complexity increases [8,9]. In the area of fire resistance of separating elements, relatively good accuracy has been demonstrated for predicting temperature distribution inside some materials e.g. gypsum plasterboard. Nevertheless, effects such as the cracking and fall-off of gypsum, which significantly influence the fire resistance of the separating element, are difficult to predict.

The development of correlations between different scale tests is an approach that is sometimes used in research and development [10–12]. Nevertheless, these models are not general and hence the applicability of these correlations is limited.

There are several reasons for the limitations in present-day model performance:

1. Major uncertainties of the parameter values describing material properties and boundary conditions (both in standard fire tests and in realistic fires). Uncertainties in material properties are due to the inhomogeneity of materials' chemical and physical structures. The uncertainties in boundary conditions are due to the wide variations of possible fire scenarios, and a lack of control over different heat transfer modes in standard fire tests;

2. Many coupled processes that take place simultaneously, which makes the computations resources demanding. These processes include heat and mass transfer, material degradation and decomposition, gas phase mixing and combustion chemistry, turbulence, radiative heat transfer, etc. Some of these processes are not yet sufficiently understood;

3. The large physical size of real-life systems (in order of tens of metres), which requires significant computational resources and allows small uncertainties in material properties and boundary conditions to contribute to large errors in overall system fire performance.

The future challenge for fire safety scientists and engineers is to apply modelling methods to a wider range of materials, products and systems in different heat exposures. The purpose of this thesis and the appended papers is to address some of these complexities.

1.1 The FIRETOOLS Project

Model development initially requires identifying processes and understanding the underlying laws that govern them. Splitting the complexity of system fire behaviour in sub-problems is useful, as these sub-problems are easier to understand when isolated from the entire system. The main principle of the FIRETOOLS project, which forms basis of this thesis, was a multi-scale approach that is illustrated in Figure 1. In the FIRETOOLS project, the complexity of the system's fire behaviour is broken down in terms of the physical scale, assuming that simplified geometry and composition will result in the isolation of processes that govern the overall fire behaviour [13].
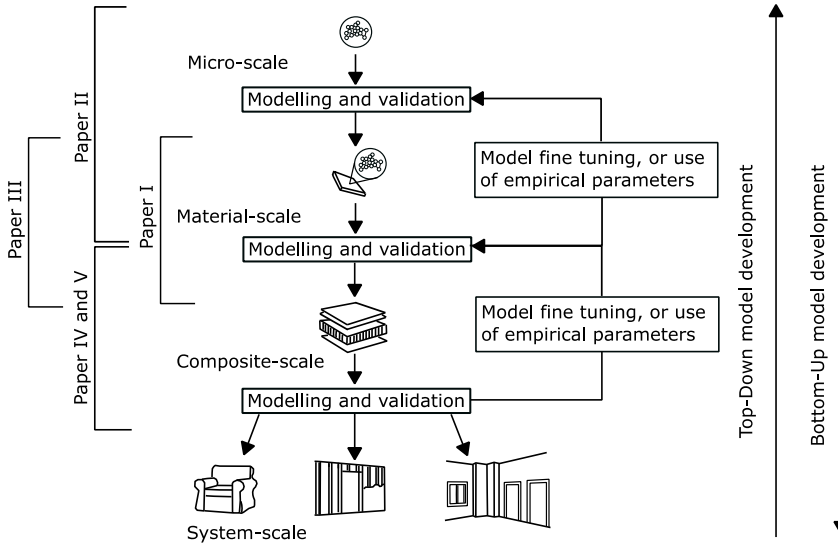
Figure 1: Multi-scale approach employed in project FIRETOOLS and its relation to the appended papers

This thesis covers parts of the micro-, material- and composite-scales as presented in Figure 1. Micro-scale is the material physical scale, with mass in order of mg, where the heat gradients upon heating can be assumed to be absent. Hence, in micro-scale, reaction kinetics can be studied as a process that is de-coupled from heat transfer. Material-scale is a physical scale with the dimensions in the order of cm, where considering both reaction kinetics and heat transfer is important. Material-scale is considered one-dimensional and the complexities associated with interactions with other materials are neglected. Composite-scale represents multilayer elements with dimensions in the order of a few centimetre to metres, if heat exposure influences at least two layers of the construction. Composite scale is a simplified representation of a finished product scale, as it does not include different seams, fixings and other

8

features of a real-life system. System-scale is a full-size construction system, including the detailing and different orientation of surfaces. This system may be a separating element (e.g. wall or ceiling tested for fire resistance), façade system (tested for reaction to fire) or building content (e.g. sofa or chair tested for burning behaviour).

The overall scope of the FIRETOOLS project was limited to system-scale behaviour in applications of fire separating elements, construction products and building contents. Larger scales, above system-scale, can easily be imagined, consisting of several systems that interact with each other and even include environmental (e.g. wind) and societal (evacuation or fire-fighting activities) influences.

1.2 Problem statement

One example of the discussed points and focus of this thesis is ventilated façade systems, which are complex and relatively new construction systems (Figure 2 and Figure 3). Noteworthy façade fire incidents involving ventilated façade systems include the Knowsley Heights fire [14] and Grenfell Tower fire [15] and the Marina Torch Tower (2015 and 2017) [3]. These incidents have triggered some research into the fire behaviour of ventilated façades [3,14,16–19]. A ventilated façade system consists of cladding material fixed on the building's exterior wall. The cladding is fixed on horizontal and vertical railing, hence forming an air cavity between the cladding and building's exterior wall. Typically, thermal insulation and moisture barriers are located in the interior of the cavity. Real life examples of ventilated cavities are presented in Figure 2 and Figure 3. Figure 2 shows the schematics of a façade with different material layers and supporting elements. Figure 3 presents an example of a ventilated façade during the construction process and on an actual building.

The overall fire behaviour of a ventilated façade system (shown in Figure 2 and Figure 3) depends on the thermal and flammability properties of individual components, mechanical behaviours in the supporting structures (rails and studs), mechanical resistance of cladding, heat feedback inside the cavity geometry etc. The performance of façades is typically assessed using façade testing e.g. DIN 4102-20, BS 8414, PN-B-02867:2013, LEPIR 2, MSZ 14800-6, ÖNORM B 3800-5, SP Fire 105, ISO 13785 -1, ISO 13785 - 2 [20] or the reaction to fire performance of individual components [21]. Full scale façade testing is resource-demanding and, in principle, covers only one single fire scenario. The component-based assessment, on the other hand, cannot capture the performance of this material inside the geometric

context of the façade. Both of these strategies provide a relative ranking of different façade systems in a specific fire scenario.
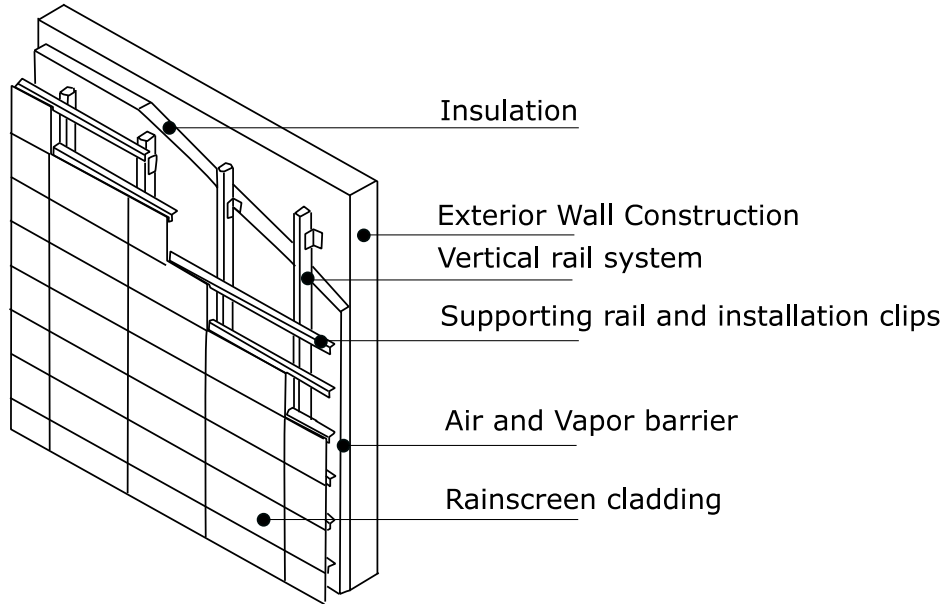
Figure 2: Ventilated rainscreen façade system schematics

For the purpose of this thesis, the complex system of a ventilated façade, as presented in Figure 2 and Figure 3, is simplified as a cavity between two parallel vertical walls, as shown in Figure 4. This simplified arrangement does not consider the cladding support system, fire barriers inside the cavity, etc.

Compared to surface flame spread in the open, the air inflow rate is different in a narrow cavity scenario, governed by limited space and the chimney effect. Ignition and the efficiency of combustion is controlled by pyrolysis rates and the rate of air inflow. Flame geometry is influenced by cavity width. Heat transfer from flames and radiation effects from the protecting layer (e.g. cladding) will determine the heating rate and heated area of the virgin material. Thermal decomposition and degradation will take place in the materials that compose the system. Some thermal insulation materials will shrink or melt when exposed to heat, thereby increasing the cavity's width. Typically, cladding material is relatively thin, making it more prone to ignition when exposed from both sides. The presence of a cavity has been shown to contribute to the ignition of the cladding system [19].

(a)

(b)

Figure 3: Example of a ventilated façade on a building in Riga, Latvia, (a) during construction with exposed insulation and railings (b) over the entire façade of a high rise building

Studies of fire dynamics inside a narrow cavity require the consideration of three-dimensional space in order to take flows into account. The parts of this study that refer to fire dynamics (i.e. Paper IV and Paper V) are therefore investigated at the composite scale (refer to Figure 1). On the other hand, investigating the materials that compose the boundaries of the ventilation cavity is useful, assuming one-dimensional or two-dimensional approximations. The parts of this study that relate to the thermal response of solids (i.e. Paper I, Paper II and Paper III) are investigated at the material scale in one dimension. Material thermal response modelling is supported by investigating material properties (e.g. reaction kinetic parameters) at the micro scale (non-dimensional approximation is used in this case).

The influence logics between different thermally driven processes are presented in Figure 5. This thesis investigates heat transfer and exothermic and endothermic reactions, surface recession and heat transfer from flames in narrow cavities, as shown in Figure 5 (b). The scope of the research is therefore limited by excluding material flammability from the analysis.
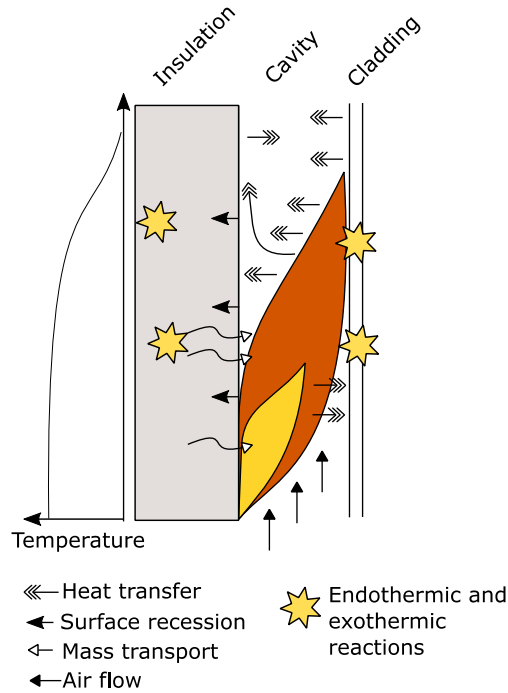
Figure 4: Processes taking place in flame spread in narrow cavity space

1.3 Objectives

The overall objective of this thesis is to contribute to the understanding of fire dynamics and the thermal response of materials in relation to fires in narrow, concealed spaces. This objective is achieved through the provision of new experimental data, outcomes of modelling attempts and model performance analysis, as well as experience-based discussions. The specific objectives of this thesis are:

Objective 1: To identify the properties needed to predict temperature distribution inside common building materials and to establish a link between the material properties obtained with micro-scale (mg of material) and material-scale (specimen size in the order of 10 cm) test methods and the temperature distribution in fire tests;

Objective 2: To investigate the modelling results' level of sensitivity to uncertainties in the modelling input;

Objective 3: To investigate how the cavity's geometrical parameters influence fire exposure inside the cavity and the capabilities and limitations of numerical modelling in replicating this influence.

(a)
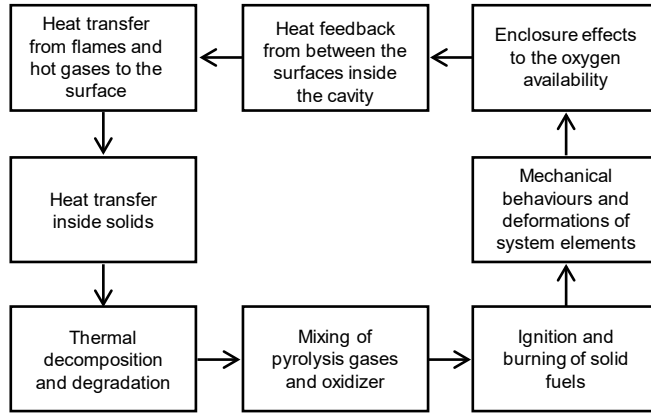
(b)
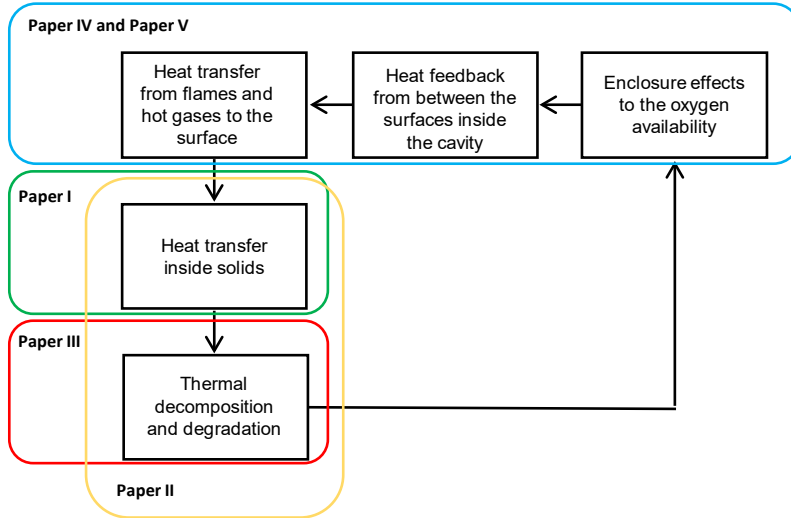
Figure 5: Influence logics diagram (a) detailed process diagram (b) simplified process diagram as considered in this thesis

1.4 Limitations and implicit assumptions

The research methodology (Figure 1) implicitly assumes that fire behaviour at smaller physical scales is easier to describe mathematically, and that it is possible to establish a link between the different physical scales. In this thesis, materials (mostly thermal insulation materials used in construction) were studied at the micro scale and material scale, and their relationship to the composite scale is discussed. The

13

heat exposure conditions, relevant to the air cavity systems, were studied at the composite scale.

The experimental and numerical setups were only very simplified versions of real-life constructions, therefore it must be noted that this work does not represent the system scale.

Furthermore, this thesis focuses on thermal processes. Mechanical behaviours, ignition and flaming combustion are not discussed (an exception is smouldering combustion in the organic contents of stone wool, as discussed in Paper II). It is evident that these processes are important for characterizing the fire behaviour of façade systems and therefore require research attention in the future. Figure 5 presents influence diagrams for façade fire behaviour. Figure 5 (a) is a more realistic and detailed diagram, including the interactions between heat transfer, combustion and mechanical processes in the façade. Figure 5 (b), on the other hand, shows a simplified diagram that is followed in this thesis.

Fire safety engineering provides a framework for using deterministic, probabilistic and comparative approaches to tackle safety and economical challenges related to fire incidents [1]. A deterministic approach is mostly used in this thesis.

1.5   Outline of the thesis

This thesis is a collection of papers, appended in Annex B [22–26]. The introductory summary is divided in 9 chapters.

Chapter 2 presents a brief overview of the theory of diffusion flame heights in different configurations and heat transfer for fire safety application. Chapter 3 presents the research tools and methods used in this thesis.

The following three chapters relate to the process diagram that is presented in Figure 5 (b). Chapter 4 is a summary of the appended Paper I and Paper II, providing a discussion and case study for heat transfer calculations in solids. Chapter 5 is a summary of Paper III and presents the work done on measuring the surface recession of materials under heat flux. Chapter 6 is a summary of Paper IV and Paper V and presents the experimental and numerical study of fire induced flows and flame heights between parallel walls.

Thereafter, the discussion is presented in Chapter 7 and the conclusions are presented in Chapter 8. Finally, Chapter 9 lists future research needs.

2 Theoretical Background

A typical example of a construction system with an air cavity is a ventilated façade system. Other constructions, such as gypsum cavity walls etc., also fall into the category of concealed narrow space constructions that can promote fire spread between compartments. It has been shown that fires often start and develop in concealed spaces, which is a significant contributor to fire losses[27].

A ventilated façade system with the rain screen cladding has a 0.02 - 0.06 m wide cavity to ensure drainage and ventilation. The material layers covered by the rain screen cladding in these systems are water-resistant breathable membranes and thermal insulation (e.g. mineral fibre insulation or phenolic foam). Fire propagation through and over ventilated façade systems has been addressed in several literature reviews and large-scale experimental studies [14,16–19]. According to the testing experience at BRE, flames in ventilation cavities can extend up to ten times, compared to flames outside the cavity, as reported by Colwell et al. [18]. An air cavity also contributes to increased burning rates in the cladding system [19]. In addition, a number of studies have been performed to investigate double skin façades that are exposed to flames emerging from a post-flashover compartment [28–31]. These studies demonstrated that air cavity width is a significant factor in influencing flame characteristics and heat exposure on the surfaces inside the cavity.

Only a limited number of studies, however, have been carried out to investigate fire behaviour in narrow spaces using well-controlled laboratory size experiments or numerical simulation tools. Fire dynamics in concealed spaces is different to that of enclosure fires, considering the traditional fire resistance and reaction to fire testing [32]. Fires in narrow cavity spaces, compared to enclosure and external fires, will have different dynamics. Firstly, air entrainment in the combustion zone will be more influenced by physical obstructions, both the cavity enclosure walls and real-life construction detailing (e.g. railings, fixings). Knowledge about flame heights and different configurations of other characteristics is required to understand the influence of restricted air entrainment. Furthermore, heat feedback will be promoted between the obstacles due to tighter geometrical configuration.

The characteristics of parallel plate arrangements, which allow increased fire exposure to the specimen, are successfully used in ANSI FM 4880, the American National Standard for evaluating the fire performance of insulated building panel assemblies and interior finishing materials. One element in this standard is 16 ft (approximately 4.9 m), the distance between the parallel plates is approximately 0.53 m and they are 1.1 m wide. A sand burner is used on the entire width of the cavity with a standard heat output of 360 kW. Due to the parallel wall arrangement, this test method can expose the specimen to heat fluxes of approximately 100 kW/m^2, which is higher than most alternative exterior envelope test methods [33,34]. Flame spread for cardboard in this parallel wall configuration has been studied experimentally and numerically using FireFOAM software by Chaos et al. [35].

The main areas of interest in studying this problem are heat transfer in solids, heat transfer from the environment to surfaces and between solid bodies, flame geometry and chemical characteristics. This chapter very briefly covers two topics: diffusion flame heights and the fundamentals of heat transfer.

2.1 Diffusion flame heights

Flame height marks the position at which the combustion reaction is, in general, completed. Nevertheless, it is typically defined using some luminosity characteristics. The transition between the easily observable flame region closer to the fuel bed and the smoke plume is not easily definable, because the upper parts of a flame are not steady. Intermittency, I, is used to define the mean flame height where I(z) is a fraction of time where at least part of the flame is observed above the elevation z. It is suggested to define the flame height at I=0.5 [36].

2.1.1 Burning in the open, next to a wall and in a corner

Diffusion flames are created in situations where the fuel and oxidizer are initially separate and are continuously mixing by diffusion while combustion takes place. The flame front is the position where the fuel and oxidizer meet at stoichiometric proportions and combustion occurs. Visible flames indicate the combustion reaction zone [37]. The time scale for reactants (fuel and oxidizer) mixing by diffusion is longer than the time scale at which the chemical combustion reaction takes place [38]. As a result, the flame speed is controlled by the diffusion process. Diffusion flames are characteristic of the burning of solids and liquids in fires.

Most previous research on flame heights has been done in an open environment, with using circular or square burners on flat, horizontal surfaces. The flame height dependency on $\dot{m}_c^2/D^5$ was established by Thomas et al. [39]:

$$\frac{L}{D} \propto (\frac{\dot{m}_c^2}{D^5})^n$$

where $\dot{m}$ is the volumetric gas flow of gaseous fuel (m³/s), D is the characteristic dimension of the fuel bed (m) and L is the flame height (m).

Later, the dimensionless heat release rate $\dot{Q}^*$ was suggested as one of the most influential parameters in determining flame height [40]:

Equation 1: Non-dimensional heat release rate

$$\dot{Q}^* = \dot{Q}_c/(\rho_a T_a c_{p\,a}\sqrt{gD}D^2)$$

where $\dot{Q}_c$ is the heat release rate (kW), ρ_a is the air density (kg/m³), T_a is the ambient environment temperature (K), c_{pa} is the specific heat capacity of ambient air (J/(kg·K)), g is the gravitational acceleration (=9.8 m/s²) and D is the diameter of the fuel bed (m). L/D versus $\dot{Q}^*$ for burning in an open is presented in Figure 6 and several regimes were identified in this relationship. For $\dot{Q}^* < 0.1$, L/D scales with the dimensionless HRR as $\left(\dot{Q}^*\right)^2$. For $0.2 < \dot{Q}^* < 0.5$, L/D scales almost linearly, two-thirds power law apply for $0.5 < \dot{Q}^* < 7$ and 2/5 power law apply above $7 < \dot{Q}^*$[41,42]. Transition between the regimes is not strictly defined, but is gradual.
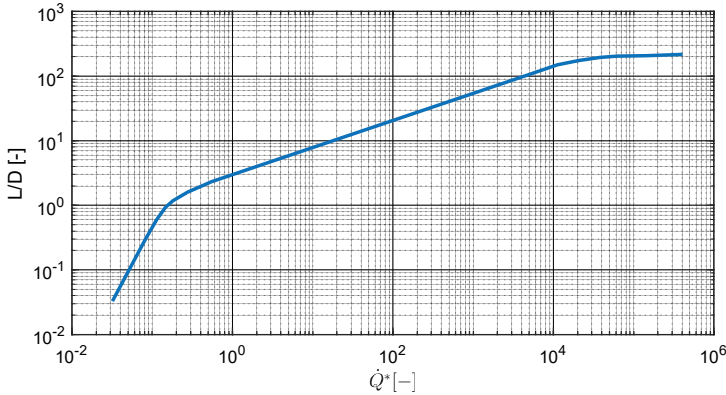
Figure 6: L/D versus dimensionless heat release rate. Reproduced from reference [41]

Heskestad has collected data from a large amount of studies to derive flame height correlation for axisymmetric fires and summarized them in Equation 2 [43]. Heskestad showed that Equation 2 is valid for N (Equation 3) between 10^{-5} and 10^5.

Equation 2: Flame height divided by the burner diameter

$$\frac{L}{D} = 15.6 * N^{1/5} - 1.02$$

Where the non-dimensional group N is given in Equation 3,

Equation 3: Non-dimensional group N used in flame height correlation by Heskestad

$$N = \left(\frac{c_p T_a}{g\rho_a^2 \left(\frac{\Delta H_c}{r}\right)^3}\right)\frac{\dot{Q}_c^2}{D^5}$$

Fire plumes from burners with large aspect ratios had been investigated by Hasemi & Nishihata [44], who suggested flame height proportionality with heat release rate:

$$L \propto \dot{Q}_c^{2/3}$$

For flame height correlations, Hasemi & Nishihata [44] suggested using modified non dimensional HRR, including the burner dimensions as:

Equation 4: Modified non-dimensional HRR

$$\dot{Q}^*{}_{mod} = \dot{Q}_c / (\rho_a T_a c_{p\,a}\sqrt{g}a^{3/2}b)$$

where a is the smallest burner dimension (m) and b is the largest burner dimension (m).

Fire plumes, flame characteristics [45] and fire-induced flows [46] are influenced by physical obstructions in their surroundings. Some examples discussed in the literature are burning next to a wall, in a corner or flame deflection along the ceiling. The principles of how the obstructions influence flame heights are suggested to be related to the limited air entrainment in the fire plume, forcing combustion to take place higher above the fuel bed.

A common belief in the past was that flame heights next to a wall can be calculated by assuming a mirror image of the burner on the wall and calculating the flame heights as if the fire of the real and the mirrored burner were burning in an open environment. This theory was refuted by Hasemi & Tokunaga (1984) and Mizuno & Kawagoe, who showed that the flame heights of gas fires only slightly increase when placed next to a wall [41,47]. Later, Back et al. showed that open burning flame height correlations fit well with experimental observations for the burning adjunct of a wall [48].

Flame height increase has been observed in corner configurations for gas diffusion burners [45,49], combustible liquid fires [50] and upholstered furniture [47]. The

flame will generally lean towards the nearby corner. Takahashi et al. showed that dimensionless flame height increased for rectangular corner fires, as the burner is moved closer to the corner, and suggested that the flames extended almost twofold compared to free burning conditions [45]. An approximately 36% increase in flame heights was observed for upholstered chair fires [47], when burning in a corner.

2.1.2   Narrow spaces between walls

Burning in narrow spaces is characterized by limited air supply for combustion and the influence of a chimney (or stack) effect. Radiation feedback from nearby walls and limited heat losses may further increase the flame spread rate in narrow configurations.

Burke and Schumann [51] studied cylindrical and flat diffusion flames. Their test setup consisted of two tubes, placed inside one another. A combustible gas flowed through the inner tube and the air was provided in the space between the tubes. They proposed a mathematical description of flame front geometry based on a theoretical analysis of fuel and air mixing by diffusion. Burke and Schumann [51] concluded that the height of the flat flame is directly proportional to the width of the ducts.

Some research on fire plumes in concealed spaces has been done on fires between rack storages, both for two dimensional and three dimensional cases [52–54]. The main investigated parameters were the visual flame heights, the temperatures and the heat fluxes to the surfaces between the racks. Figure 7 presents a comparison of observed flame heights by Hasemi & Nishihata [44] and Ingason [53]. Hasemi & Nishihata performed burn test in free environment with the largest burner aspect ratio 0.1 × 1.0 m2 (aspect ratio 0.1). Ingason [53] performed tests free burning and enclosed flames between rack storage with horizontal separation distance between 0.05 and 0.1 m. The burner used by Ingason was 0.02 m × 0.59 m (aspect ratio 0.034). It can be seen that the data for free burn fits well and that cavity configuration results in extended flames.
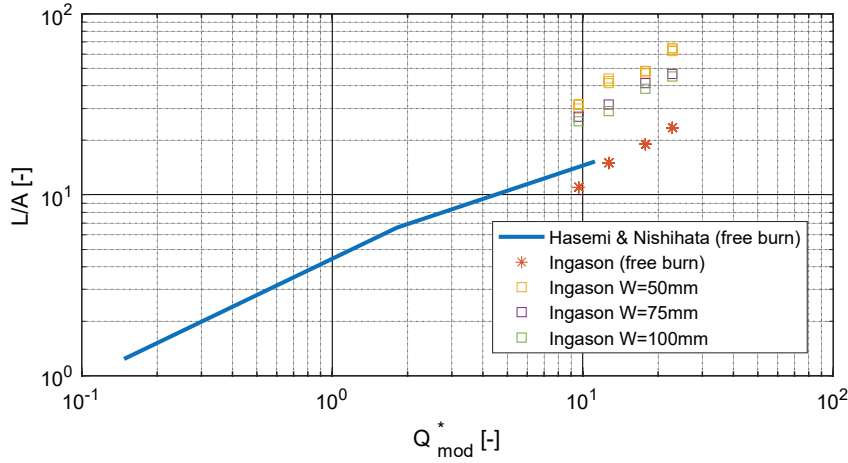
Figure 7: $\dot{Q}^{*}_{mod}$ versus L/D, where A is the smallest dimension of the burner. Data by Hasemi & Nishihata [44] using a burner with a=0.1 m and b=1.0 m, and Ingason [53]a=0.02 m and b=0.59 m

Ingason developed a theoretical model for predicting flame heights, air flow and temperature in a two-dimensional rack storage configuration and showed that the air leakage through the horizontal flues is insignificant, meaning that the results are not influenced by the vertical distance between rack storage boxes [55]. Furthermore, Ingason also performed a three-dimensional arrangement at 1:3 scale and full-scale tests with corrugated cardboard box arrays and measured the centreline temperatures and gas velocities between the racks [54,56].

Foley & Drysdale [57] varied the cavity width W (minimum 0.06 m), burner location, air flow conditions and Q', and demonstrated the importance of the air inflow conditions by opening and closing the base of their test setup, which was a parallel wall configuration. Air availability influenced the flame shape inside the gap. Yan & Holmstedt used Foley & Drysdale's results to validate a mathematical model that they had developed [58]. Hu et al. [59] investigated flame heights between two parallel walls with cavity widths equal to and greater than 0.14 m, and different orientations of the line burner relative to the walls. Hu et al. found that in the investigated range, flame heights were not influenced by cavity width when the long edge of the burner was perpendicular to the walls. In the cases where the burner's long edge was parallel to the walls, flame heights were found to increase when cavity width was decreased.

Foley & Drysdale [57] also showed that the total heat flux to the inner surface increases as the cavity width is reduced. Several different fuels were used in a study by Ris & Orloff [60], showing that the heat flux from flames is sensitive to the flames' sootiness and parallel wall configuration.

2.2 Basic concepts of heat transfer in fire

2.2.1 Heat transfer mechanisms

Heat transfer deals with the transport of thermal energy. Transport of thermal energy is the main driver for material behaviours created by fires, such as thermal decomposition, thermal degradation, pyrolysis, ignition, flame spread, heat impact on human health, etc. The three fundamental modes of heat transfer are thermal conduction (referred to as conduction in this thesis), thermal radiation (referred to as radiation in this thesis) and convection.

Conduction is heat transfer in a stationary medium – solids and fluids. Conduction is the diffusion of thermal energy from regions with higher temperature to regions with lower temperature. The significance of conduction is related to temperature distribution inside solids. The influence of conduction on heat transfer in fluids is relatively smaller than in solids, because the energy in fluids is mostly transported by the bulk motion of the fluid's molecules. Temperature distribution inside solids not only depends on their conductivity, but also on their specific heat capacity and density.

Radiation heat transfer is the thermal energy exchange between two bodies at a distance from each other. Thermal radiation is emitted by all bodies with a temperature above 0 K; it propagates using electromagnetic waves and is absorbed by bodies reaching this energy. No medium is required for radiation heat transfer. Radiation significance is related to the heat transfer from flames or heated objects to the fuel bed. The radiation heat flux has a 4th power dependence on the temperature difference between the objects that exchange the energy. Just like receiving the heat, the hot object also loses the thermal energy through radiation.

When a solid is in contact with a fluid that has a different temperature, molecules in the fluid exchange energy with molecules in the solid via conduction and radiation[61]. The peculiarity of heat exchange between fluids and solids is that fluids are typically in motion, and the energy transferred to the solid's surface will depend on the properties of this motion. Therefore, this process is commonly regarded as a separate heat transfer mechanism called 'convection'. Technically, convection is heat transfer due to the bulk movement of molecules in fluids, but in fire safety engineering, including this thesis, it is frequently defined as the heat transfer between the fluid and the solid. Convection is important in problems involving the cooling of heated bodies, e.g. on the unexposed surface of the standard

fire resistance test specimen, and in problems that involve heating solids, leading to ignition and flame spread.

2.2.2 Convective heat transfer to a solid boundary

Thermal energy is transferred between fluids and solids though conduction and radiation. However, the fluid's motion differentiates this heat transfer process from heat transfer inside solids or between two stationary bodies. The heat between the fluid and the surface is exchanged in a very narrow region on the boundary between the solid and the fluid, called the 'boundary layer'. For practical reasons, the heat transfer is typically related to flow properties in the region outside the boundary layer, called the 'free stream' region. This free stream region is where the relative velocity, pressure and temperature are unaffected by the solid boundary. Temperature and velocities in the boundary layer are different to those in the 'free stream' region in the fluid further from the solid boundary. Boundary layer thickness is determined by properties of the flow, fluid and solid. This process is therefore separate and referred to as convection. Convective heat flux is calculated as shown in Equation 5,

Equation 5: Convective heat transfer

$$\dot{q}''_c = h\left(T_g - \mathrm{T}_s\right)$$

where h is the convective heat transfer coefficient (W/(m²·K)), T_g is the free stream fluid temperature (K) and T_s is the solid surface temperature (K). The convective heat transfer coefficient is therefore a proportionality coefficient between the temperature difference and the convective heat flux. The convective heat transfer coefficient describes the system in which the heat transfer takes place – it is dependent on the properties of the flow, fluid and solid.

Natural and forced convection are distinguished and different equations are used to calculate the convective heat transfer coefficient, depending on the geometry of the system. These equations can be found in heat transfer textbooks, such as reference [62].

The typical range for convective heat transfer coefficients relevant to this thesis is from 2 W/(m²·K) (expected in natural cooling) up to about 60 W/(m²·K) (expected order of magnitude in façade testing and during the initial stages of standard fire resistance tests).

2.2.3 Radiation heat transfer to a solid boundary

Heat transfer via electromagnetic waves is called radiation. All objects with a temperature above 0 K emit thermal radiation. This emitted thermal radiation is received by other objects, whereupon it can be absorbed, reflected or transmitted through this object. Objects simultaneously receive and emit thermal radiation and, consequently, depending on the balance between the received and emitted thermal radiation, will either lose or gain heat. Radiation heat transfer does not require a physical medium and heat can be transferred from the emitter to receiver over a distance. Thermal radiation is via electromagnetic waves from 10^{-1} to 10^2 µm and spectral normal emissivity is a function of wavelength. Grey body approximation is commonly used in fire safety engineering, assuming that the emissivity is independent of wavelength. Emissivity is a value between 0 and 1. Radiation energy balance on a solid surface, assuming grey body approximation, is given in Equation 6,

Equation 6: Net radiation heat flux at the surface of the receiver

$$\dot{q}''_r = \alpha\, \dot{q}''_{inc\,r} - \varepsilon\sigma T_s^4$$

where $\dot{q}''_{inc\,r}$ is the incident radiation heat flux (W/m2), α is the absorptivity (-), ε is the emissivity (-) and σ is the Stefan-Boltzmann constant (=5.6704 × 10–8 W/(m²·K⁴)).

The incident radiation heat flux from the emitter to the receiver is calculated as shown in Equation 7,

Equation 7: Incident radiation from the emitter to the receiver

$$\dot{q}''_{inc\,r} = \phi\varepsilon\sigma T_s^4$$

where ϕ is the configuration factor (-). The configuration factor (also called the view factor) covers aspects of the geometry of the receiver and the emitter as well as the distance between them. Configuration factor values are presented in textbooks [41,62].

The emitted thermal radiation energy is proportional to $T_s{}^4$. Considering the high temperatures reached in fire problems, radiation often becomes the dominant heat transfer mechanism for heating solids. A typical order of magnitude for radiative heat flux in fire problems is 0 to 300 kW/m², where the upper limit of 300 kW/m² is close to being representative for heat flux in standard fire resistance tests with furnace temperatures of about 1200 °C.

2.2.4 Heat conduction in solids

Heat transfer inside solids is governed by thermal conduction according to Equation 8,

Equation 8: Heat flux by conduction, one-dimensional form

$$\dot{q}''_x = -k\frac{dT}{dx}$$

where k is the thermal conductivity (W/(m·K)), T is the temperature in different space locations inside the material (K) and x is a distance between two locations in the solid.

Equation 9 presents an energy balance in partial derivative form, as used in heat conduction modelling to predict temperature distribution inside the material, assuming a one-dimensional transient case.

Equation 9: transient heat conduction equation, including heat source

$$\rho(T)c_p(T)\frac{\partial T}{\partial t} = \frac{\partial}{\partial x}\left(k_x(T)\frac{\partial T}{\partial x}\right) + \frac{\partial}{\partial y}\left(k_y(T)\frac{\partial T}{\partial y}\right) + \frac{\partial}{\partial z}\left(k_z(T)\frac{\partial T}{\partial z}\right) + \dot{Q}_{gen}'''$$

The material's properties are as follows: ρ is the density (kg/m³), c_p is the specific heat in constant pressure (J/(kg·K)) and k is the thermal conductivity (W/(m·K)). The values of these properties commonly change with the temperature, with enough significance that they should be considered. $\dot{Q}_{gen}$ is the heat source term (W/m3) that represents heat generation or heat sink inside the solid due to chemical reactions or phase changes.

As shown in Equation 9, in transient heat conduction analysis the material's thermal properties are thermal conductivity, density and specific heat. These properties are typically obtained from material testing and used as input parameters in a numerical model. These parameters are relevant for all materials in transient heat conduction analysis, although in some cases simplifications are possible:

- One-dimensional systems;
- Lumped thermal capacity analysis;
- Effective (apparent) and temperature independent thermal properties;
- Steady state solutions.

One-dimensional approximation can be used when the heat in the system is transferred in one direction. This simplification converts Equation 9 to Equation 10.

Equation 10: One-dimensional transient heat conduction with source term

$$\rho(T)c_p(T)\frac{\partial T}{\partial t} = \frac{\partial}{\partial x}\left(k(T)\frac{\partial T}{\partial x}\right) + \dot{Q}_{gen}{}'''$$

Another simplification used in this thesis is called lumped thermal capacity [24,25]. Lumped thermal capacity analysis assumes that the temperature distribution over the thickness of material is negligible, thereby eliminating thermal conductivity from the analysis. This can be used if the heat transfer inside the material occurs at a much higher rate than the heat is transferred to the surface of material and/or if the material is thin. The applicability criteria for lumped thermal capacity analysis is the Biot number (Equation 11),

Equation 11: Biot number

$$Bi = \frac{l * h}{k}$$

where l is the material's thickness (m), h is the convective heat transfer coefficient (W/(m²·K)) and k is the thermal conductivity (W/(m·K)). It is assumed that the Biot number below 0.1 allows this simplification [41]. Lumped heat capacity analysis reduces the transient heat conduction equation to energy balance, as shown in Equation 12,

Equation 12: One-dimensional energy balance inside a solid, assuming lumped thermal capacity analysis

$$\dot{q}''_{in} - \dot{q}''_{out} = \rho c_p l \frac{\partial T}{\partial}$$

where subscripts in and out refer to incoming and outgoing heat flux.

The discussion here assumes that heat conduction alone governs the heat transfer inside solids. When it comes to most of the real-life materials used in construction, this assumption is merely a simplification. Many materials, e.g. stone wool, gypsum and concrete, are porous, so the heat transfer process includes radiation and convection in the pore spaces. Additionally, mass transport (such as water vapour) influences heat transfer. The numerical interpretation of radiation and convection is much more complex than for conduction. An effective (or apparent) thermal conductivity is commonly used to include all processes governing the heat transfer inside solids, and reducing the heat transfer in materials to conduction therefore

simplifies the required calculations. Examples include apparent thermal conductivity, which includes radiation and gas phase conduction [63,64] and/or moisture movement [65], and apparent specific heat capacity including reaction kinetics [66–69]. This approach suggests that the success of models relies on the error elimination principle – that the errors introduced by dismissing some of the physical processes are eliminated by errors in the thermal property values that are used in the models. As a consequence, each property may have a number of different values that fulfil the need for model requirements to fit with experimental observations. Hence the need for a precise and thorough description of each value from this perspective is somewhat diminished, including the need to consider the temperature dependency. Nevertheless, there are benefits to using thermal property values as accurately as possible from the physical perspective available to the researcher:

1. Temperature dependence gives more degrees of freedom to tune the model input parameters to achieve fit with the experimental observations;

2. Using accurate thermal property values supports the identification of the influence of previously unidentified processes in material behaviours. These processes will reveal themselves as a mismatch between the model predictions and test observations, as they would not be hidden by introducing errors in the material property values (e.g. the use of effective material properties). A more detailed picture of material thermal process would therefore be obtained, allowing more refined optimization of materials during the development process;

3. Similarly to the previous point, a more detailed description of the material's thermal response would allow the model to be applied to different heat exposures with higher reliability. This would be especially useful for considering material performance in realistic compartment fires for fire safety engineering.

Sometimes, if the exposure conditions are constant and the material is exposed to these conditions for very long durations, solving for a steady state solution, rather than transient solution, is more optimal. Steady state solution eliminates the time dependent term on the right-hand side of Equation 9, and therefore the specific heat and density properties disappear, as shown in Equation 13,

Equation 13: Steady state one-dimensional heat conduction equation

$$\frac{\partial}{\partial x}\left(k(T)\,\frac{\partial T}{\partial x}\right) + \dot{Q}_{gen} = 0$$

The nature of enclosure fires is transient with temperature changes in order of several hundred degrees during tens of minutes. Therefore, the steady state assumption is not applicable in most fire related problems.

The heat source term, previously shown in Equation 9, Equation 10 and Equation 13, represents energy input or consumption due to physical or chemical changes in the material, rather than from the external boundaries of the material (e.g. heat flux from the fire). Thermal energy inside the material is used to decompose the material and this thermal energy therefore needs to be subtracted from the heat conduction equation. Decomposition includes material pyrolysis, the drying and release of chemically bound water, melting, etc. Similarly, some processes inside the material result in added heat to the system. For example, some porous materials are prone to smoulder and hence release combustion energy inside the material matrix. When explicitly considered, the heat source term is typically calculated using the Arrhenius equation, Equation 14,

Equation 14: The Arrhenius equation

$$\dot{Q}_{gen} = AY\,exp\left(\frac{-E}{RT}\right)\Delta H$$

where A is the pre-exponential constant (-), E is the activation energy (MJ/mol), ΔH is the heat of reaction (MJ/g) and Y (-) is the remaining energy fraction. These material-related properties can be obtained by analysing the output from micro scale test methods (i.e. on physical scales which are so small that heat transfer can be neglected). Some of the micro-scale test methods mentioned in this thesis are TGA, DSC and MCC.

Solving the heat conduction equation requires fixed boundary conditions on the surfaces of the solid. Three types of thermal boundary conditions relevant for fire problems are [70]:

1. Specified surface temperature (Dirichlet boundary condition) as shown in Equation 15,

Equation 15: Specified surface temperature BC

$$T(x_0) = T_0$$

2. Specified heat flux boundary condition, as shown in Equation 16,

$$\dot{q}''_x = -k\frac{dT}{dx}\bigg|_{x=x_0}$$

3. Natural BC as shown in Equation 17. According to this boundary condition, the heat transferred to the surface is proportional to the difference between the surrounding and surface temperatures.

$$h(T_g - T_s) = -k\frac{dT}{dx}\bigg|_{x=x_0}$$

Most often, a combined specified heat flux and convection boundary condition is used in fire-related problems. Nevertheless, to apply this boundary conditions, the surface temperature, convective heat transfer coefficient and emissivity must be known.

3 Research Tools and Methods

The experimental, numerical and data analysis tools used in this research are presented in this chapter. Experimental and testing methods can be divided into two categories. The first category is testing to obtain the material properties to be used in numerical modelling. Methods in this category include a custom-made simplified slug calorimeter test, micro combustion calorimetry (MCC), thermogravimetric analysis (TGA), bomb calorimetry (BCA) and surface recession testing. The second category is the testing of material or system behaviour in fire or to study fire dynamics. Methods in this category include fire resistance furnace testing and parallel wall test setups for studying flame heights.

Numerical tools used in this thesis include heat conduction and computational fluid dynamics (CFD) calculations with finite element method (FEM) and finite difference method (FDM). Data gathering and analysis tools include Monte Carlo simulations and functional analysis. These tools were used to perform research activities in relation to the published research papers presented in Table 1.

This chapter discusses some of the research tools used in this thesis and appended papers. The research methods described in this chapter are of a 'standard' nature – they are often used by scientists and engineers and some of them have specific standards.

Some of the methods used in this thesis have been specially designed for a specific research purpose. These 'non-standard' methods are described in the relevant chapters of this thesis. The non-standard methods include:

- Numerical heat conduction model written in Matlab® software;

- Non-standard test setup for measuring material recession rates;

- Experimental setup for studying flame heights and heat exposure between two parallel plates.

Table 1: Research activities in relation to the research papers

	Experimental	Numerical	Data analysis
Micro scale	Study of reaction kinetics of stone wool (Paper II)	Determination of the reaction kinetic parameters of stone wool (Paper II)	
Material scale	Study of thermal conductivity of stone wool (Paper II) Shrinking rates of EPS (Paper III)	Modelling heat transfer through stone wool and stone wool composites (Paper I and II)	Sensitivity study (Paper I). Comparing experimental and numerical results (Paper II)
Composite scale	Study of flame heights and heat transfer between parallel plates (Paper IV)	Modelling of flame heights and heat transfer between parallel plates (Paper V)	Comparing experimental and numerical results (Paper V)

3.1 Test methods

3.1.1 Custom-made slug calorimeter

The custom-made slug calorimeter method was used to study heat transfer inside stone wool specimens and to determine the effective thermal conductivity. It was also used as a test case for coupled heat conduction and validation of the reaction kinetics model.

The slug calorimeter test is a non-steady state method using the principle of inverse calculation of the material's thermal properties, based on the temperature difference between the exposed surface and inside the material. Slug calorimetry is described in references [71–74]. A custom-made, simplified version of the slug calorimeter was used in Paper II.

The sample in the custom-made slug calorimeter test consisted of a metallic plate (the 'slug') with a temperature measurement device, squeezed between two identical specimens. The sample is then placed between retaining plates and guard insulation and placed in an electrical oven. The oven temperature is increased at an approximately constant rate. The temperatures of the slug and retaining plates are measured using type K thermocouples. The custom-made slug calorimeter test setup is shown in Figure 8.

The thermal conductivity is thereafter calculated according to Equation 18,

Equation 18 Thermal conductivity calculation from the slug calorimeter test

$$k = \frac{Fl(m_{sl}c_{p\,sl} + m_m c_{p\,m})}{2A_{sl}\Delta T}$$

where F is the heating rate (K/s), l is the specimen thickness (m), m is the mass (kg), c_p is the specific heat capacity (J/(kg·K)), A_{sl} is the cross-section area of the slug (m2), ΔT is the temperature difference between the retaining plates and the slug (K) and subscripts sl and m refer to the slug and specimen material respectively. To obtain the thermal conductivity, specific heat and density must be known.
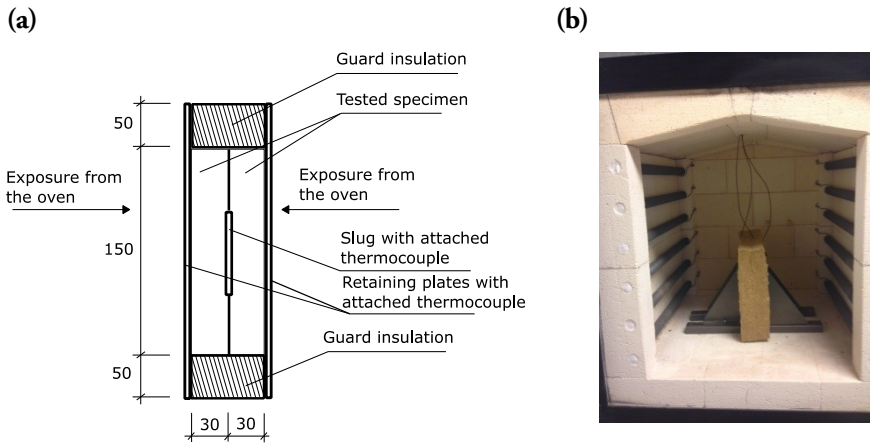
Figure 8: Custom-made slug calorimeter used in the study (a) schematic of the sample (b) photo of sample placed in an electrical oven

The slug calorimeter was chosen mostly due to its robustness and simplicity. The measurements are relatively quick, because it is not necessary to wait for a steady state of temperature distribution throughout the sample. One disadvantage of the slug calorimeter is that interpreting the results is not straightforward. For example, reactions in the material influence the measured output.

3.1.2 Thermogravimetric analysis, TGA

TGA was used to study the reaction kinetics of stone wool samples. Thermogravimetric analysis (TGA) [75] is a method for measuring specimen mass as a function of time or temperature. The specimen mass is typically 5 – 10 mg and it is exposed to a controlled temperature programme of thermal decomposition. For fire-related problems, typically a 5 – 20 K/min dynamic temperature programme is

used [76]. Due to the relatively small specimen size and slow temperature increase, it is assumed that there is no temperature gradient inside the specimen when heated. This assumption allows the separation of heat transfer and reaction kinetics. TGA can be used in different atmospheres (typically, air or nitrogen are used). The use of different atmospheres allows the identification of pyrolysis reactions from thermo-oxidative decomposition. In this thesis, TGA was used due to its widespread application in the field of fire science for studying thermal decomposition in polymers and retrieving reaction kinetic parameters for modelling polymers [8,9,77], the dehydration of gypsum plaster [66] and reactions in stone wool [78–80]. TGA was used in the appended Paper II [25] to study reactions taking place inside stone wool.

3.1.3 Micro combustion calorimetry, MCC

MCC was used to study reaction kinetics and the heat of combustion of stone wool. Micro combustion calorimetry (MCC) [81] uses oxygen consumption calorimetry to measure the HRR of specimens with mass of a few mg that are exposed to the prescribed temperature programme [82,83]. MCC consists of a two-stage reactor, where the specimen is exposed to the prescribed atmospheric and temperature conditions in one compartment and the pyrolysis gases are mixed with oxygen and combusted in second chamber. A typical temperature programme is 60 – 300 K/min. The schematics of MCC is presented in Figure 9.
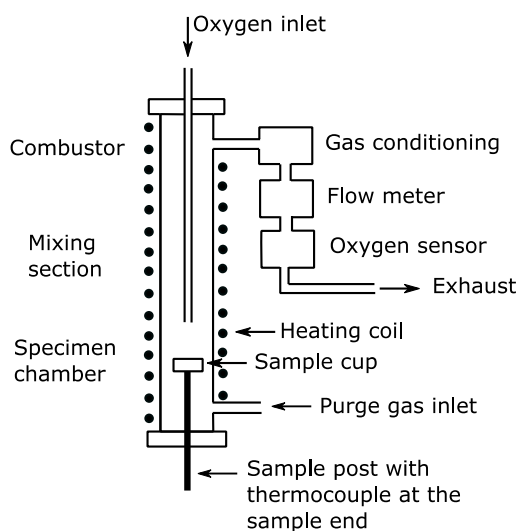
Figure 9: MCC schematics. Reproduced from reference [81]

MCC methodology allows the identification of reactions that are related to combustion (or thermo-oxidative decomposition) and in this study it was used as an alternative method to the more traditionally used TGA.

3.1.4 Bomb calorimetry

Bomb calorimetry (ISO EN 1716) [84] was used to obtain the gross heat of combustion (calorific valie) of stone wool in a pure oxygen environment. Specimens with a mass of approx. 1 g are used. The specimen is combusted under 30 bar pressure in pure oxygen inside a stainless-steel container. The released energy is obtained from the temperature increase of water in a vessel around the container.

Bomb calorimetry results in a single value, so does not provide information about the dynamics of decomposition. Also, the water generated by the combustion will condense close to the fuel due to the test setup, so the heat of condensation will be included in the measured heat of combustion [85].

3.2 Numerical Tools

3.2.1 Fire Dynamics Simulator, FDS

Fire Dynamics Simulator (FDS) software version 6.7.0 [86,87] was used to predict flame heights, surface temperatures and flow velocities for fire scenarios between two parallel walls with a separation distance of 0.04 m. FDS is a computational fluid dynamics (CFD) programme for computing low speed thermally driven flows, developed for fire safety related problems. Large eddy simulation (LES) or direct numerical simulation (DNS) approaches are implemented in FDS. In the LES approach, only the largest length scales are computed, while the sub-grid length scales are solved using sub-grid models. The DNS approach directly resolves all length scales. DNS requires very fine mesh, and therefore large computational power and time resources are required, therefore it is only practical in a very limited range of cases.

The main application area for FDS is smoke transport in fires. In this thesis, FDS was used to calculate flame heights and the thermal impact of flames and hot environments on the solid surfaces of building elements [88,89].

3.3 Data Analysis Tools

3.3.1 Functional analysis

Functional analysis is a tool for comparing two data sets. The overview of functional analysis in fire-related problems was performed by Peacock et al. [90] and, since then, it has been applied by various researchers [91–93]. The main advantage of functional analysis is its ability to quantify differences through the entire data set, not only differences in discrete values. Most commonly in this thesis, these data sets are time versus temperature output from tests or numerical models. Three parameters were used: effectively Euclidean relative distance (ERD), Euclidean projection coefficient (EPC) and secant cosine (SC).

ERD calculates the difference between the data points in two data sets. If ERD=0, then the data sets are equal. The ERD calculation is shown in Equation 19.

Equation 19: Euclidean relative distance (ERD)

$$\text{ERD} = \frac{\sqrt{\sum_{i=1}^{n}\left(T_{max,i} - T_{min,i}\right)^2}}{\sqrt{\sum_{i=1}^{n}\left(T_{max,i}\right)^2}}$$

EPC calculates the general tendency of both data sets. An EPC calculation gives an opportunity for inconsistency elimination and estimates the average behaviour of the data sets. This is valuable if one of the data sets has a high level of noise, but still results in the same mean values as the second data set – without noise. Low EPC values indicate that both data sets are equivalent. The EPC calculation is shown in Equation 20.

Equation 20: Euclidean projection coefficient (EPC)

$$\text{EPC} = \frac{\sum_{i=1}^{n}\left(T_{max,i} \cdot T_{min,i}\right)}{\sum_{i=1}^{n}\left(T_{max,i}\right)^2}$$

SC calculates the derivatives of both data sets between two data points. The SC calculation shows the overall tendencies of both data sets, but does not consider the absolute values. SC values close to unity indicate equivalent shapes of the data sets. However, as a result of the calculation procedure they can be shifted. The SC calculation is shown in Equation 21,

Equation 21: Secant cosine (SC)

$$SC = \frac{\sum_{i=s+1}^{n} \frac{(T_{max,i} - T_{max,i-s})(T_{min,i} - T_{min,i-s})}{s^2(t_i - t_{i-1})}}{\sqrt{\sum_{i=s+1}^{n} \frac{(T_{max,i} - T_{max,i-s})^2}{s^2(t_i - t_{i-1})} \sum_{i=s+1}^{n} \frac{(T_{min,i} - T_{min,i-s})^2}{s^2(t_i - t_{i-1})}}}$$

where s is a data point interval. Choosing parameter s above unity allows smoother the data sets and is useful in reducing the effect of short period oscillations. Here, $s = 1$ was used, because the data sets did not present any significant oscillations.

Functional analysis was used in Paper I to compare the model output depending on the input parameter values, and in Papers II, III and IV to compare the model predictions with test measurements.

4 Predicting the Thermal Response of Solids – Case Study of Stone Wool

The previous chapter provided a brief introduction to flame properties and thermal processes in fires. Flame characteristics are different in narrow cavities, in contrast to the previously discussed open, corner and wall configurations. Absorption of heat from the flames and hot surfaces results in a rise in material temperature, which is a fundamental driver of the material's thermal degradation [94] and decomposition [76], and, as a result, it governs material flammability, construction integrity, insulation properties and load bearing capacity. From the perspective of fire resistance and reaction to fire, it is therefore important to understand heat transfer inside solids.

After the flame enters the narrow ventilation cavity, the inner materials will be directly exposed to radiation from flame and fire induced flows. Heat transfer inside solids in context of this thesis is presented in Figure 10. This chapter presents a numerical model for calculating temperature distribution inside stone wool sample and material testing for obtaining the necessary modelling input parameters.

This chapter covers heat transfer in stone wool insulation products. Stone wool is a type of mineral wool insulation and is often used in ventilated façade systems. The two main types of mineral wool are stone wool and glass wool. The main components of mineral wool are fibres and organic binders, which hold the fibres together. Stone wool fibres are produced from volcanic rock and glass wool fibres are made from sand or recycled glass [95,96].

4.1 Problem description

Heat transfer in stone wool is complex, involving many processes that are also typical of other construction materials. Because of the large void space around the inorganic

fibres, in addition to solid phase conduction, heat transfer also includes radiation and gas phase convection in the void space [64,97]. Secondly, stone wool is relatively inhomogeneous, and therefore its thermal properties cannot be characterised with a single value, and uncertainty levels need to be understood for both the material property values and model predictions. Stone wool fibres are held together with an organic binder and include low values of other organic compounds, which generate heat when exposed to elevated temperatures. These reactions have been observed to start at approximately 200°C [78,80,98] and, as a result, the heat source term must be addressed in modelling. Stone wool is nevertheless rated as non-combustible [95], and for many practical engineering purposes it is unnecessary to consider flaming gas-phase combustion in the analysis.
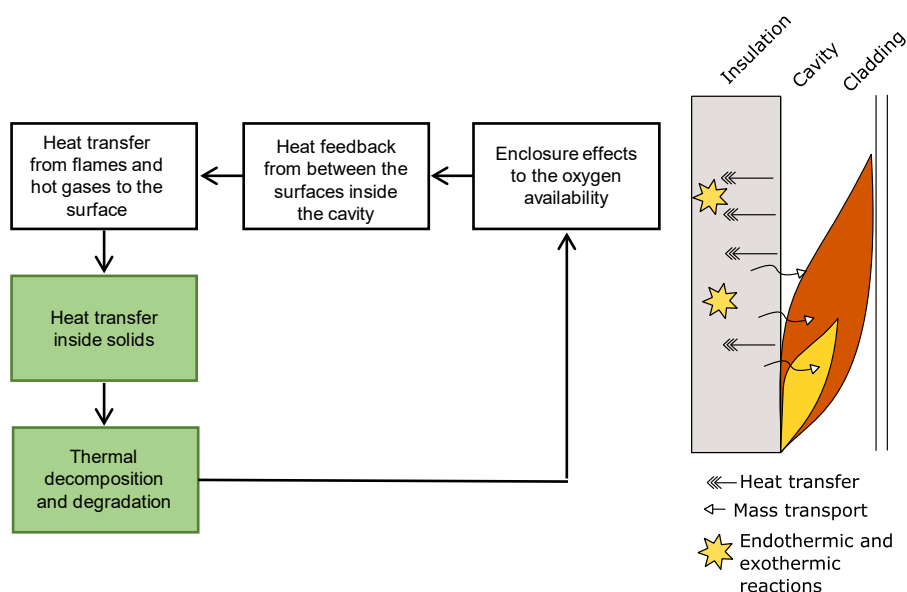
Figure 10: Processes covered in chapter 4 of the thesis

It is very difficult to account for conduction, radiation and convection modes explicitly and, for engineering purposes, they are typically lumped in an apparent (or effective) thermal conductivity k_{eff}. Obtaining the apparent thermal conductivity by material testing is relatively easy compared to obtaining the parameters needed to calculate the convection, radiation and conduction processes separately. In order to account for convection and radiation, it is expected that a detailed geometrical description of the matrix, permeability, porosity, diffusion coefficient, etc. is necessary. Using apparent thermal conductivity also allows the simplification of the heat transfer analysis for the heat conduction calculations, e.g. Equation 9.

Characterizing all heat transfer processes using only apparent thermal conductivity would create some challenges. Assuming that the apparent thermal conductivity is obtained in material testing using one heating rate, the use of this property may have limitations in different heat exposures. The potential limitation could be related to the fact that heat flux transferred by radiation is proportional to the temperature difference in the fourth power, whereas convection and conduction are linear to the temperature difference. Furthermore, convection also depends on the flow properties and material permeability (potentially influenced by fibre distribution and size), which may not be the same in different testing conditions. For example, in standard fire resistance tests, a pressure gradient of 8.5 Pa per metre over the height of the furnace is expected [99].

This chapter describes the experimental and numerical work presented in Paper I and Paper II on four different types of stone wool (referred to as types A to D). The main differences between the types were their density and organic content. An overview of the principal property values at 20°C is presented in Table 2.

Table 2: Properties of stone wool types investigated in Paper II

Material	Density*, ρ (kg/m3)	Organic content*, (%)	Thermal conductivity at 20°C, k** (W/(m K))
A	36.8±1.2	2.50±0.06	0.037
B	60.7±1.2	3.75±0.01	0.033
C	105.1±2.4	4.36 ±0.06	0.041
D	153.6±6.8	3.48±0.07	0.040

* Measured prior to testing

** Reported by the producer

Density was measured for the samples later used in conductivity measurements as a ratio of specimen mass and dimensions. Organic content was measured as a mass difference prior to and after exposing the specimens to 500°C in an electrical furnace for two hours.

Several simplifications have been included in this work. One-dimensional heat transfer analysis is performed and lumped heat capacity analysis was used of steel plates [24,25]. In some cases in the appended papers, the c_p and ρ values of stone wool have been assumed to be constants. This simplification is possible only if the property values of the temperature variations are relatively small. Apparent thermal conductivity, covering several processes, has mostly been used in this work. This also includes calculations of the heat source term $\dot{Q}_{gen}$ in Equation 9, which is important for materials that undergo exothermic or endothermic reactions.

4.2 Experimental and numerical studies – methodology and results

4.2.1 Thermal properties

The apparent thermal conductivity was obtained for four different stone wool materials using a custom-made slug calorimeter method [71,73,74]. Thermal conductivity was calculated according to Equation 18 using the temperature measurements on two sides of test sample. Specific heat capacity was assumed to be a constant value of 840 J/(kg·K) based on previous research work [100]. This value corresponds to the specific heat of basalt rock, which is principal stone wool fibre material, at 100°C [101]. Further refinement of the specific heat value would include using temperature dependent values and in cooperating the air's influence on the effective specific heat of the stone wool product. Density was calculated as a ratio of the volume and mass of each specimen. It is expected that the sample's density depends on the compression of each specimen during the measurement.

The specimens were tested in two heating regimes in custom-made slug calorimeter tests: 5 K/min and 15 K/min. Thermal conductivity was obtained only from the 5 K/min tests and was later used in numerical modelling to replicate the results of the 15 K/min tests. Hence, it aimed to show the applicability of thermal conductivity at different heating rates.

It was observed that upon the heating the temperature inside the stone wool samples (i.e. the slug temperature) increased above the retaining plate temperature (refer to Figure 8). This observation was consistent with the previous studies and attributed to the combustion of the organic content inside the stone wool [78,79]. Combustion of the organic binder is discussed in the next section. To avoid the influence of the heat generation when thermal conductivity is obtained, two heating cycles in the electrical oven were run. During the first cycle, the material went through the heat generation reactions. The first cycle was run only up to approximately 800 °C. The second cycle was afterwards used for calculating the thermal conductivity.

The apparent thermal conductivity values of the four specimens are presented in Figure 11. A noteworthy difference between this study and the previously obtained thermal conductivity is the steep increase of the calculated thermal conductivity above 800 °C. The steep rise in this research can be attributed to the exothermic reactions, that were not eliminated during the first heating cycle above 800 °C.
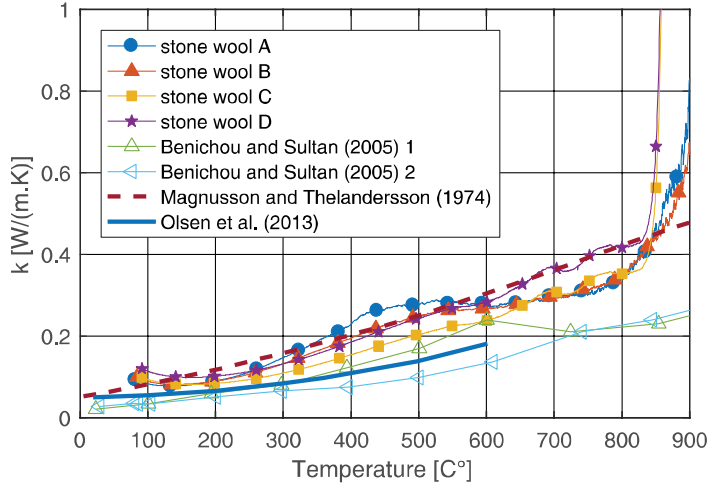
Figure 11: Thermal conductivity obtained in study in Paper II and studies by other researchers [78,102,103]

When integrated between 200°C and 800°C, the maximum difference in thermal conductivity between the four investigated stone wool types was 19%. Type D had the highest integral value and type C had the lowest value. When the mean value of all stone wool conductivity values was compared to the individual values, the maximum deviation was 20%. Nevertheless, no clear correlation is evident between the apparent thermal conductivity at elevated temperatures and the density, organic content or thermal conductivity at 20°C.

4.2.2 Heat source

On heating the slug in the custom-made slug calorimeter test, it was observed that its temperature rose above that of the retaining plate, indicating heat generation inside the stone wool. This occurred only when the stone wool was first exposed to heat and was attributed to the combustion of the organic content. This process had been observed by researchers, but it has been a challenge to account for it in numerical modelling [78,79].

The heat source term in the heat conduction equation is typically calculated using the Arrhenius equation (Equation 14) and the required input parameters are the reaction kinetic that describes the parameters of activation energy E, pre-exponential constant A, and order of reaction n, and thermochemistry describing the parameter for heat of reaction ΔH. The heat source term, previously shown in Equation 9, Equation 10 and Equation 13, represents energy input or consumption due to physical or chemical changes in the material, rather than from the external

boundaries of the material (e.g. heat flux from the fire). Thermal energy inside the material is used to decompose the material and this thermal energy therefore needs to be subtracted from the heat conduction equation. Decomposition includes material pyrolysis, the drying and release of chemically bound water, melting, etc. Similarly, some processes inside the material result in added heat to the system. For example, some porous materials are prone to smoulder and hence release combustion energy inside the material matrix. When explicitly considered, the heat source term is typically calculated using the Arrhenius equation, Equation 14,

Equation 14: The Arrhenius equation

$$\dot{Q}_{gen} = AY \exp\left(\frac{-E}{RT}\right)\Delta H$$

Reaction kinetics parameters for three types of stone wool material were obtained using TGA [75] and MCC [81]. Both TGA and MCC tests showed three identifiable reactions at temperatures that were consistent for both tests. The TGA tests were performed in air and nitrogen environments. In the air environment, TGA resulted in two positive mass loss rate peaks, followed by one negative mass loss rate peak. In the nitrogen environment, only one positive mass loss rate peak was observed. This indicated that the first reaction did not require the presence of oxygen (it could be gasification or pyrolysis) and that the second reaction was associated with the thermo-oxidative decomposition of the organic content. The third reaction was also thermo-oxidative decomposition reaction, but more research is required to analyse it. The comparison between TGA tests in the air and nitrogen environments is presented in Figure 12.
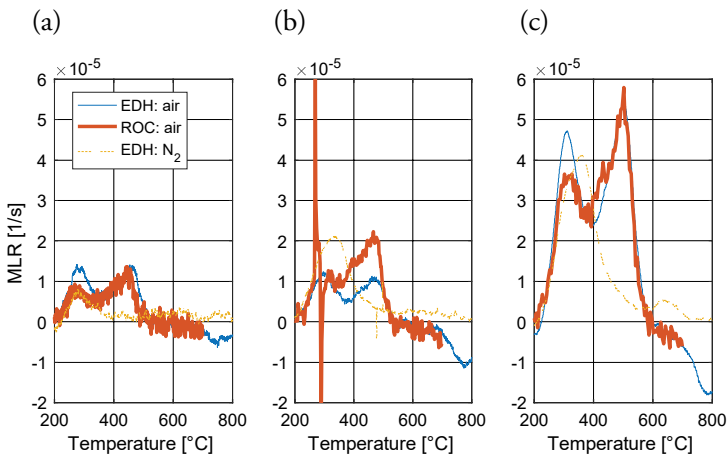
Figure 12: TGA results for stone wool A. EDH refer to the test done at the University of Edinburgh and ROC refer to test done at Rockwool International AS. (a) 5 K/min (b) 10 K/min (c) 20 K/min

MCC tests were performed in an air environment, up to 600°C. Two peaks in the rate of HRR were observed in similar temperature ranges to the TGA test [25]. Since the first reaction was observed in both TGA and MCC, the conclusion was that the pyrolysis or gasification products from the stone wool matrix were prone to combust in an exothermic reaction.

The procedure implemented in Fire Dynamics Simulator FDS [86] was used to calculate the reaction kinetics parameters from the TGA and MCC test outputs. The results are presented in Table 3. Both methods resulted in relatively similar values for activation energy, whereas the pre-exponential constants were significantly different. The TGA and MCC results are compared with the results obtained with the calculated parameters and the Arrhenius equation are presented in Figure 13 and Figure 14. The TGA and MCC tests were not performed with stone wool type C specimens due to technical issues, so these results are not presented in Table 3.

There are several differences between the TGA and MCC methods, as presented in Table 4. It is possible that both TGA and MCC provide results of limited applicability to heat source modelling. TGA and MCC are mostly associated with the creation of pyrolysis and gasification products, and neither of these methods provide information about the temperatures at which gas phase products ignite. Secondly, the influence of the transient atmospheric conditions inside a porous media cannot be captured using these tests. Furthermore, TGA requires assumptions about relation of the mass loss to the heat source, and MCC, on the other hand, does not cover heat loss due to endothermic reactions.

Table 3: Reaction kinetics parameters of stone wool

Reac.	Param.	Stone wool A		Stone wool B		Stone wool D	
		TGA	MCC	TGA	MCC	TGA	MCC
1	E (J/mol)	72.4E+3	57.3E+3	46.5E+3	59.4E+3	52.5E+3	53.0E+3
	A (1/s)	13.9E+3	4.53E+3	37.2	5.630	12.5 E+1	84.4E+1
	n (-)	1	1	1	1	1	1
2	E (J/mol)	12.2 E+4	10.3E+4	11.7 E+4	10.3E+4	14.8 E+4	13.3E+4
	A (1/s)	14 E+5	3.01E+5	44.3E+4	30.1E+4	91.3 E+6	31.0E+6
	n (-)	1	1	1	1	1	1
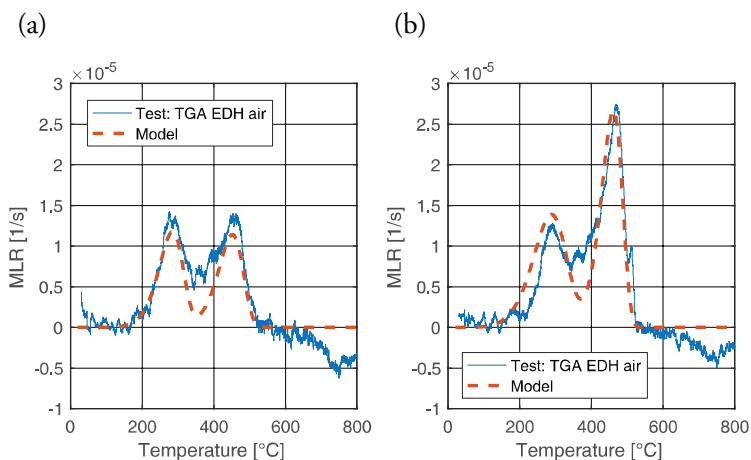
Figure 13: TGA tests (EDH) at 5 K/min and model results. (a) Stone wool A (b) Stone wool D
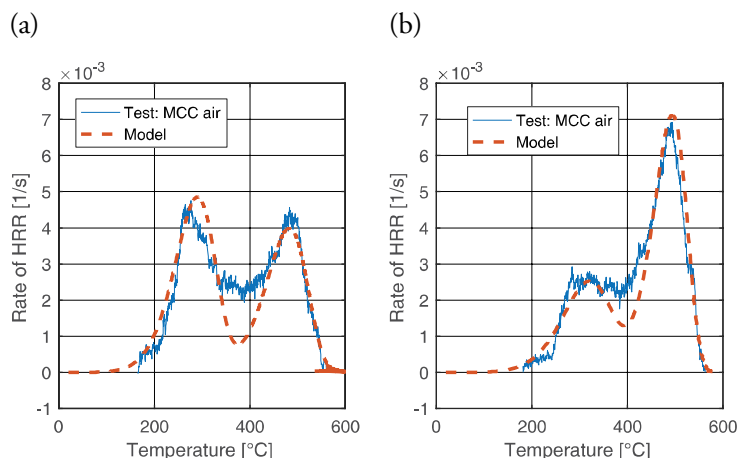
Figure 14: MCC test and modelled results (a) Stone wool A (b) Stone wool D

Both the TGA and MCC tests gave an output with a high noise level, most likely due to the low content of the reactant – organic content in the stone wool was between 2.50% and 4.37% of its mass. Therefore, the test results had to be filtered, thereby possibly reducing the precision and reliability of the micro-scale test results. In addition, the distribution of the organic content in the fibre matrix is not expected to be uniform and so negatively influenced the repeatability of the tests. The main conclusion is that testing stone wool in the presented micro scale tests has significant limitations. Testing compounds in the organic content separately is advisable, in order to avoid limitations related to the sensitivity of the testing equipment and to avoid noise.

The gross heat of combustion was measured with the bomb calorimetry method [84] and the net heat of combustion was calculated as an integral of the HRR output from MCC tests. The measured heat of combustion is presented in Table 5. The net heat of combustion showed lower average values for all tested stone wool types. Nevertheless, considering the uncertainty levels, both measurements should be considered similar. It must be noted that bomb calorimetry combusts the material in pure oxygen, hence complete combustion, and higher heat of combustion is to be expected. Nor did MCC measurements cover the third reaction above 600°C.

Table 4: Differences between the TGA and MCC test methods and implications for reaction kinetics properties

	TGA	MCC
Measured output quantity	Mass loss. Heat source is directly associated with the mass loss.	Heat release rate per unit mass of sample. Heat source does not consider reactions that do not result in oxygen depletion in the atmosphere (e.g. phase change)
Heating rate (as used in this thesis)	5-20 K/min	60 K/min. Fast heating rate may contribute to the thermal gradient in the specimen.
Specimen mass	7-14 mg	3-4 mg. Small specimen mass will decrease the thermal gradient during testing.
Combustion temperature	None	900°C

Table 5: Gross heat of combustion from three repeated tests of bomb calorimetry and net heat of combustion from MCC

Stone wool type	$\Delta H_{SW\ BC}$ (kJ/g $_{wool}$)	$\Delta H_{SW\ MCC}$ (kJ/g $_{wool}$)
A	0.89±0.03	0.84±0.26
B	0.93±0.04	0.85±0.08
D	1.07±0.03	0.93±0.33

Based on the data presented in Table 2 and Table 5, heat of combustion was calculated per unit mass of the stone wool's organic content (rather than per unit mass of stone wool) using Equation 22. The results are presented in Table 6, indicating that the heat of combustion per kg of the organic content is between 22.7 and 35.6 kJ/g. If the same organic compounds are used, the information in Table 6 allows modelling of the internal combustion effect in wools with different contents.

Equation 22: Calculation of heat of combustion per mass of the organic content

$$\Delta H_{OC} = \frac{\Delta H_{SW}}{Y_{OC}}$$

ΔH_{oc} is the heat of combustion per unit mass of the organic content (kJ/g), ΔH_{sw} is the heat of combustion per unit mass of stone wool (kJ/g) and Y_{oc} is the mass fraction of the organic content in stone wool (-).

Table 6: Calculated heat of combustion of organic content in the investigated stone wool

Stone wool type	$\Delta H_{OC\ BC}$ (kJ/g $_{oc}$)	$\Delta H_{OC\ MCC}$ (kJ/g $_{oc}$)
A	35.6±0.3	33.4±9.6
B	24.8±1.0	22.7±2.1
D	30.7±0.2	26.5±8.9

4.2.3 Numerical model

A one-dimensional transient heat conduction model, with a heat source term, was written using the Matlab® software. The thermal property values and reaction kinetics parameters, presented in the previous section, were used as the model input and the modelling results were compared to the slug calorimeter test results. An implicit formulation was used to compute the heat conduction, while the input for the heat source term was based on the previous time step. Equation 10 and Equation 14 were used as the governing equations with the specified temperature boundary condition (Equation 23) on the exposed side and the insulation boundary condition (Equation 24) on the 'unexposed' or slug centreline side.

Equation 10: One-dimensional transient heat conduction with source term

$$\rho(T)c_p(T)\frac{\partial T}{\partial t} = \frac{\partial}{\partial x}\left(k(T)\frac{\partial T}{\partial x}\right) + \dot{Q}_{gen}{}'''$$

Equation 14: The Arrhenius equation

$$\dot{Q}_{gen} = AY\ exp\left(\frac{-E}{RT}\right)\Delta H$$

Equation 23: Specified temperature boundary condition

$$T_{x=x_0} = T_{exp}$$

Equation 24: insulation boundary condition

$$\dot{q}_s'' = 0$$

The slug temperature was calculated using the lumped thermal capacity simplification, as presented in Equation 12. The governing equation was discretized with the finite difference method and was solved with the iterative Jacobi method. Each time step was iterated until the sum difference of the temperature calculations between the previous and ongoing iteration was less than or equal to 0.05 K. Modelling was performed for both heating cycles of the custom-made slug calorimeter test. Modelling of the first cycle included the heat source term (Equation 14), while the second heating cycle, in which the material had already undergone reactions up to 800°C, was modelled without the heat source.

Modelling the second heating cycle resulted in very good fit with the experimental results (refer to paper I in the appendix), both for 5 K/min and 15 K/min heating rates. This result indicated that the thermal conductivity obtained at 5 K/min was reasonably valid for predicting the temperature distribution also in heating rates up to 15 K/min. The results of the first heating cycle (including the heat source) are presented in Figure 15 and Figure 16. The model overpredicted the maximum slug temperature during the exothermic peak in all cases. Results for stone wool A and B are somewhat comparable between the test and model. Using kinetic parameters that were obtained from TGA data resulted in slightly better predictions for stone wool type A and B, compared to when using parameters from MCC data. The maximum temperature percentage difference between the test and model was 25 % and 35 %, when kinetic parameters from TGA data were used. As shown in Figure 16, modelling the stone wool D, resulted in very high temperature peak overshoot, whereas the experiments showed a moderate temperature increase lasting for a long time.
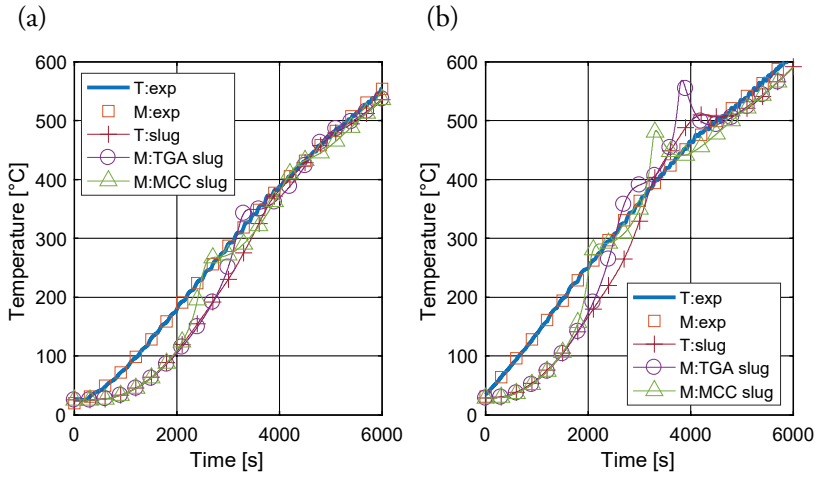
Figure 15: Test and model prediction of the slug's temperature, placed between the stone wool specimens in the custom-made slug calorimeter test. M refers to model predictions and T refers to test results (a) stone wool type A (b) stone wool type B
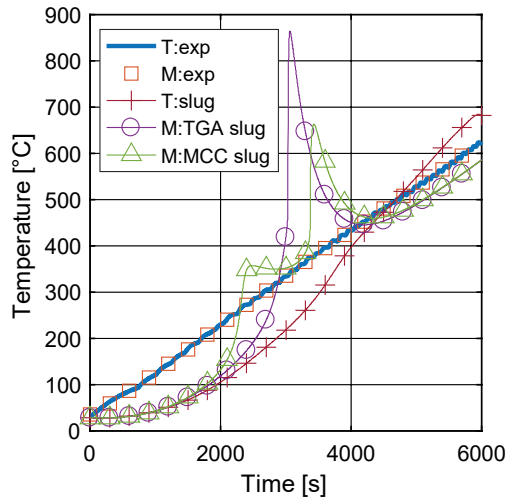
Figure 16: Test and model prediction of the slug's temperature, placed between the stone wool specimens in the custom-made slug calorimeter test. M refers to model predictions and T refers to test results. Stone wool type D.

4.3   Model sensitivity - methodology and results

The model input parameters can be divided into material properties and the boundary condition describing parameters, as presented in Table 7. The previous sections only covered material properties.

Table 7: Modelling input parameter categories and examples relevant to this thesis

Input parameter category	Input parameter example
Material properties	Thermal conductivity, density, specific heat, pre-exponential constant, activation energy, order of reaction,
Boundary condition describing parameters	Surface emissivity, surface absorptivity, convective heat transfer coefficient, ambient gas temperature, incident radiation heat flux

One challenge in material modelling is defining the values of these input parameters. It is often challenging to define a single reliable value. Uncertainties about material properties, for the same group of materials, can expected due to:

- Wide variety of commercially available materials (even within the same family of materials), with slight differences in chemical composition and physical structure;

- Inhomogeneity of typical construction materials;

- Limitations and uncertainties of methods used to obtain these properties.

Uncertainties in boundary condition describing parameters are expected due to:

- Limitations and uncertainties of methods used to obtain these parameters;

- Simplifications and approximations in physical analysis and modelling work (e.g. the use of empirically based convective heat transfer coefficient or grey body approximation).

All these uncertainties in the model's input will result in uncertainty in the model's predictions. Modelling results will have a different level of be sensitivity to each of these parameters.

If the uncertainty limits can be described, sensitivity analysis is a useful approach for quantifying intervals in the expected results. Paper I presents a global and local sensitivity analysis of the temperature predictions for the unexposed surface of a sandwich construction exposed to the standard ISO 834 cellulosic fire curve. It is important to note that these conditions are not the same as presented in the previous section and did not include reaction kinetics inside the stone wool. Nevertheless, the methods presented in this section are applicable to any exposure conditions.

Global sensitivity was investigated by performing Monte Carlo simulations, with several parameters varied at the same time. The parameter values were randomly chosen from set minimum and maximum values, as presented in Table 8. The 'unifrnd' function in Matlab® was used to generate the random values of the input

parameters. This function returns numbers from a continuous uniform distribution with prescribed upper and lower endpoints. In the local sensitivity study the parameters were varied individually to the minimum and maximum values. The resulting curves were evaluated based on functional analysis [90]. Different thicknesses of stone wool between the steel sheets were investigated: 0.01 m, 0.05 m and 0.1 m. It was shown that the model's sensitivity to the input parameters depend on the thickness of the construction. 0.05m and 0.10 thick stone wool is realistic for fire separating constructions, whereas 0.01m stone wool would not be enough to reach the minimum fire resistance classification ranking. The modelling input parameters used in this study were partly based on testing presented in Paper II or gathered through literature research and are presented in Table 8.

Table 8: Chosen parameters as used in Paper I for the sensitivity study

		Reference value (most probable)	Min value	Max value	Value probability distribution
Exposed surface boundary conditions	h (W/m^2/K)	25	20	60	Uniform
	ε (-) and α (-)	0.9	0.8	1.0	Uniform
Unexposed surface boundary conditions	h (W/m^2/K)	4	4	10	Uniform
	ε (-) and α (-)	0.65	0.55	0.75	Uniform
	k (W/m/K)	Figure 17 (based on paper II)			Uniform
Stone wool material properties	c_p (J/kg/K)	840	756	924	Uniform
	ρ (kg/m^3)	105	103	107	Uniform

The results of the local sensitivity analysis, in form of functional analysis parameters ERD, EPC and SC are presented in Figure 18. The functional analysis concepts are previously presented in chapter 3. ERD values close to 0 and EPC and SC values close to 1 represent a close fit between the two compared data sets (two sets of temperature predicted by numerical model in this case). As presented in Figure 18, for stone wool thicknesses of 0.05 m and 0.1 m (representing realistic thickness for thermal insulation in real life constructions) the investigation concluded that, from the thermal properties, the model is the most sensitive to the thermal conductivity and then to the specific heat capacity. The influence of the convective heat transfer coefficient on the unexposed surface is significant, especially as the thickness of the stone wool increases. Nevertheless, h_{cold} only seems to be significant for the ERD and EPC parameters and is relatively less sensitive to the SC parameter.
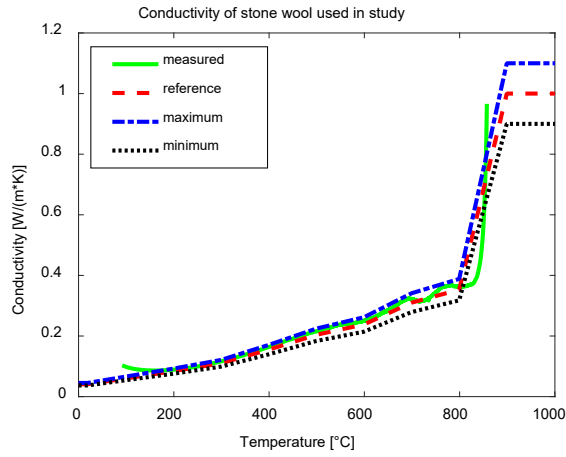
Figure 17: Thermal conductivity values used in Paper I
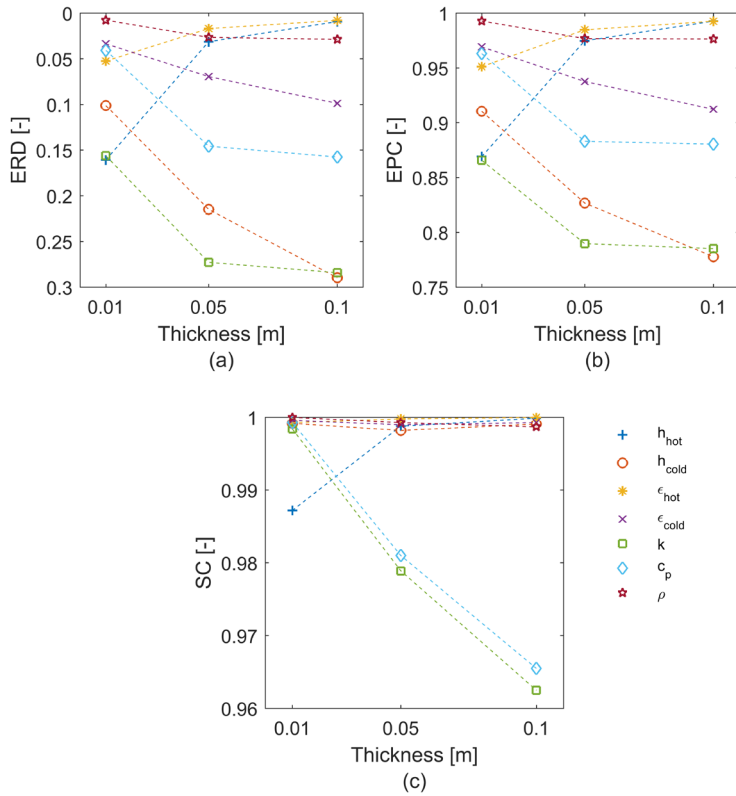
Figure 18: Calculated ERD, EPC and SC values for stone wool and boundary properties in standard fire resistance tests. Notice the differences in the y axis between the subplots

Figure 18 also shows that for narrow constructions (0.01 m), the processes at the exposed surface, as described by emissivity and the convective heat transfer coefficient ε_{hot} and h_{hot}, play more significant role. In fact, for a 0.01 m construction, the model is the most sensitive to the convective heat transfer coefficient at the exposed surface. This can be explained by a) high uncertainty in the h_{hot} values as presented in Table 8 and b) early failure times for this thin construction. Due to the early failure, the exposure temperatures are still relatively low and heat transfer to the surface may be more governed by convection, rather than by radiation.

The model's sensitivity will depend on the value limits set for the input parameters. Lowering the uncertainty levels for one parameter would result in this parameter having less influence on uncertainty. It is therefore necessary for sensitivity studies to be constantly updated, based on the studied materials and improved material property test methodologies, which will reduce these uncertainties.

4.4 Summary

This chapter presented a case study the focuses on obtaining thermal properties and using them as model input parameters to predict the temperature field in stone wool, based on findings presented in Paper I and Paper II.

The thermal conductivity of four types of stone wool was obtained using a custom-made slug calorimeter test, assuming a constant specific heat capacity of 840 J/(kg·K) and constant density, depending on the type of stone wool. Two heating cycles were performed to separate the exothermic/endothermic reactions from the heat transfer inside the stone wool. Two heating rates of 5 K/min and 15 K/min were used and the obtained thermal conductivity from the lower heating rates applicability to predictions of higher heating rate was studied. TGA and MCC tests were performed to obtain the kinetic reaction parameters for solving the heat source term. Bomb calorimetry and MCC were used to obtain the gross and net heat of combustion. Monte Carlo and functional analysis methods were presented to study the model sensitivity to the uncertainties of input parameters.

The conclusions from this work include:

- The custom-made slug calorimeter provided a simple, yet sufficiently precise method for measuring the effective thermal conductivity of a wide range of stone wool materials. The products should be pre-heated and studied without the organic content. Further improvements could be made

by using more accurate cp values (e.g. obtained with DSC test result analysis);

- The temperature distribution in low density and low organic content stone wool products was predicted with relatively good accuracy. The maximum temperature difference in modelled slug calorimeter tests was 35%, using the kinetic parameters from TGA;

- Predicting the temperature distribution in high density and high organic content stone wool was not done with sufficient accuracy;

- To improve temperature distribution predictions, more knowledge of mass diffusion in stone wool is needed to account for the local oxygen levels and movement of gas phase organic content products. In the conventional test methods for studying the reaction kinetics, TGA and MCC, it is difficult to account for the transient oxygen levels that are expected in real life configurations;

- The TGA and MCC tests resulted in a high noise level. The suggestion is that the organic content should be investigated separately, without the stone wool fibres. However, the products are typically only commercially available in their end form;

- The heat transfer model is the most sensitive to the uncertainties in stone wool thermal conductivity, followed by uncertainties in the specific heat capacity. In standard fire resistance testing, another parameter to which the model is sensitive, is the convective heat transfer coefficient on the unexposed surface.

5 Solid Surface Recession

The previous chapter discussed heat transfer in solids exposed to heat flux, representative of fire conditions. This chapter adds to the previous discussion by explicitly covering materials' morphological and shape changes when exposed to heat. A material's morphological changes and deformations in fire conditions create challenges for material testing and modelling. Morphological changes in the fuel occur as it is consumed by fire or during thermal degradation and decomposition. It can also be caused by be shrinking due to moisture loss, melting and dripping or volume increase due to chemical reactions. The problem of a material's morphological and shape changes in the context of cavity fire behaviour is presented in Figure 19. As shown by the green box in Figure 19, the morphological changes are related to the thermal decomposition and thermal degradation induced by heat transfer in the decomposing materials. Thereafter, material shrinkage influences the width of cavity in which the burning takes place. Furthermore, many shrinking and melting materials are also prone to burning, therefore decomposition, shrinking/melting and fire spread are coupled processes.
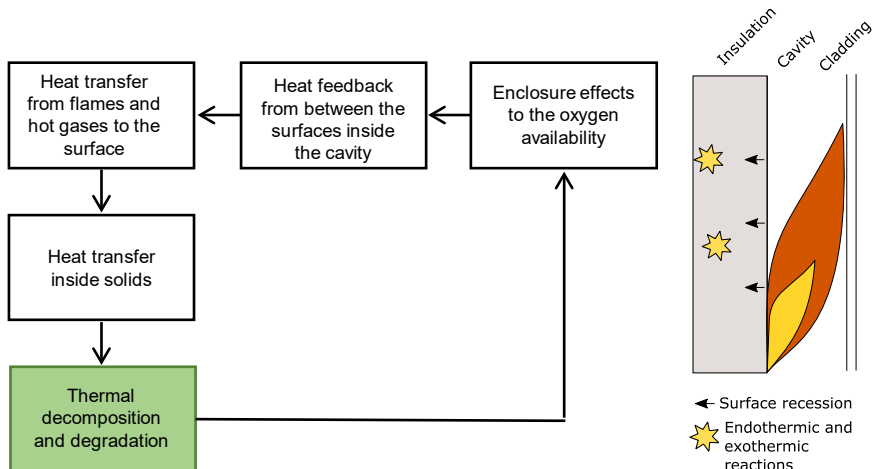
Figure 19: Processes covered in chapter 5 in the overall thesis

5.1 Problem description

Some materials that undergo significant volumetric changes when exposed to heat include expanded polystyrene EPS [23,104–108], extruded polystyrene XPS, flexible polyurethane foams FPUF [9,109–111], glass fibre insulation [68,94,102]. EPS, XPS and glass fibre insulation are widely used as insulation products in construction and in façade systems. The importance of EPS' shrinking and melting behaviour is recognized, e.g. in ETICS façade systems [112]. This chapter focuses on development of a new test method and uses EPS and FPUF as example materials.

EPS is a rigid, moulded bead foam based on a polystyrene polymer. EPS is an thermoplastic, therefore after reaching a critical temperature it softens and loses its bead structure, and melts [104,108]. Melted EPS hardens again during cooling. EPS is used as a core material in sandwich panels and structural insulated panels, and the fire-related risks due to its flammability, melt and melt flow properties are critical [107,113]. EPS is observed to shrink in temperatures around 100 °C or when exposed to heat fluxes as low as 2 kW/m^2 [23,104–108]. It has been noted that the initial shrinking is due to the material's loss of structure, and glass transition and melting occur at higher temperatures [106]. EPS is used as thermal insulation in ETICS façade systems and structural insulated panels [107,113]. In addition to recession of the exposed surface, EPS is prone to forming flaming droplets that pose significant risks of fire spread.

FPUF foam is an open cell thermoset polymer foam and its main components are polyol and isocyanate. Under heat exposure it decomposes into gas and semi-liquid products [8]. The term 'collapse' is sometimes used to denote the process of rapid shrinking and loss of structural stability [110]. PU foams are also prone to smouldering [114]. Flexible polyurethane FPUF is observed to collapse when exposed to heat, and the materials' morphological changes significantly influence their burning behaviour [9,109–111]. The collapse is explained by thermal decomposition – the loss of isocyanate leaves polyol in a 'semi liquid' form. Studying flexible polyurethane in TGA allows a distinction to be made between two reactions; the first starts at around 200 °C and can be linked to the decomposition that results in collapse [9,109].

EPS and FPUF were chosen for this study because of the relatively different characteristics of these materials. Other shrinking materials include glass fibre insulation at approximately 500°C – 800°C, and rock fibre insulation, which melts at higher temperatures [68,94,102]. Furthermore, thermoplastics are prone to melting and the melt flow drives the fuel away from the heat source. Nevertheless,

the most obvious example of surface recession is the consumption of the solid by the fire or 'burn away', to which all combustible materials are exposed to during fire.

Reduction of the effective solid volume or mass, when exposed to heat, introduces several problems. In most reactions to fire tests a fixed position heat source is used and the incident heat flux to the surface of the tested material depends on the distance between the heat source and the receiving surface. If the material surface recedes during the test, it can be argued that the testing methodology is not consistent between morphologically non-stable and stable materials. An example of such a typical reaction to fire test is the cone calorimeter test [115]. Studies have shown that the incident heat flux reduces in the cone calorimeter as the distance from the cone heater increases, and this reduction percentage depends on the cone heater's output [116–118]. Similarly, in material modelling, changes in the form of the burning item will influence the boundary conditions of the exposed surface and the changing volume and mass will influence heat transfer inside the material.

Building products rarely consist of a single material. Usually, materials are used in combination to ensure the end-product utilizes the beneficial properties of each material. Materials ensuring the thermal insulation of the construction are typically those prone to morphological changes and are used as the core material and protected from the external environment with other materials. Examples of such constructions are:

- Sandwich panels composed of a steel skin and a polymeric or mineral fibre core;

- Polymeric insulation protected by cladding in façade systems;

- ETICS façade system with render that protects polymeric insulation;

- Gypsum and mineral wool insulation separating elements.

This will have implications both if a fire becomes established in between the material layers and if the heat exposure comes from the exterior of the construction. Change in the solid material's volume will advance the widening of the cavity between the material layers, which will further influence fire dynamics in a cavity fire scenario. The change in the solid material's volume will influence the heat transfer processes inside the construction system and the transition from solid phase heat transfer (described by the effective thermal conductivity) and gas phase heat transfer modes (radiation and convection). To predict the fire performance of products composed of such morphologically unstable materials, it is important to understand the nature of the morphological changes and their rates of development in various heating conditions.

Attempts at numerical modelling for melting or burn away have been done for fire situations, with the resulting models being complex and thus of limited practical applicability [119,120]. The development of new testing tools and establishing simple empirical correlations, on the other hand, may result in the development of simplified modelling approaches.

5.2 Methodology

This research examined the rate of material surface recession and the critical temperature at which it starts to recede in contact with a hot surface. A novel method was proposed, with a test setup based on the ISO 5657 ignitability test apparatus [121] and presented in Figure 20.

(a)

(b)
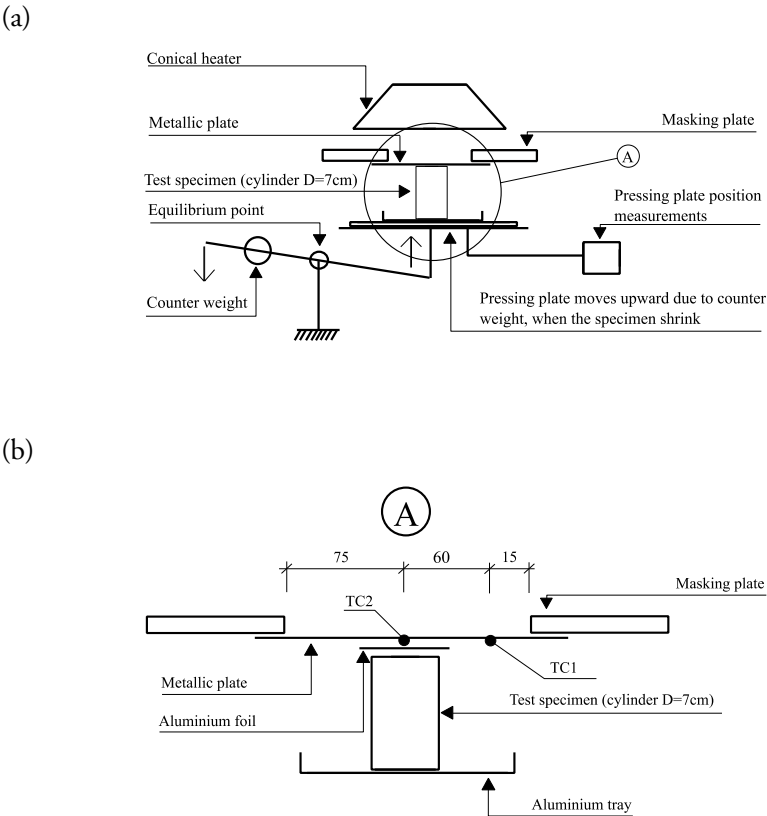
Figure 20: Schematic of material surface recession test (a) test apparatus (b) specimen position. Dimensions in mm

The ISO 5657 ignitability test apparatus consists of a conical heater and the test specimen being fixed between the pressing and masking plates. The force required to fix the specimen in position is provided by a counterweight that pulls down a steel rod on the opposite side of a supported equilibrium point. For the purpose of this study, the ignitability test was modified to measure material shrinkage during exposure to heat. A metallic plate (aluminium or stainless steel) was placed between the specimen and masking plate. In this arrangement, the metallic plate was exposed to the heat flux from the conical heater and transferred the heat to the specimen surface by conduction. As the critical temperature for recession was reached and the material begun to shrink, the pressing plate started to move upwards. The shrinkage rate was measured with the Temposonics® E-series magnetostrictive position meter attached to the pressing plate. A type-K thermocouple was placed between the test specimen and the metallic plate, to measure the critical temperature at which the material starts to recede. Another type-K thermocouple was fixed to the unexposed surface of the metallic plate; this was used to monitor the exposure and keep it constant during the tests. Figure 21 is a photo of the test setup. The setup is explained in more detail in the appended Paper III [23].

Two sets of tests were performed in this study. During the first set of tests, materials were tested in five different temperature regimes to evaluate the test's repeatability and the material's response to heat. Three repeated tests were done for each temperature regime in the first set of tests. During the second testing programme, the methodology was further investigated in detail by assessing the results' sensitivity to the pressure from the metallic plate being applied to the test specimen's exposed surface.

The specimen is fixed between the pressing plate and the metallic plate (there is no specimen in this image). The conical heater provides heat to the metallic plate.

The counter weight presses upward on the pressing plate. The pressing plate presses the specimen to the metallic plate and hence the specimen is fixed in the position.

The position meter is located next to the apparatus.

Position meters wire is attached to the pressing plate. It measures the distance the pressing plate moves upwards as the test specimen shrinks.

Figure 21: The ISO 5657 ignitability test and its modification for the purpose of measuring material recession rates

Commercially available non-fire retarded EPS and FPUF specimens, cut in a cylindrical shape with a diameter of 0.07 m and a height 0.048 m, were used. The used materials are presented in Table 9.

Table 9: Materials used in preliminary shrinkage tests

Material	Measured density [kg/m3]	Specimen size diameter × height [m × m]	Notes
EPS	26	0.07×0.048	Commercially available. Non-fire retarded.
FPUF	23	0.07×0.048	Commercially available. Non-fire retarded.

5.3 Results

The results of average recession rates as a function of exposure temperature during the first set of tests are presented in Figure 22. Polynomial fits were calculated and the coefficients are presented in Table 10. EPS was observed to start receding at temperatures between 140°C and 170°C. The FPUF started to recede when exposed to 260°C to 290°C. The tests showed good repeatability and polynomial fits with R^2 above 0.98 were obtained for both materials.
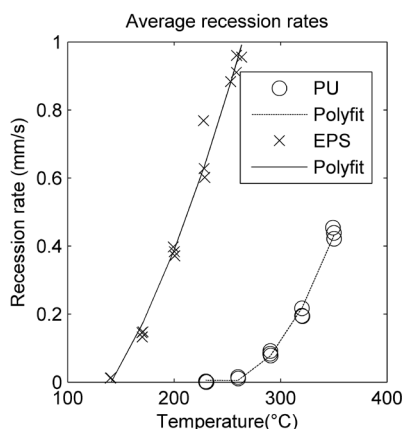
Figure 22: Surface recession rate when exposed to a hot metallic plate at different temperatures

Table 10: Polynomial fitting coefficients for p(x)=A*x2+B*x+C

Material	A	B	C	R2
EPS	2.39e-05	-0.0015	-0.2517	0.986
PU	3.96e-05	-0.0194	2.3809	0.993

60

During testing it was noticed that the thermocouple temperature between the metal plate and the FPUF specimen (see TC2 in Figure 20) increased above the monitoring temperature (TC1 in Figure 20). This was not observed when testing EPS and it indicated exothermic reactions in the FPUF specimen. Exothermic reactions in FPUF may therefore influence the recession rate beyond the exposure from the test apparatus and make it difficult to interpret the results.

The second set of tests was done to investigate the influence of the applied pressure from the pressing plate on the test results. The pressure changed as the counter-weight moved relatively to the equilibrium point. Depending on the counter-weight's position the pressure was assessed as changing from approximately from 4.2 kPa to 7.2 kPa. Results showed that EPS is relatively insensitive to the different applied pressures with a recession rate increase of 12 % at the highest mechanical pressure. On the other hand, FPUF had a 136 % increased recession rate.

Figure 23 and Figure 24 present the test specimens after testing. Discolouration of the exposed surface can be seen on the FPUF specimens, indicating a smouldering reaction. The EPS specimens are characterized by a distinct melted/hardened zone on the exposed surface. Typically, the beads forming the EPS structure were intact below the melted material zone.

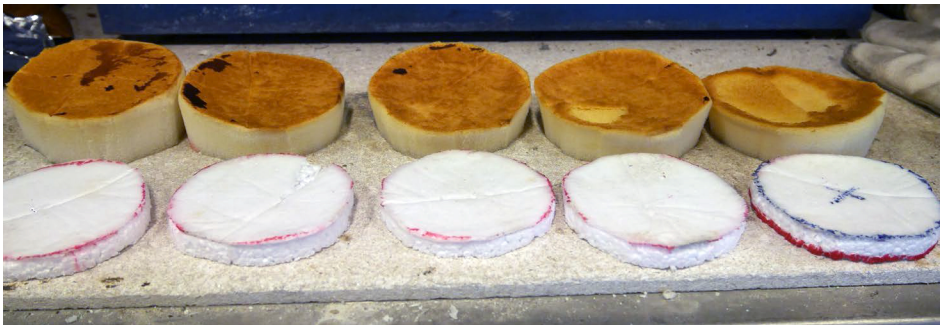**Figure 23:** Test specimens after recession rate testing. FPUF specimens in the top row and EPS specimens in the bottom row

Figure 24: Close-up of an EPS specimen after the test

5.4 Summary

A methodology for studying material surface recession due to heat exposure was proposed and described in this chapter. The material's shape change, such as shrinkage and melting, but also expansion, is an expected behaviour that could influence the geometry of narrow construction cavities. Depending on the process, the cavity can either increase in width or become narrower, thereby influencing the fire dynamics, as discussed in the appended Paper IV and Paper V and in the following chapter of this thesis.

The method presented here was based on standard ignitability test apparatus. The purpose of such testing would be to rank materials based on their shape stability when heated and to suggest empirical correlations for recession as a function of exposure for modelling purposes. The test's repeatability and sensitivity to the counterweight's position were investigated along with the recession behaviour of the EPS and FPUF specimens.

Significant recession in EPS was observed at temperatures between 140°C and 170°C. Flexible PU foams started to recede when exposed to 260°C to 290°C. The proposed test methodology had good repeatability, with up to 24% difference for EPS and 16% difference for FPUF during periods of significant recession (i.e. excluding low exposures when very slow or no recession was observed). The results had bad repeatability for PU foams at relatively low temperatures when the foam only just started to recede (approximately 230°C for FPUF).

Repeatability is influenced by several factors, which should be further investigated: the inhomogeneous structure of materials; deviations in temperature of the metallic plate's temperature; slight variations in the specimen's dimensions; and variations in cooling conditions around the perimeter of the specimen. Further investigations should include discussion of the boundary condition around the perimeter of the sample. FPUF proved to be sensitive to the applied mechanical pressure due to its flexible characteristics, hinting at a potential challenge when dealing with flexible materials.

Temperature runaway was observed for FPUF samples at the interface between the specimen's surface and metallic plate. This behaviour creates challenges for the interpretation of the results. Specifically, whether the temperature increase on the surface should be considered as the material's response or whether the interface's temperature change should lead to adjusting (i.e. lowering) the exposure during the test. The answer depends on the purpose of the testing. If the test data is to be used in mathematical modelling that explicitly calculates for heat source due to

exothermic reactions, the suggestion is to adjust the exposure from the conical heater during the test to compensate for the heat generation in the sample. If, however, the testing is for ranking purposes, the exposure from the test should be kept constant independently of the material's response to it.

The suggested test methodology provides only a one-dimensional case, with the main heat transfer and resulting recession in one direction only. In real-life fire conditions, the exposure would not be uniform across the fuel bed – local areas of high temperature are expected due to local flame attachment to the surface, as shown in Figure 19. The applicability of the derived recession rate correlations (Figure 22 and Table 10) should therefore be sought in two or three-dimensional test arrangements. Furthermore, in a realistic fire situation, the exposure would be due to radiative and convective heating, rather than conduction from a hot object, as presented here. Numerical modelling of deforming materials is a challenge and should be improved for fire-related problems.

6 Fire-Induced Flow in Narrow Air Cavities

Previous chapters discussed material responses to heat exposure in fire conditions. The heat exposure from fires in narrow cavities is discussed in this chapter. Furthermore, the influence of the cavity's dimensions on flame heights and upward flows was studied as part of this research. Flame heights are of interest, because they influence the area subjected to direct flame contact, and fire-induced flows influence heating by convection. The problem of flame characteristics and fire-induced flows in narrow spaces in the context of this thesis is presented in Figure 25. As shown by the green boxes in Figure 25, the cavity's geometry influences the air supply that is available to support combustion, as well as the flow characteristics that can determine the shape of the flame. The heat transfer in a narrow space is also influenced by thermal feedback between the boundaries of the cavity.
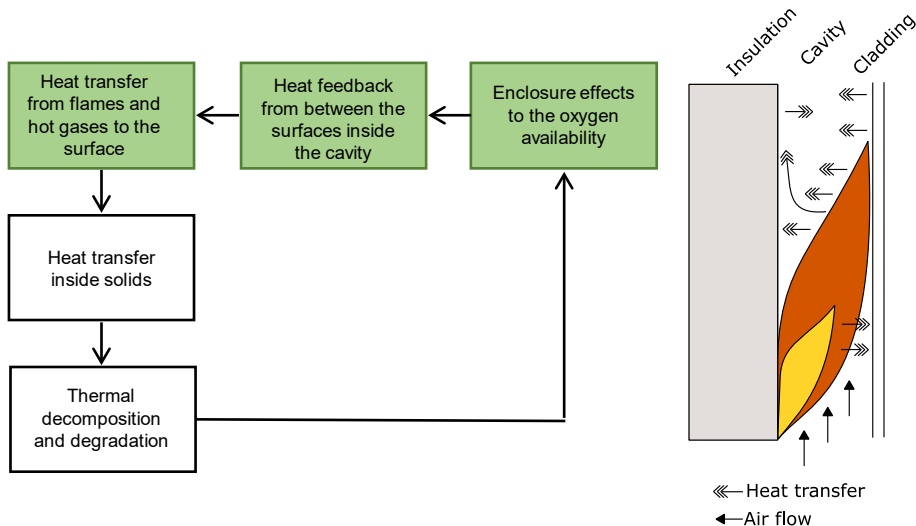
Figure 25: Processes covered in chapter 6 in the overall thesis

6.1 Problem description

It is recognized that the fire dynamics are influenced by the physical obstructions surrounding the burning item. Senez et al., and Johansson & van Hees proposed dividing building fires into groups based on the proximity of physical obstructions: fires in structural elements (or fires in concealed spaces), compartment fires, and fires in large enclosures (or exterior fires) [27,32,122]. Compartment fires and fires in large enclosures have traditionally been the main focus of fire safety engineering and science. A typical example of fires in structural elements (e.g. inside walls, roof constructions) is fire spread inside narrow cavities between the construction elements or material layers. Fires in structural elements are more difficult to observe during fire accidents, compared to external flaming, for example, but can potentially lead to fire spread between compartments, or the re-emergence of a fire after it was thought to be extinguished. The issue of fires in structural elements and cavity fires is recognized [32,123–125], but there is still a considerable lack of knowledge about the conditions that influence fire dynamics in narrow spaces. Although this thesis applies to façade ventilation cavities, the findings of this work can be more generally used in other fire situations in structural elements. The dimensions of real-life structural elements are in the order of several metres and above. Real life façade systems are particularly large as they cover the entire boundary of a building. The research presented in this thesis, nevertheless, is done using simplified constructions with reduced dimensions to capture the fundamental principles of the studied processes.

It can be suggested that more tightly enclosed fires are more likely to be controlled by the air inflow. The chimney effect in a construction's vertical narrow spaces will therefore play a significant role in fire dynamics, flame shape and heat transfer. Various studies and observations have shown that the flames extend and the heat fluxes to the surface increase as cavity width (the distance between the enclosure boundaries) is reduced [18,52].

An experimental study was performed as part of this research, to develop a correlation between the flame height and incident heat flux to the surface as a function of the cavity's width. Thereafter, FDS simulations were performed to assess its capability to produce accurate predictions of flame heights and exposure conditions in a cavity arrangement.

6.2 Experimental study – methodology and results

6.2.1 Methodology

An experimental programme was performed to study the influence of the distance between two parallel facing walls on flame heights and heat fluxes between these walls.

The experimental setup consisted of two parallel facing calcium silicate boards (thickness 20 mm), lined with a ceramic insulation layer (2 mm). A propane burner, with a gas outlet area of 8 × 391 mm, was placed between the walls, next to one of the walls (referred to as 'near wall'). The burner opening included a metal grid to redistribute the gas flow over the outflow area. The experimental setup is presented in Figure 26.
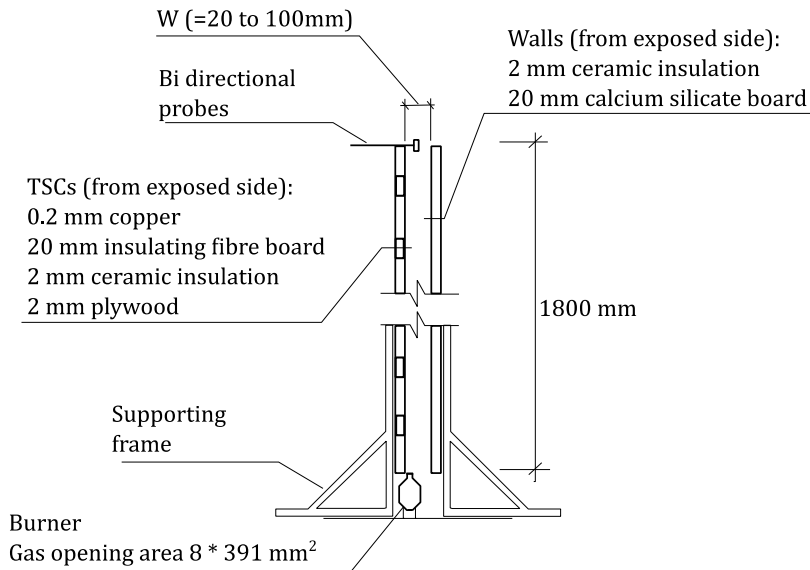
Figure 26: Experimental setup used to study flame heights between parallel plates

The experimental programme consisted of tests with two varied parameters: the distance between the walls (W) and the propane gas mass flow rate. In individual tests, the distance between the walls varied between 2 and 10 cm. Additional tests with only one wall were performed (referred to as 'one-wall' tests). Four different gas mass outflow rates were used with a resulting target HRR between 6.5 kW and 15.8 kW. This HRR output is referred to as 'target HRR' because up to 10% deviations in actual propane mass flow rate during and between the tests were observed and

67

because the actual HRR was not measured as part of the experimental programme. In total, 77 tests, including repetitions, were performed. In most cases three repeated tests were performed for each experimental arrangement. The overview of the experimental programme is presented in Table 11. The main differences to previous research [52,53] into similar fire scenarios were the narrower cavity width and the different burner location in this study.

Table 11: Summary of tests in parallel wall experimental programme

Experimental series	HRR (kW/m)	HRR (kW)	W, m
I	16.5	6.5	0.1, 0.06, 0.05, 0.04, 0.03, 0.02, one wall
II	24.8	9.7	0.1, 0.06, 0.05, 0.04, 0.03, 0.02, one wall
III	32.3	12.6	0.1, 0.06, 0.05, 0.04, 0.03, one wall
IV	40.4	15.8	0.1, 0.06, 0.05, 0.04, one wall

The three main measured parameters in the study were visual flame heights, exposure to the near wall and vertical flow velocity. Flame heights were measured with visual observations from 30 photos taken during each test. The photos were taken at one second intervals, resulting in the 30-second average flame height. Only the main body of flame was considered in the analysis (detached flames were ignored). Exposure to the near wall was measured with custom-made thin skin calorimeters, TSCs. The TSCs were composed of a type K thermocouple welded to a thin copper disc with diameter of 4 cm. The disc was insulated on the back and the TSC was mounted in a round hole drilled in the near wall. The TSCs measured the transient temperature of the exposed copper disc. The heat transfer from a hot environment to such devices is summarized by Ingason & Wickström [126]. For the purpose of this study, the incident heat flux was used as parameter to characterize the exposure, consisting of absorbed incident radiation and convective heat exchange on the surface of the copper plate. The incident heat flux is defined as presented in Equation 25,

Equation 25: Incident heat flux at the surface

$$\dot{q}''_{inc} = \alpha\, \dot{q}''_{inc\,r} + h(T_g - T_s)$$

where α is the absorptivity (-), h is the convective heat transfer coefficient (W/m2K), T_g is the surrounding gas temperature and T_s is the surface temperature.

To relate the measured TSC temperature to the incident heat flux, a heat transfer model with FEM was used. Specifically, back calculations were performed to calculate the required incident heat flux to atchieve the measured TSC temperature.

In addition, vertical flow velocity at the top of the setup was measured with bi-directional probes with diameter of 0.016 m [127].

6.2.2 Results

In Figure 27 and Figure 28 the resulting flame heights are compared with the studies by Karlsson et al. [52], Ingason [53] and Hasemi & Nishihata [44]. It was observed that flame heights increased as the distance between the parallel plates was reduced. It must be noted that, in some cases, the flames in one wall configuration were observed to be taller than in the widest investigated cavity. This can be seen in Figure 28.
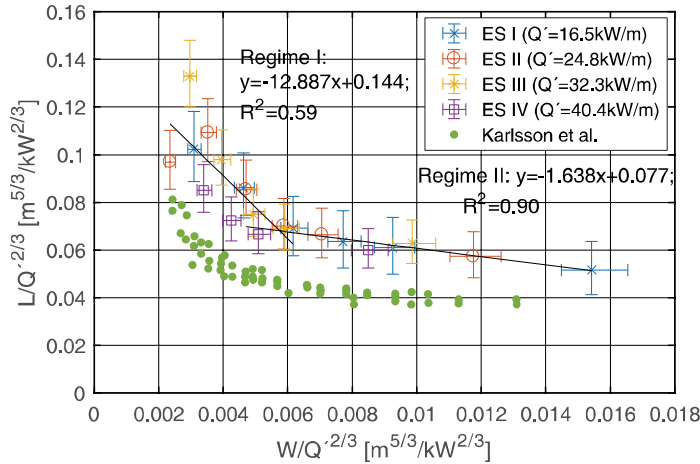
Figure 27: Average flame heights from this study (excluding one wall tests) and the study by Karlsson et al. [52]

Comparing the flame heights for when the burner is located next to a single wall and an arrangement with a 0.02 m cavity, the maximum observed flame extension was 2.2 times. Plotting the results $L/Q'^{2/3}$ versus $W/Q'^{2/3}$ allowed two regimes to be distinguished (Figure 27) and a linear correlation was suggested for each of these regimes. A relatively gradual increase in flame heights with decreasing cavity width is observed for $W/Q'^{2/3} > 0.006$. A steeper increase with a higher result distribution level is observed for very narrow cavities or large HRR fires where $W/Q'^{2/3} < 0.006$. As presented in Figure 27, the observed flame heights in this study were higher than those observed by Karlsson et al. [52]. This could be due to differences in

experimental setup. One of the main differences between the test setups was that in study by Karlsson et al. [52] one of the sides was closed, hence allowing air inflow from one side only. It also must be noted, that in the study performed for this thesis, due to the view angle inside the cavity, it was difficult to distinguish between a persistent flame and an intermittent flame. The flame heights in this study are more appropriately characterized as a maximum height for intermittent flame, hence they are higher than the average flame height.

As presented in Figure 28, the flame heights in this study matched well with those measured by Ingason [53], and extended the same trend to $\dot{Q}^*_{mod} < 48$. A full list of observed flame height values in the experimental programme is provided in Annex A.
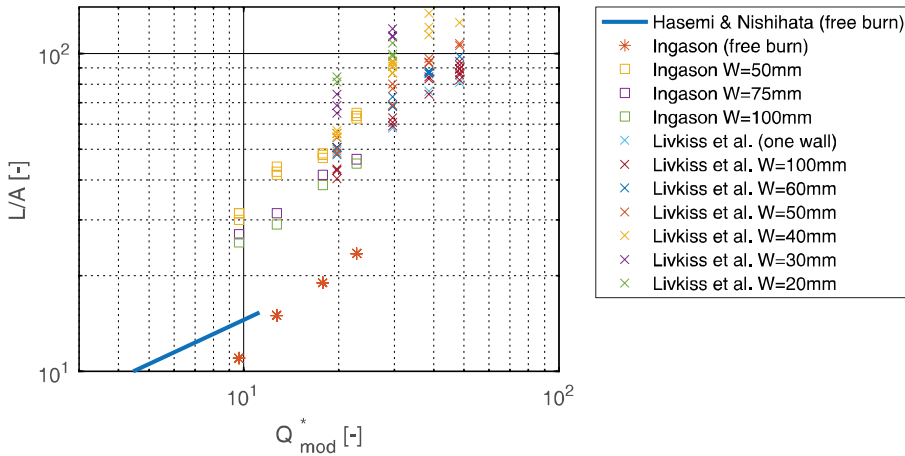
Figure 28: L/A versus modified dimensionless HRR from various studies. Axis limits are set for the clarity of the graph.

Incident heat flux to the surfaces inside the cavity was also observed to increase as cavity width was reduced, as presented in Figure 29. The results are presented for two regions of interest, because different interpretations of the results are possible. First of all, the region below the height where the flame was observed in the one wall test is presented in Figure 29 (a). In this region the increased heat flux could be explained by changes in the flame or burning characteristics in relation to the emitted heat, e.g. increased sootiness of the flame, which would increase radiation from the flame to the surface. Secondly, the region above the height where the flame was observed in the one wall test is presented in Figure 29 (b). In this region, the incident heat flux increase is also influenced by flame extension as the cavity width is reduced. In must be noted that even though this trend of increased heat flux in the flame zone

is consistent, large variations exist, as presented by the standard deviations around the mean value in Figure 29.

(a)　　　　　　　　　　　　　　　(b)
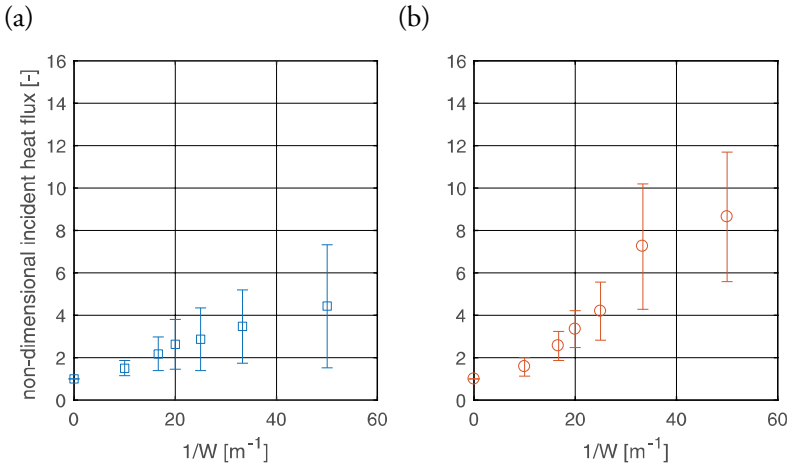
Figure 29: Relative incident heat flux increases as a function of the cavity width (a) below flame height in one wall tests (b) above the flame height in the one wall test. Error bars show two standard deviations around the mean value

6.3　Numerical study – methodology and results

6.3.1　Methodology

The LES approach with FDS version 6.7.0 was used to replicate the parallel wall experiments from the perspective of reacting flow mechanics and heat transfer. The aim was to understand the capability of FDS to predict the observed characteristics of fire driven flows, flame lengths and heat transfer in a narrow cavity arrangement. Two sub-grid scale convective heat transfer coefficient models available in FDS and the result sensitivity to the grid size were investigated.

6.3.2　Convective heat transfer modelling in FDS

In FDS several different methods can be used to calculate the convective heat transfer coefficient (hence the convective heat flux) at the solid boundary:

- Default model;

- Logarithmic law model;

- User prescribed convective heat transfer coefficient.

71

The default and the logarithmic law models were investigated. The equations used to calculate the convective heat transfer coefficient are presented in references [86,87].

In the default model, the convective heat transfer is calculated according to Equation 26 to Equation 28,

Equation 26: Default convective heat transfer calculation in FDS

$$h = max\left[C|T_g - T_w|^{1/3}; \frac{k}{L}Nu; \frac{2k}{dn}\right]$$

where k is the conductivity (W/(m·K)), L is the characteristic length scale (=1.8 m), C is an empirical coefficient (= 1.31), T_g is the gas temperature in the cell next to the wall (K), T_w is the wall temperature (K) and dn is the wall normal cell dimension (m). Nu is the Nusselt number, calculated as

Equation 27: Nusselt number calculation in FDS

$$Nu = \max[1, 0.037Re^{0.8}Pr^{0.33}]$$

where Pr is the Prandtl number (=0.7). Re is the Reynolds number, calculated as

Equation 28: Reynolds number calculation in FDS

$$Re = \frac{\rho|u|L}{\mu}$$

where μ is the dynamic viscosity (kg/m·s).

In Equation 26, the convective heat transfer coefficient is determined as the highest value of three parameters. From the left-hand side of these three parameters, the first term represents heat transfer by natural convection. Different values for the empirical coefficient C can be chosen for horizontal plate or vertical plane or cylinder in FDS (the coefficient for vertical plane was used in this study).

The middle term covers the possibility that there is forced convection on the solid. In principle, Nu refers to the ratio between the convective and conductive heat transfer in fluid at the boundary of the solid. The heat transfer is more dominated by convection if Nu is high, suggesting that there is a forced convection.

The third term, $2k/dn$, becomes the governing one if the mesh cell size is small enough near the boundary for DNS.

According to the logarithmic law wall function, the convective heat transfer coefficient is calculated in accordance with Equation 29 to Equation 31.

Equation 29: Logarithmic law convective heat transfer calculation in FDS

$$h = \frac{\rho c_p u_\tau}{T^+}$$

Equation 30: Non-dimensional temperature calculation in FDS

$$T^+ = Pr \, y^+ \qquad\qquad for \; y^+ < 11.81$$

$$T^+ = \frac{Pr_t}{\kappa} ln \, y^+ + B_T \qquad\qquad for \; y^+ \geq 11.81$$

Equation 31: Coefficient to account for resistance to the heat and momentum transport

$$B_T = (3.85 Pr^{\frac{1}{3}} - 1.3)^2 + 2.12 ln \, Pr$$

Where u_τ is the friction velocity (m/s), T^+ is non-dimensional temperature (-), ρ is the gas density (kg/m3), c_p is the specific heat capacity in constant pressure (J/(kg·K)), Pr_t is the turbulent Prandtl number (=0.5) and B_T is a coefficient to account for the resistance to the heat and momentum transport (-).

Equation 30 gives the temperature profile of the first off-wall gas cell.

6.3.3 Modelling programme

The simulation programme was limited to the one wall arrangement and 4 cm cavity arrangement for case I and case III (see Table 11). Default and logarithmic law convective heat transfer coefficient models were used with 4 mm and 2 mm mesh cell sizes. The simulation programme is presented in Table 12.

6.3.4 Model setup

The modelled computational domain was $0.8 \times 0.064 \times 1.9$ m³ (x, y and z dimensions respectively). The computational domain is presented in Figure 30. Parallel walls were built as obstructions with no thickness. The near wall was composed of the wall and the TSCs located on the wall. The wall component consisted of two materials (starting from the exposed side): calcium/magnesium/silicate CMS-based insulation (thickness 0.002 m) and calcium silicate (thickness 0.02 m). The TSCs were modelled with an exposed area 0.04×0.042 m located as a part of the wall and consisting of three material layers (starting from the exposed side): copper (thickness 0.2 mm), insulation (0.02 m) and plywood

(0.002 m). Material properties were taken from the producer data sheets as presented in the appended Paper V.

The modelled burner opening area was 8×392 mm^2. The burner output was assigned as HRR per unit area, based on the HRR calculations from propane mass flow rate during experiments.

Table 12: FDS simulation programme

Notation	HRR in simulation [kW]	Geometry	Convective heat transfer coefficient model	Cell size [mm]	Tangential velocity boundary condition at surface
A1-1	6.111	One wall	Default	4	Log law
A1-2	6.111	One wall	Log law	4	Log law
A2-1	6.511	Cavity 4 cm	Default	4	Log law
A2-2	6.511	Cavity 4 cm	Log law	4	Log law
A2-3	6.511	Cavity 4 cm	Default	4	No slip
A2-4	6.511	Cavity 4 cm	Default	2	Log law
A2-5	6.511	Cavity 4 cm	Log law	2	Log law
B1-1	12.839	One wall	Default	4	Log law
B1-2	12.839	One wall	Log law	4	Log law
B2-1	12.646	Cavity 4 cm	Default	4	Log law
B2-2	12.646	Cavity 4 cm	Log law	4	Log law
B2-3	12.646	Cavity 4 cm	Default	4	No slip
B2-4	12.646	Cavity 4 cm	Default	2	Log law
B2-5	12.646	Cavity 4 cm	Log law	2	Log law
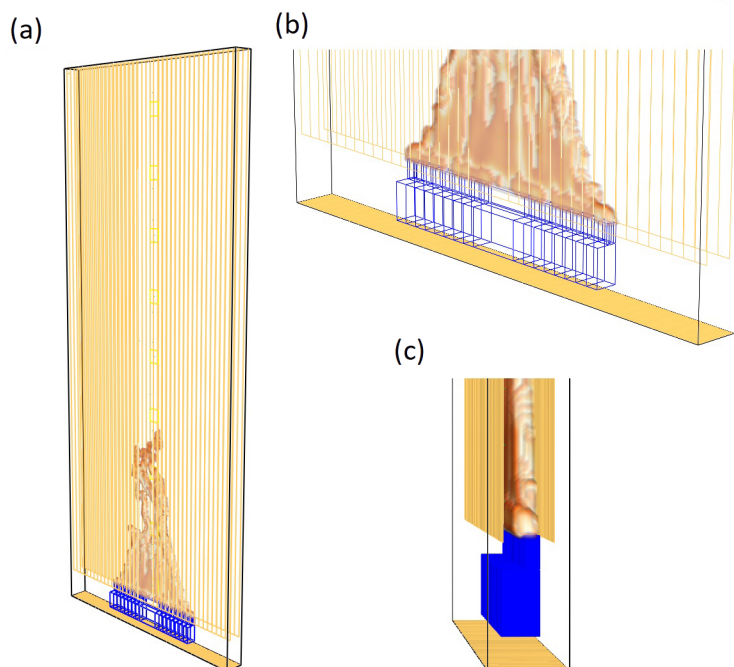
Figure 30: FDS model geometry (a) the entire computational domain with revealed mesh boundaries (b) the burner closeup with revealed mesh boundaries (c) the burner closeup

FDS employs a rectilinear grid with a recommended uniform dimension in all directions and the model's geometry was fitted according to the grid. The computational domain was split into several meshes and parallel computing was used. The main outputs were obtained along the height above the centre of the burner. This location was maintained as a single 8 cm wide mesh for simulations where 4 mm mesh cell size was used and a 4 cm wide mesh for simulations with 2 mm mesh cell size. The GLMAT pressure solver was used to ensure the correct solution for pressure equations when using several grids.

6.3.5 Results

The experimental flame heights were compared with the cumulative HRR output from the FDS simulations and are presented in Figure 31. In previous studies the height at which 95% of combustibles are burned had been shown to be a good criteria for flame heights [7]. In the presented study, the observed flame heights corresponded with 96.6% to 99.9% of the cumulative heat release rate.

(a) One-wall HRR=6.111 kW   (b) Cavity HRR=6.511 kW
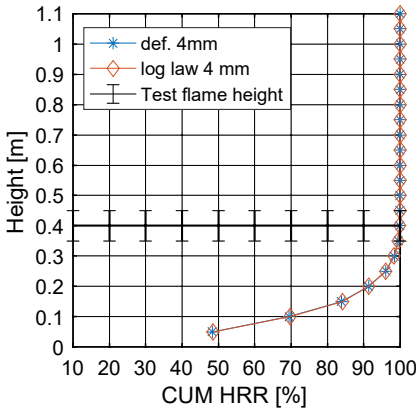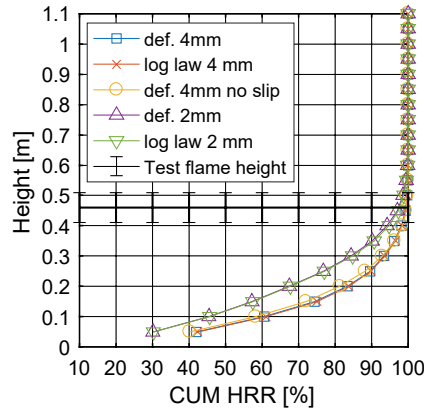
(c) One-wall HRR=12.839 kW   (d) Cavity HRR=12.646 kW
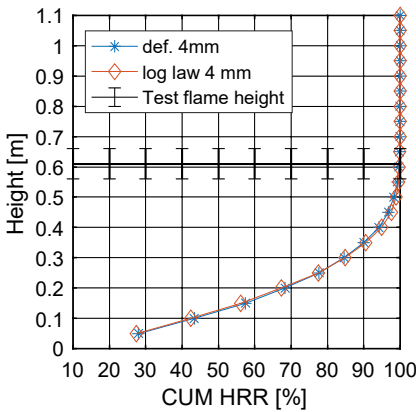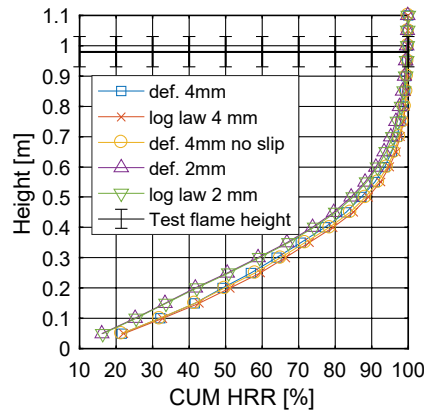
Figure 31: Cumulative HRR compared to the experimentally observed flame heights

As shown in Figure 31, the cumulative HRR near the burner is higher in simulations with a 4 mm cell size, compared to 2 mm simulations. As a result of this effect near the gas outlet boundary, slightly taller flames are predicted in 2 mm cell size simulations.

The upward flow velocities were measured in different positions at the top of the experimental setup. The measured and predicted flow velocities are presented in Table 13 and Table 14. Using 4 mm grid the upward flow velocities were under predicted down to 23 %. Refining the grid size to 2 mm increased predicted upward flow velocities. In case I, the flow velocities were overestimated by 22% compared to the experiments, whereas in case III the velocities were underestimated to -20%. Most of the predictions were inside the ± 20% error.

Table 13: Predicted and experimental upward flow velocities and deviation between the values for case I. Simulation results are seven-second averages and test results are sixty-second averages

y - position [m]	Test [m/s]	Def. 4 mm [m/s]	Log law 4 mm [m/s]	Def. 4 mm, no slip [m/s]	Def. 2 mm [m/s]	Log law 2 mm [m/s]
middle	2.44	2.44 (0%)	2.27 (-7%)	2.22 (-9%)	2.96 (21%)	2.78 (14%)
near wall	2.32	2.22 (-4%)	2.06 (-11%)	1.89 (-19%)	2.83 (22%)	2.61 (13%)
far wall	2.52	2.34 (-7%)	2.19 (-13%)	2.08 (-17%)	2.85 (-13%)	2.74 (9%)

Table 14: Predicted and experimental upward flow velocities and deviation between the values for case III. Simulation results are seven-second averages and test results are sixty-second averages

y - position [m]	Test [m/s]	Def. 4 mm [m/s]	Log law 4 mm [m/s]	Def. 4 mm, no slip [m/s]	Def. 2 mm [m/s]	Log law 2 mm [m/s]
middle	3.47	2.77 (-20%)	2.66 (-23%)	3.05 (-12%)	2.96 (-15%)	2.78 (-20%)
near wall	3.00	2.58 (-14%)	2.45 (-18%)	2.62 (-13%)	2.83 (-6%)	2.61 (-13%)
far wall	3.26	2.66 (-18%)	2.60 (-20%)	2.89 (-11%)	2.85 (-13%)	2.74 (-16%)

TSC temperature predictions and measurements are compared in Figure 32 and Figure 33. In this study, when using 4 mm cell size, excellent temperature predictions were obtained in the flame region (see subplots (e) and (f) in Figure 32 and (d) and (e) in Figure 33). However, the same simulations showed greater deviations from the experimental results in the plume region, where the temperatures were mostly under-predicted. Using logarithmic law, the convective heat transfer coefficient model results in slightly better predictions for the locations above flames. When a 2 mm cell size was used, the correspondence with the experimental results was worse in the flame region. Nevertheless, the predictions in the plume region were better compared with the 4 mm simulations (see subplots (a) in Figure 32 and (a) and (b) in Figure 33).

FDS showed the ability to predict flame lift-off observed in case III, which resulted in the temperature of the lowest TSC having a lower temperature than the TSC one position higher, as presented in Figure 33 subplots (e) and (f). Nevertheless, the extent of this temperature difference is not predicted with sufficient accuracy.

6.4 Summary

An experimental and numerical investigation was performed for flame characteristics and incident heat fluxes to the surface in 0.02 to 0.1 m wide cavity spaces and flames near a wall. During the experiments, extended flames and increased incident heat fluxes to the wall were observed when the cavity width was reduced. Narrower cavities than in previous research were investigated, hence contributing to the data sets and reinforcing conclusions from previous studies by other authors.

In this study, the maximum flame extension between flames in a 0.02 m cavity and flames next to one single wall was 2.2 times. Empirical correlations for flame heights versus burner output were established and compared to the previous research. The research presented in this thesis corresponded well with the previous research [53] in regions where the dimensionless HRR overlaps. Nevertheless, it also showed higher flames than in a study performed at Lund University in 1995 [52], probably due to differences in the test setup.

FDS showed good potential to predict flame heights and temperature measurements on the exposed wall surface. Considering the narrow and wide geometry, finding right grid resolution is a challenge. In this study cavity width to cell size ratio of 10 showed good results when comparing with the experimental results and further grid refinement did not result in improved prediction of the measured parameter. Nevertheless, the differences were observed in parameters that are not simple to measure experimentally. For example, simulations showed that grid refinement close to the burner gas outlet (boundary) resulted in 25% lower cumulative heat release next to the burner. Lower cumulative HRR was also seen on entire flame height, nevertheless converging with the course grid predictions as the height increased. The heat transfer from the flames and hot gases to the solid is still considered as a major challenge in CFD application for fire simulations.
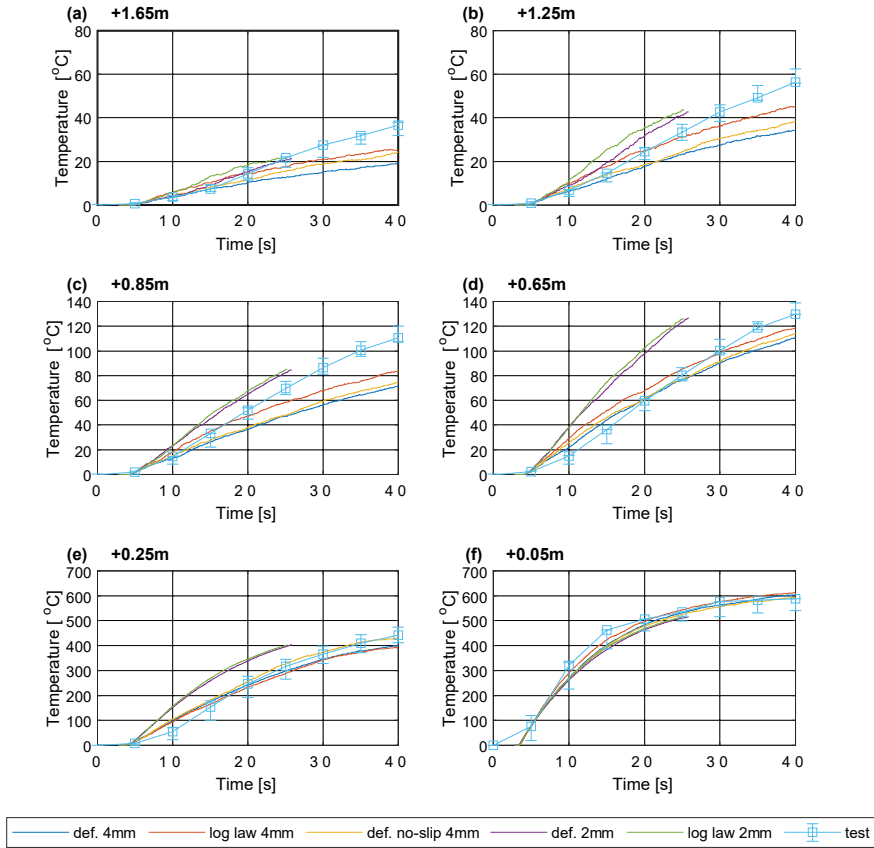
Figure 32: Relative TSC temperatures from tests and FDS model for case I

In the context of flame and smoke spread inside façade ventilation cavities, this investigation used an assumption that the flame had already entered the cavity. The mechanisms of how this occur was not discussed and requires more research. Furthermore, in real systems, such as façade systems, it is expected that other construction features would influence the fire and smoke spread. It could be influenced by limited availability of fresh air to sustain the burning. Furthermore, in some arrangements the flame may be suffocated in the cavity space allowing only the combustible gases to travel upward, and potentially ignite at the outlet of the cavity.
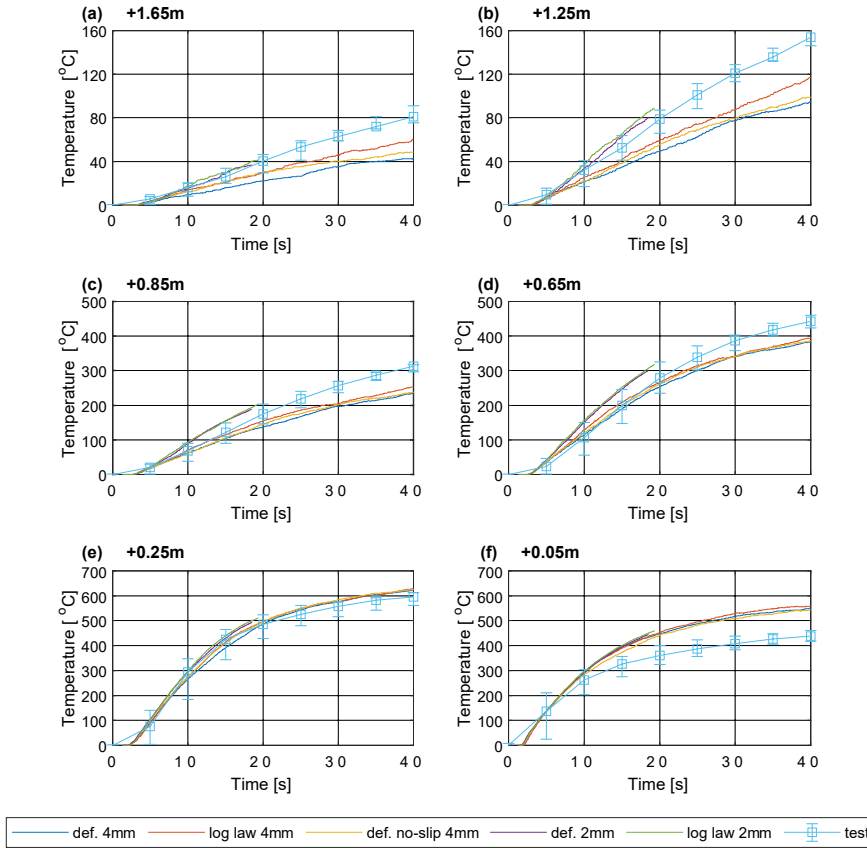
Figure 33: Relative TSC temperatures from tests and FDS modelling for case III

7 Discussion

The problem of fire dynamics and material fire behaviour in narrow cavities was divided into two sub-problems. First of all, the material's fire behaviour was discussed. The thermal response of a commonly used thermal insulation material, stone wool, was examined, both from testing and numerical perspectives. Furthermore, morphological changes in thermoplastics were studied with a new suggested test method. Material fire behaviour in a narrow cavity scenario is of interest in relation to the temperatures reached in the materials, thermal feedback in the cavity and widening of the cavity due to the material's shrinkage. Secondly, the fire induced flows and flame shapes were studied as a function of the cavity width. This task was undertaken using both experimental and numerical studies.

7.1 Materials' fire behaviour

In this thesis, the thermal behaviours of stone wool [24,25], EPS [23] and flexible PU foams [23] were studied under exposure to high temperatures. A material's behaviour in fires is related to thermal impact and heat transfer inside materials, leading to thermal decomposition and degradation. Stone wool insulation was used as an example for discussing the heat transfer in building materials from physical and modelling perspectives. Same processes, which take place in heated stone wool (e.g. heat conduction, heat source due to reactions, transport of air and decomposition products) are also relevant to many other real-life materials used in built environments. Furthermore, aspects in relation to material deformations due to the thermal decomposition and degradation are discussed for PUR and EPS.

Stone wool consists of mineral fibres held together by organic adhesives, composing an open porous structure [96]. In stone wool, heat transfer occurs by conduction in the fibres and conduction, convection and radiation in the space between the fibres [64,97]. Other porous construction materials are glass wool, gypsum, concrete etc. Mathematical descriptions and numerical solutions for convection and radiation in a porous medium is the main challenge in addressing all heat transfer modes

separately. To perform convection and radiation calculations, the material's structure must be described with a sufficient precision (i.e. describing the distribution and geometry of space between fibres). Secondly, additional mass transport related parameters (e.g. diffusion coefficient) are difficult to a obtain experimentally. A typical simplification in heat transfer analysis is using effective conductivity as a parameter that includes all heat transfer modes [63].

Exothermic and endothermic processes take place inside stone wool upon heating [78–80]. Typically, exothermic and endothermic processes in fire safety science are studied with micro scale methods, such as TGA, DSC and MCC. The Arrhenius equation is used to relate the output of micro scale measurements to large scale solid behaviour [76]. All micro scale methods have limitations, and their application to engineering calculations at a larger scale is straightforward. For example, even though it is possible to determine the temperatures at which an oxidative reaction takes place and when pyrolysis gases are generated, the gas state ignition process is not quantified with micro scale methods. Ignition is related to the mixing of pyrolysis gases with oxygen to achieve a mix prone to ignition and the temperature for this ignition to occur. It also leads to the second limitation - the conditions inside the real-life construction are difficult to resolve (e.g. oxygen content). Therefore, the rate at which the energy is released or consumed on a scale larger than the micro scale is unknown. Furthermore, if the pyrolysis gases do not ignite instantaneously upon creation, they are transferred through the matrix by diffusion and convection. The mass transfer process was not explicitly examined in this research, because it was not possible to obtain a sufficiently good description of the porous matrix, fluid and flow properties. It was observed that due to the low combustible content of stone wool, the micro scale methods were very sensitive to the test conditions. TGA and MCC measurements resulted in very noisy readings and required significant filtering.

Most of the modelling work for a material's thermal performance in fire safety engineering relies on effective material properties or other model parameters that are tuned to give the best model prediction fit with the observations of a chosen specific test. It can be argued that the use of these fitted models is acceptable for a limited range of similar situations (e.g. similar exposures and materials). Up to now, predicting just the thermal behaviour of the building construction is typically either not accurate (if the input parameters are not tuned to fit with the test results) or not reliable for other exposure conditions (if the input parameters are tuned to fit with the test result). If more general models are to be developed, some complexities ought to be addressed. The complexities of material behaviour modelling can be grouped under the following headings:

- *Understanding the processes that take place inside materials exposed to heat and their influence on the material's temperature:*

  Nowadays, relatively simple numerical heat transfer models (typically limited to heat conduction) are used for fire engineering calculations and many complex processes are addressed with fitted modelling parameters. This result in gross simplifications of the problem and possibly contributes to the model's inaccuracy when used for different exposures.

  Convection and radiation within porous materials are typically included in effective conductivity. Mass (e.g. water vapour) transport is also sometimes covered by effective conductivity [65]. Furthermore, the influence of thermal contact resistance between the layers of different materials in constructions is mostly ignored.

  In this thesis, reaction kinetics and heat generation were explicitly included in the model of heat conduction in heated stone wool. An effective thermal conductivity obtained from a custom-made slug calorimeter was used. This approach nevertheless resulted in sufficient predictions of the temperatures inside a few stone wool products, with a low density and low organic content.

  Morphological changes in solids exposed to heat are not sufficiently understood and addressed. These include the recession of the exposed surface or expansion, crack formation, spalling, formations of bubbles on the surface, etc. Some of these processes have been studied (e.g. surface recession [23,110] and crack formation [128]), but still require more research. The research presented in this thesis suggests a simple small-scale test method for determining the recession rates of materials that are exposed to heat. This method is more appropriate for rigid materials that cannot be easily compressed.

- *Developing a mathematical description of the processes:*

  After understanding the principles of the processes that take place during heating, a mathematical description can be developed. Theoretical principles of heat conduction and heat source modelling are agreed upon. Exothermic/endothermic reactions are often modelled explicitly, but sometimes the effects are included in apparent thermal properties for the sake of simplicity.

  Mass transport processes through porous media still require adequate mathematical descriptions to be used in fire safety science and engineering. These transport processes include the transport of pyrolysis gases through the material to the material surface, moisture transport after drying, air diffusion into porous materials upon heating, etc. In the work presented in this thesis, an

empirical description of pyrolysis gas transport in stone wool was suggested. It showed improved results for temperature predictions inside a heated stone wool sample, hence indicating the need for further development in this area.

Other processes that are not sufficiently described mathematically are related to changes in the physical structure of the material – shrinkage, cracking, etc. Fitting parameters are sometimes proposed to cover material surface recession in modelling [9,109]. Attempts to model melting and melt flow had been performed with a numerical model with motional nodes [119,120,129] and ALE [130]. More extensive verification, validation and improved feasibility are still required for these models.

- *Obtaining the model's input parameters:*

The model's precision strongly depends on the input parameters, including material properties. Methods for obtaining these properties require further development. Uncertainties and errors in the existing material property testing methods must be addressed. These errors and uncertainties are created by the material property testing methodologies (both precision and validity are important).

As additional processes become explicitly modelled, there will be a need to obtain new input parameters. Examples include the diffusion coefficient, permeability and porosity for mass transport calculations [131], viscosity for resolving melt flow and dripping [119]. To obtain these parameters, methods appropriate for fire-related problems then must be developed. An especially challenging issue is the need for temperature-dependent values.

- *Dealing with the material's inhomogeneity, the wide variation of commercial materials and quality control during production:*

A wide selection of construction materials is now available on the market. The materials and products in the same family have slight differences due to different manufacturing processes and raw materials. Furthermore, materials produced at the same manufacturing facility can have differences due to poor quality control.

This wide variety of commercially available materials is not sufficiently reflected in the scientific literature. Generic material descriptions are typically used when reporting the material's properties. As the result, a range of material properties for the 'same' materials are reported in literature, as shown for thermal conductivity in Paper II. These reported properties should thus be used with care and may lead to imprecise engineering calculations. Fire safety science should therefore focus on developing simple and reliable methods for obtaining

the thermal properties of each specific material. Fire safety engineers should use these simple test methods each time an uncertain material is included in the assessment, rather than relying on scientific literature about the material's properties.

An alternative approach would be to use material property value distributions. A probabilistic, rather than deterministic, approach may be taken in material modelling. An example of this was presented in the uncertainty study presented in the appended Paper II [24].

- *Addressing the increase in the model's uncertainties due to its increased complexity:*

  Bal [132] has pointed out that increasing the model's complexity (i.e. including more input parameters to resolve more processes) results in increased model output uncertainty. This uncertainty is related to the uncertainties and errors of input parameter values and numerical solutions. Hence, a balance between the model's complexity and precision should be sought in relation to the purpose of the model.

7.2 Modelling heat exposure

In this thesis, the heat exposure of materials was investigated from two perspectives, CFD simulations of reacting flows inside a narrow cavity and prescribed boundary conditions, to produce a heat conduction model for standard fire resistance tests. In principle, CFD simulations would allow the explicit calculation of exposure conditions on the surface. Nevertheless, mathematical descriptions and solutions for calculating heat transfer from a fire environment to constructions is currently one of the most challenging aspects of fire-related CFD calculations [133]. Modelling uncertainties and errors are present in these calculations, related to uncertainties in input parameter, numerical solution methods and the equations used. CFD calculations for relevant physical dimensions are time consuming, hence different approaches are employed to make the simulation time shorter, typically at the expense of the solution's accuracy.

The prescribed boundary conditions for heat conduction analysis is an approach that avoids explicit calculation of the fluid domain. The drawback of this approach is that the parameter values must be known to the engineer or scientists for each fire scenario. This approach typically does not allow feedback from the solid to the gas phase.

- *Use of LES and the boundary layer problems:*

  For efficient CFD calculations, LES is a typical approach that provides a compromise between accuracy and simulation time. LES uses mesh cell sizes that are larger than the typical length scales of the processes taking place in the flow. However, it requires well established and reliable empirical correlation to capture the sub-grid scale processes. One challenge is sub-grid scale models at the boundary between the flow and solid. Thermal and velocity boundary layers are distinguished and treated with different wall functions. In this research, the size of the cavity width required the use of a very fine grid (with mesh cell sizes down to 2 mm). This is not a typical application for the FDS software, which is often used with a mesh cell size of several cm for engineering applications or less than a millimetre for resolving DNS for research purposes. In other words, this research aimed to use the LES approach with a mesh cell size so small that it was outside the recommended dimensionless wall distance y+ values. Revision of the sub-grid scale models for low y+ regions in FDS is therefore recommended.

- *Correlations of convective heat transfer in realistic fire problems in CFD:*

  A characteristic of empirical correlation, including sub-grid scale models used in CFD, is that it is valid only for a specific case with defined limitations and assumptions. As a result, for the accuracy and reliability of the model's predictions, these empirical correlations should be reconsidered for every new simulation case. The empirical correlations used in FDS currently have a relatively limited application range. It this work specifically, sub-grid scale models for the convective heat transfer coefficient were of interest. Correlations for forced internal flow in channels would be the most appropriate way of modelling the fire scenario in a narrow ventilation cavity presented in this research, but this is not available in FDS.

  However, extending the choice of empirical correlation does place additional responsibility on the user of the model. The user would have to be more educated to wisely choose the appropriate simulation settings.

- *The position of the exposed surface relative to the heat source:*

  In every model, significant changes in the geometry of the computational domain influence the simulation results. As shown in the experimental study, heat fluxes and flame heights change as the distance between two parallel facing walls is decreased. The transient predictions of the material geometry hence become especially important in narrow geometries, where uncertainties in distance play critical role. The geometrical changes are nevertheless difficult to

model. In the research presented in this thesis, a simple empirical correlation between the exposure temperature (temperature of a hot plate attached to the specimen) and the recession rate was established for PUR and EPS.

- *Lack of understanding of the unexposed surface conditions in standard fire resistance tests:*

When the temperature distribution in constructions exposed to standard fire resistance tests is modelled, radiative and convective heat transfer is typically prescribed at the boundaries. One of parameters that most influences the model's predictions was shown to be the convective heat transfer coefficient on the unexposed surface of the construction [24]. Values between 4 and 10 W/(m²·K) are typically used. From a physical perspective, the coefficient depends on surface temperature, flow properties and properties of solid and fluid. As a result, the convective heat transfer coefficient is not expected to be constant during the fire resistance test and over the sample geometry. Secondly, environmental conditions in the testing facilities may potentially influence the test/modelling results.

The author's observations also show that, in some cases, hot gas leakages from the furnace to the outside are possible during fire resistance testing. This occurs as a result of overpressure in the testing furnace and deformations of the tested construction. When a leak occurs, the hot furnace gas typically rises due to buoyancy close to the specimen's unexposed surface, locally increasing the temperature of fluid around the measurement devices. It is therefore clear that a simple specification of the convective heat transfer coefficient is not possible, and that this parameter is used as a fitting value. Without refining the understanding of this parameter, a development to more generic models is not possible. A potential solution may be the use of CFD models to model the unexposed side conditions during the test and coupled structural calculations (deformations) and CFD calculation, both for the furnace inside and the unexposed side.

7.3 Transferring research to industry

Scientific findings should bring technological advancement, so the question of how to effectively transfer academic knowledge to industry for practical use is important. The research presented in this thesis was conducted as a part of an industrial PhD, aiming to bridge the gap between academia and industry. The potential practical

application of this research is reducing the resources needed for product development and supporting the introduction of new products and solutions to the market, while still maintaining acceptable safety risk levels. Recourse reduction would be fulfilled with use of screening tests and numerical models for making informed decisions during the product development.

The physical size scales considered in this thesis are small and constructions are simplified compared to real-life building systems. It is therefore not expected that system producers and fire safety practitioners will be able to directly apply the data and conclusions presented here to solve their full-scale system problems. Nevertheless, some comparative assessments can be made based on this research. It provides possibility of comparing the thermal performance of stone wool with different organic content compositions, and estimating the expected fire resistance test performance using numerical modelling. Material shrinking rates can be compared using the methodology presented in this thesis. Insight in the comparative assessment of thermal heat impact in different cavity widths can be used to assess the worst-case façade system to be tested in standard tests. Furthermore, the thesis contributes to the understanding of the possibilities and limitations of material property testing and CFD modelling in narrow cavity cases.

Scientific progress is a long-term investment, which aims to support the production of optimal building products and assemblies. Many of the research challenges discussed in this thesis, such as the wide variety of constructions and inhomogeneity of materials' structures, could be addressed by contributions to the manufacturing industry. Academia, on the other hand, can provide the development of research tools and methods for working with the material data provided by the industry.

8 Conclusions

Three objectives were specified in section 1.3 and addressed in this research. In this chapter, the research outcomes are described in relation to each objective.

Objective 1: To identify the properties needed to predict temperature distribution inside common building materials and to establish a link between the material properties obtained with micro-scale (mg of material) and material-scale (specimen size in the order of 10 cm) test methods and the temperature distribution in fire tests:

Thermal conductivity, specific heat capacity and density are the three main heat transfer parameters that describe energy transport inside solids. Using stone wool as an example material, it was demonstrated that exothermic reactions inside the material can significantly influence temperature distribution. The micro-scale methods of TGA and MCC were used to obtain the reaction kinetics parameters, which were thereafter used as input parameters in addition to thermal conductivity, specific heat and density in the heat transfer modelling (appended Paper II). The developed model was shown to provide a good fit for stone wools with a low density and low organic content [25].

The temperature field for high density and high organic content stone wools was not predicted with sufficient accuracy, thereby identifying a need for future research. The model overpredicted the temperature peaks created by the combustion of the organic content in the stone wool. It was suggested that the main reason was the absence of a way to account for the limited oxygen content in the porous matrix of the stone wool. The potential influence of limited oxygen levels and mass transport through empirical fitting parameters was included in the upgraded model [25]. The upgraded model, which uses the empirical parameters, is of very limited applicability, and more general ways to account for the mass transport processes inside porous materials needs to be found.

Furthermore, a small-scale method was developed to quantify the shrinkage of polymer foams when exposed to heat (appended Paper III). This shrinkage or surface recession occurs during the degradation and decomposition of some materials and, in addition to the thermal processes, influences temperature development in materials, products and systems [23]. One example of how this influences the

temperature distribution is in multilayer systems, where the exposed material is relatively inert, but the unexposed material is prone to shrinking. In this case, the initial energy transfer through the material system is determined by direct thermal contact. But due to shrinking, this thermal contact is lost and energy is transferred via radiation and convection in the established gap. The influence of cavity width on fire dynamics was experimentally demonstrated and analysed in this research (appended Paper IV), and numerical modelling was performed (appended Paper V).

Objective 2: To investigate the modelling results' level of sensitivity to uncertainties in the modelling input:

Objective 2 was fulfilled in two parts. First of all, a sensitivity analysis was performed to investigate a numerical heat conduction model for predicting temperature distribution inside stone wool exposed to the ISO 834 standard fire resistance fire curve. Secondly, FDS model result sensitivity to the chosen sub-grid scale models and grid size was investigated for fire-induced flows in a narrow air cavity.

A numerical heat conduction model was used to calculate the stone wool and steel sheet sandwich panel systems, when exposed to the cellulosic fire curve described in ISO 834. The model's sensitivity to the uncertainties of the input parameters was studied (appended Paper I). In sensitivity studies, all modelling input parameters are often varied in a certain range (e.g. ±10 %), hence the performance of the model itself is studied. A different approach was taken in this project, where the input parameters were varied based on the existing understanding of the expected values. As a result, different percentage variation was applied to each input parameter. This study relates more to the practical use of the models and was focused on identifying the parameters that require better description. As the result, the suggestion is to improve the knowledge of the stone wool's thermal conductivity, specific heat and the convective heat transfer coefficient on the unexposed surface in standard fire resistance tests [24]. Therefore, materials' high temperature thermal conductivity and specific heat testing methods should be improved to decrease the levels of measurement uncertainty, and quality control during the material manufacturing process is required. Sensitivity to the cooling processes on the unexposed side needs to be better controlled in fire resistance testing facilities. It could be suggested that there should stricter control in this area to ensure the correspondence of the test results between fire testing laboratories. In principle, specific requirements could be defined similarly to the way that exposure is controlled.

FDS was used to predict flame heights and the heat exposure of a surface inside a narrow cavity. Two grid sizes were investigated (2 mm and 4 mm). The finer grid model predicted relatively higher flames and more severe exposure of the surface.

Using a 2 mm grid gave better predictions for the wall exposure in the plume region, above the flames. The 4 mm grid size, on the other hand, provided better predictions of the heat fluxes to the wall inside the flame region. Using a 2 mm grid in this study proved impractical, due to the computational resources required. However, in many cases, a 4 mm grid showed significant under-predictions of the exposure using FDS, compared to the experimental results. Furthermore, two sub-grid scale models for convective heat transfer coefficient were investigated (the default model and the logarithmic law model). The logarithmic law model provided slightly closer results to the experimental results for the heat impact to the wall, especially in regions above the flames. It also resulted in an up to 70% higher convective heat transfer coefficient compared to the default model. It also resulted in higher convective heat flux for the logarithmic law model early in the simulations.

Objective 3: To investigate how the cavity's geometrical parameters influence fire exposure inside the cavity and the capabilities and limitations of numerical modelling in replicating this influence:

Flame heights and incident heat fluxes to the inner surfaces as a function of cavity width and burner output were investigated. Correlations were established, showing that both the flame heights and the incident heat fluxes to the surface increase as cavity width is reduced in the investigated ranges (appended Paper IV) [22].

Numerical modelling was attempted, to reproduce the heating of the inner surface of the cavity, with FDS (appended Paper V). The challenges in this modelling work included the need to use a relatively fine grid and the need to define methods for calculating the convective heat transfer coefficient. Due to the geometry of the computational domain, the grid was too fine to accurately calculate the convective heat transfer coefficient. It was, nevertheless, too big to perform DNS, thus avoiding the need to have sub-grid scale models. Despite the challenges, FDS showed a good predictive ability.

9 Insights for the Future

The researcher can choose between bottom-up or top-down approaches when investigating prediction methodologies for the fire performance of building materials, products and systems.

In this research, a bottom-up approach was implemented. The materials were studied at micro and small scales and this knowledge was applied to predict fire behaviour at the material and composite scales. Furthermore, the ventilated façade system's performance was analysed based on extremely simplified geometry and identifying only one component of the complex set of processes that control fire spread in real systems. An alternative to the bottom-up approach is investigating the complete full-scale systems and to determine what features of the failure contributed the most to the performance of the complete system. Then, based on the developed hypothesis, experimental conditions may be changed to investigate the full system's response in different exposures or with slight changes in the system. This approach is referred to as a top-down approach.

In the author's opinion, both approaches should be undertaken by researchers and both approaches would contribute to the overall understanding of fire behaviour in building systems. This chapter proposes a few topics for investigation.

9.1 Bottom-up research needs

- *Heat generation and smouldering in fibrous insulation materials, and their relationship to temperature distribution inside the material:*

  This research found limitations in predictions of the temperature field in high density stone wool with a high organic content, when exposed to heat from one side. Specifically, the challenge was to correctly predict the effect of exothermic reactions which lead to temperatures inside the stone wool increasing above the exposure temperature. It was proposed that the inability to predict the temperature field is related to a lack of understanding of mass transport in stone

wool and heat generation in low oxygen conditions in insulating porous materials. The highly inhomogeneous nature of stone wool is a potential challenge in describing these processes. The ability to account for these exothermic reactions would allow more precise predictions of whether the product can achieve the desired insulation criteria, e.g. in standard fire resistance testing, and the surface temperatures of stone wool insulation, e.g. in ventilated façades.

- *Understanding patterns and reasons for the physical behaviours of materials that influence their structure and morphology when exposed to heat:*

    This thesis mainly deals with material shrinkage due to degradation or decomposition. Melting, melt flow and the formation of combustible pools or flaming droplets are relatively little studied processes, which are nevertheless important in the practical application of flame spread problems. When these processes are understood, complex numerical methods that allow the capture of deformations, such as ALE [130] or the particle finite element method [119,120,129], could be further developed.

    Secondly, the processes and conditions governing crack formation and fall-off of parts of the material are important in predictive façade tests (e.g. fall-off of cladding), and standard fire resistance tests (e.g. fall-off of gypsum boards in separating elements or passive fire protection for steel elements).

- *Heat transfer from reacting flows to solid surfaces using LES:*

    LES relies on empirical correlations to simulate sub-grid scale processes. The sub-grid models need to be further validated and developed to describe the boundary layer between the fluid and solid with sufficient precision. Furthermore, radiation from flames and how this is absorbed by the structure still requires further study before being used in practical applications (e.g. feasible CFD simulations).

- *Smoke and flame travel in narrow, enclosed environments:*

    Some aspects of fire-driven flows and flame characteristics in narrow spaces are discussed in this thesis. This work needs to be further developed by expanding the limits of experimentally studied cases, measuring the efficiency of combustion inside the narrow spaces, characterizing flame temperatures, etc. These investigations will lead to an understanding of flame spread in façade ventilation cavities.

9.2 Top-down research needs

- *Investigation of system level features in relation to typical failure mechanisms during fires:*

  Academic research has mostly been focused around heat transfer, which, as discussed, is a basic initial process that influences the loss of fire resistance, and ignition and flame spread. However, the failure of the structure often happens at the seams and connection points of the structure, possibly due to crack formation or significant deformations and stresses in the materials. Therefore, addressing mechanical behaviours is becoming more and more important, now that there have been advances in predicting the thermal response of materials. A systematic grouping of the most probable failure mechanisms in full-scale constructions is therefore necessary to guide bottom-up research in the right direction.

- *Investigation of fire spill plumes and mechanisms for entering the façade's cavity:*

  More focused investigations should be undertaken regarding how window spill plumes and external fires can enter the ventilation cavity. This would allow the identification of critical fire scenarios in which flame spread in the cavity is expected, and how fire stops act to prevent this occurring. From a practical safety perspective, it also essential to understand the reliability of fire stops that are installed in real buildings. Deviation from the design when installed, or failure during other external influences over time are likely, and could influence fire stop and overall façade performance in fire situations.

- *Investigating standard test conditions with the aim of reducing uncertainties in test conditions:*

  The boundary conditions in standard testing still need to be better understood in order to predict fire test results. The results of this study suggest that the unexposed surface's heat losses have a significant influence on the insulating performance of separating elements, yet there is a lack of precise values for prescribing as modelling input. Even more problems are expected in façade testing. Firstly, due to the complexity of heat transfer between flames and fire-induced flows and the solid boundaries of the construction. Secondly, because of the less controlled nature of façade fire testing, which includes open flames from liquid or solid fuels (i.e. heptane pool fired or wood cribs) in larger physical geometries.

References

[1]   ISO/TR 13387-1:1999 Fire safety engineering - Part 1: The application of the fire performance concepts to design objectives, Geneve, 2000.

[2]   A. Hofmann, A. Webb, Changes in facade regulations, in: Proceedings of 15th International Fire Science and Engineering Conference Interflam, Intercience Communications Limited, London, 2019: pp. 183–197.

[3]   E. Guillaume, T. Fateh, R. Schillinger, R. Chiva, S. Ukleja, Study of fire behaviour of facade mock-ups equipped with aluminium composite material-based claddings, using intermediate-scale test method, Fire and Materials. 42 (2018) 561–577. doi:10.1002/fam.2635.

[4]   M. Mcnamee, B. Meacham, P. Van Hees, L. Bisby, W.K. Chow, A. Coppalle, R. Dobashi, B. Dlugogorski, R. Fahy, C. Fleischmann, J. Floyd, E.R. Galea, M. Gollner, T. Hakkarainen, A. Hamins, B. Merci, Y. Ohmiya, L. Hu, P. Johnson, G. Rein, A. Trouv, Y. Wang, B. Weckman, IAFSS agenda 2030 for a fire safe world, Fire Safety Journal. 110 (2019). doi:10.1016/j.firesaf.2019.102889.

[5]   X. Dai, S. Welch, A. Usmani, A critical review of "travelling fire" scenarios for performance-based structural engineering, Fire Safety Journal. 91 (2017) 568–578. doi:10.1016/j.firesaf.2017.04.001.

[6]   SP Technical Research Institute of Sweden, External wall assemblies and facade claddings Reaction to fire, 1 (1994) 1–16.

[7]   K. McGrattan, S. Hostikka, R. McDermott, J. Floyd, C. Weinschenk, K. Overholt, Sixth Edition Fire Dynamics Simulator Technical Reference Guide Volume 3 : Validation, 1 (2018) 1–147. doi:http://dx.doi.org/10.6028/NIST.SP.1018-1.

[8]   L. Bustamante Valencia, Experimental and numerical investigation of the thermal decomposition of materials at three scales: application to polyether polyurethane foam used in upholstered furniture. PhD thesis, L'Ecole Nationale Superieure de Mecanique et d'Aerotechnique, 2006.

[9]   A. Camillo, Multi-scale investigation of fire behaviour of a seat and wall panel from european railway transport system. PhD thesis, Ecole Nationale Superieure de Mecanique et d'Aerotechique - Poitiers, PhD thesis, Ecole Nationale Superieure de Mecanique et d'Aerotechique - Poitiers, 2013.

[10]   P. van Hees, J. Axelsson, Modelling of Euroclass Test Results by Means of the Cone Calorimeter, in: C.G. Duquesne S., Magniez C. (Ed.), Multifunctional Barriers for

Flexible Structure, Springer, Berlin, Heidelberg, 2007. doi:https://doi.org/10.1007/978-3-540-71920-5_12.

[11]   B. Sundstrom, CBUF: fire safety of upholstered furniture. The final report on the CBUF research programme, European Commission Measurements and Testing, London, 1996.

[12]   P. Van Hees, T. Hertzberg, A.S. Hansen, Development of a Screening Method for the SBI and Room Corner using the Cone Calorimeter, SP Report 2002:11, SP Swedish National Testing and Research Institute, Borås, Sweden, 2002.

[13]   P. van Hees, B. Andersson, F. Guay, D. Lauridsen, A. Bhargava, K. Livkiss, B. Andrés Valiente, F. Vermina Lundstrom, K. Wilkens, Simulation of fire technical properties of products and construction barriers to support efficient product development in industry (firetools), in: Proceedings of the 13th International Conference Interflam, Interscience Communications Limited, Egham, UK, 2013.

[14]   N. White, M. Delichatsios, Fire Hazards of Exterior Wall Assemblies Containing Combustible Components, The Fire Protection Research Foundation, Quincy, Massachusetts, 2014.

[15]   P. Reina, A. Wright, Grenfell Tower Fire Tragedy Sparks Safety Dispute, Architectural Record. 205 (2017).

[16]   D.I. Kolaitis, E.K. Asimakopoulou, M.A. Founti, A full-scale fire test to investigate the fire behaviour of the "'ventilated facade'" system, Proceedings of 14th International Fire and Engineering Conference Interflam. 2 (2016) 1127–1138.

[17]   R. Weghorst, B. Hauzé, E. Guillaume, Determination of fire performance of ventilated façade systems on combustible insulation using LEPIR2. Extended applications approach based on multiscale tests, Proceedings of 14th International Conference Interflam. 2 (2016) 1139–1149.

[18]   S. Colwell, T. Baker, Fire Performance of external thermal insulation for walls of multistorey buildings, 3rd editio, IHS BRE Press, Garston, 2013.

[19]   L. Boström, C. Skarin, M. Duny, R. McNamee, Fire test of ventilated and unventilated wooden façades, SP Report 2016:16, Borås, Sweden, 2016.

[20]   L. Boström, R. Chiva, S. Colwell, I. Móder, P. Tóth, A. Hofmann-Böllinghaus, D. Lange, J. Anderson, Development of a European approach to assess the fire performance of facades, Publications Office of the European Union, Luxembourg, 2018. doi:10.2873/954759.

[21]   LBN 201-15 Būvju Ugunsdrošība (in Latvian), Latvian construction standard, Riga, 2015.

[22]   K. Livkiss, S. Svensson, B. Husted, P. van Hees, Flame heights and heat transfer in façade system ventilation cavities, Fire Technology. 54 (2018) 689–713. doi:https://doi.org/10.1007/s10694-018-0706-2.

[23]   K. Livkiss, P. Van Hees, Development of a dynamic shrinkage/collapse measurement method for cellular polymer foams, in: Proceedings of 14th International Fire and

Engineering Conference Interflam, Interscience Communications Limited, 2016: pp. 991–1002.

[24]   K. Livkiss, B. Andres, N. Johansson, P. van Hees, Uncertainties in modelling heat transfer in fire resistance tests: a case study of stone wool sandwich panels, Fire and Materials. (2017). doi:10.1002/fam.2419.

[25]   K. Livkiss, B. Andres, A. Bhargava, P. van Hees, Characterization of stone wool properties for fire safety engineering calculations, Journal of Fire Sciences. 36 (2018) 202–223. doi:10.1177/0734904118761818.

[26]   K. Livkiss, B.P. Husted, P. van Hees, T. Beji, Numerical study of a fire-driven flow in a narrow cavity, Fire Safety Journal. (2019). doi:10.1016/j.firesaf.2019.102834.

[27]   P.L. Senez, K.D. Calder, H.H.I. Li, Fire loss statistical considerations in relating failure and building damage to the building code objectives, Proceedings of the 13th International Conference Interflam. (2013).

[28]   N.C.L. Chow, S.S. Han, A study on building-integrated photovoltaic system fire with double-skin façade by scale modeling experiment, in: 2nd European Symposium of Fire Safety Science, Nicosia, 2015.

[29]   W.K. Chow, W.Y. Hung, Effect of cavity depth on smoke spreading of double-skin facade, Building and Environment. 41 (2006) 970–979. doi:10.1016/j.buildenv.2005.04.009.

[30]   C.L. Chow, Numerical studies on smoke spread in the cavity of a double-skin facade, Journal of Civil Engineering and Management. 17 (2011) 371–392. doi:10.3846/13923730.2011.595075.

[31]   J. Li, X. Xing, C. Hu, Y. Li, C. Yin, S. Liu, Numerical studies on effects of cavity width on smoke spread in double-skin facade, Procedia Engineering. 45 (2012) 695–699. doi:10.1016/j.proeng.2012.08.225.

[32]   N. Johansson, P. Van Hees, A case study of fires in structural elements, in: MATEC Web of Conferences, Proceedings of 2nd International Seminar for Fire Safety of Facades, 2016. doi:10.1051/matecconf/20164606001.

[33]   G. Agarwal, Evaluation of the fire performance of aluminum composite material (ACM) assemblies using ANSI/FM 4880, FM Global Research Technical Report, Boston-Province Turnpike Norwood, 2017.

[34]   G. Agarwal, Y. Wang, S. Dorofeev, Fire performance evaluation of cladding wall assemblies using the 16-ft high parallel panel test method of ANSI/FM 4880, in: Proceedings of 15th International Conference Interflam, Interscience Communications Limited, London, 2019: pp. 199–212.

[35]   M. Chaos, M.M. Khan, N. Krishnamoorthy, P. Chatterjee, Y. Wang, S. Dorofeev, Experiments and modeling of single- and triple-wall corrugated cardboard: Effective material properties and fire behavior, in: Proceedings of 12th International Conference Fire and Materials, Interscience Communications Limited, San Francisco, USA, 2011.

[36]   E.E. Zukoski, B.M. Cetegen, T. Kubota, Visible structure of buoyant diffusion flames, in: 20th Symposium (International) on Combustion / The Combustion Institute, Pittsburgh, PA, 1984: pp. 361–366.

[37]   G. Heskestad, Dynamics of the fire plume, Philosophical Transactions of the Royal Society A: Mathematical, Physical and Engineering Sciences. 356 (1998) 2815–2833. doi:10.1098/rsta.1998.0299.

[38]   A.S. Rangwala, Diffusion flames, in: M.J. Hurley, D.T. Gottuk, J.R.J. Hall, K. Harada, E.D. Kuligowski, M. Puchovsky, J.L. Torero, J.M. Watts, C.J. Wieczorek (Eds.), SFPE Handbook of Fire Protection Engineering, 5th Edition, 5th ed., Springer-Verlag New York, New York, 2016: pp. 350–372. doi:10.1007/978-1-4939-2565-0.

[39]   P.H. Thomas, C.T. Webster, M.M. Raftery, Some experiments on buoyant diffusion flames, Combustion and Flame. 5 (1961) 359–367. doi:10.1016/0010-2180(61)90117-1.

[40]   E.E. Zukoski, T. Kubota, B. Cetegen, Entrainment in fire plumes, Fire Safety Journal. 3 (1981) 107–121. doi:10.1016/0379-7112(81)90037-0.

[41]   D. Drysdale, An Introduction to Fire Dynamics, 2nd ed., John Wiley & Sons Ltd., Chichester, U.K., 1999.

[42]   E.E. Zukoski, Properties of fire plumes, in: Combustion Fundamentals of Fire, Academic press, London, 1995: pp. 101–176.

[43]   G. Heskestad, Luminous heights of turbulent diffusion flames, Fire Safety Journal. 5 (1983) 103–108. doi:10.1016/0379-7112(83)90002-4.

[44]   Y. Hasemi, M. Nishihata, Fuel shape effect on the deterministic properties of turbulent diffusion flames, Fire Safety Science - Proceedings of the 2nd International Symposium. (1989) 275–284.

[45]   W. Takahashi, H. Tanaka, O. Sugawa, M. Ohtake, Flame and plume behavior in and near a corner of walls, Fire Safety Science—Proceedings of the Fifth International Symposium. (1997) 261–271. doi:10.3801/IAFSS.FSS.5-261.

[46]   C. Qian, K. Saito, Fire-induced flow along the vertical corner wall, in: Proceedings of the First Asian Conference on Fire Science and Technology, 1992: pp. 257–262.

[47]   T. Mizuno, K. Kawagoe, Burning behaviour of upholstered chairs: part 3, flame and plume characteristics in fire test, Fire Science & Technology. 6 (1986) 29–37. doi:https://doi.org/10.3210/fst.6.29.

[48]   G. Back, C. Beyler, P. Dinenno, P. Tatem, Wall incident heat flux distributions resulting from an adjacent Fire, Proceedings of the 4th International Symposium, International Association of Fire Safety Science. (1994) 241–252. doi:10.3801/IAFSS.FSS.4-241.

[49]   O. Sugawa, M. Tobari, Behaviour of flame plume flow in and near corner fire, in: 15th Meeting of the UJNR Panel on Fire Research and Safety, National Institute of Standards and Technology, 2000.

[50]   M. Poreh, G. Garrad, Study of wall and corner fire plumes, Fire Safety Journal. 34 (2000) 81–98. doi:10.1016/S0379-7112(99)00040-5.

[51]   S.P. Burke, T.E.W. Schumann, Diffusion flames, Industrial & Engineering Chemistry. 20 (1928) 998–1004. doi:10.1021/ie50226a005.

[52]   B. Karlsson, P.H. Thomas, G. Holmstedt, Flame sizes in a small scale stack: pilot experiments, Department of fire safety engineering, Lund University, Lund, 1995.

[53]   H. Ingason, Two dimensional rack storage fires, in: 4th International Symposium of Fire Safety Science, Ottawa, Canada, 1994: pp. 1209–1220.

[54]   H. Ingason, J.L. de Ris, Flame heat transfer in storage geometries, Fire Safety Journal. 31 (1998) 39–60. doi:10.1016/S0379-7112(97)00062-3.

[55]   H. Ingason, Modelling of a two-dimensional rack storage fire, Fire Safety Journal. 30 (1998) 47–69. doi:10.1016/S0379-7112(97)00024-6.

[56]   H. Ingason, Plume flow in high rack storages, Fire Safety Journal. 36 (2001) 437–457. doi:10.1016/S0379-7112(01)00007-8.

[57]   M. Foley, D.D. Drysdale, Heat transfer from flames between vertical parallel walls, Fire Safety Journal. 24 (1995) 53–73. doi:10.1016/0379-7112(94)00033-C.

[58]   Z. Yan, G. Holmstedt, Three-dimensional computation of heat transfer from flames between vertical parallel walls, Combustion and Flame. 588 (1999) 574–588. doi:10.1016/S0010-2180(98)00092-3.

[59]   L. Hu, S. Liu, X. Zhang, Flame heights of line-source buoyant turbulent non-premixed jets with air entrainment constraint by two parallel side walls, Fuel. 200 (2017) 583–589. doi:10.1016/j.fuel.2017.03.082.

[60]   J.L. de Ris, L. Orloff, Flame heat transfer between parallel panels, Proceedings of 8th International Symposium of Fire Safety Science. (2005) 999–1010.

[61]   A. Atreya, Convection heat transfer, in: M. Hurley, D. Gottuk, J.R. Hall, K. Harada, E. Kuligowski, M. Puchovsky, J. Torero, J.M. Watts, C. Wieczorek (Eds.), SFPE Handbook of Fire Protection Engineering, 5th Edition, 5th ed., Springer, New York, 2016.

[62]   T.L. Bergman, A.S. Lavine, F.P. Incropera, D.P. DeWitt, Fundamentals of heat and mass transfer, 7th ed., John Wiley & Sons, Hoboken, 2011.

[63]   M.K. Kumaran, D.G. Stephenson, Heat transport through fibrous insulation materials, Journal of Thermal Insulation. 11 (1988) 263–269. doi:10.1177/109719638801100406.

[64]   M.K. Kumaran, D.G. Stephenson, Heat tansport through thermal insulation: an application of the principles of thermodynamics of irreversible processes, 1986.

[65]   P. Clancy, Advances in modelling heat transfer through wood framed walls in fire, 254 (2002) 241–254.

[66]   K. Ghazi Wakili, E. Hugi, L. Wullschleger, T. Frank, Gypsum board in fire - modeling and experimental validation, Journal of Fire Sciences. 25 (2007) 267–282.

doi:10.1177/0734904107072883.

[67] H. Takeda, J.R. Mehaffey, WALL2D: A model for predicting heat transfer through wood-stud walls exposed to fire, Fire and Materials. 22 (1998) 133–140. doi:10.1002/(SICI)1099-1018(1998070)22:4<133::AID-FAM642>3.0.CO;2-L.

[68] H. Takeda, A model to predict fire resistance of non-load bearing wood-stud walls, Fire and Materials. 27 (2003) 19–39. doi:10.1002/fam.816.

[69] A. Samaké, M. Taazount, P. Audebert, P. Palmili, Thermo-hydric transfer within timber connections under fire exposure: Experimental and numerical investigations, Applied Thermal Engineering. 63 (2014) 254–265. doi:10.1016/j.applthermaleng.2013.10.049.

[70] U. Wickström, Temperature calculation in fire safety engineering, Springer, 2016. doi:10.1007/978-3-319-30172-3.

[71] D.P. Bentz, D.R. Flynn, J.H. Kim, R.R. Zarr, A slug calorimeter for evaluating the thermal performance of fire resistive materials, Fire and Materials. 30 (2006) 257–270. doi:10.1002/fam.906.

[72] D.P. Bentz, Combination of transient plane source and slug calorimeter measurements to estimate the thermal properties of fire resistive materials, Journal of Testing and Evaluation. 35 (2007). doi:10.1520/JTE100033.

[73] D.P. Bentz, P.S. Gaal, D.S. Gaal, Further progress in the development of a slug calorimeter for evaluating the apparent thermal conductivity of fire resistive materials, Proceedings of Thermal Conductivity 29/Thermal Expansion 17. (2008) 403–411.

[74] ASTM E2584-14 Standard practice for thermal conductivity of materials using a thermal capacitance (slug) calorimeter, West Conshohocken, PA, 2014. doi:10.1520/E2584-14.2.

[75] ASTM E1131-08, Standard test method for compositional analysis by thermogravimetry, West Conshohocken, PA, 2014. doi:10.1520/E1131.

[76] A. Witkowski, A.A. Stec, T.R. Hull, Thermal decomposition of polymeric materials, in: M.J. Hurley (Ed.), SFPE Handbook of Fire Protection Engineering, Springer, 2016. doi:10.1007/978-1-4939-2565-0.

[77] D.M. Marquis, M. Pavageau, E. Guillaume, Multi-scale simulations of fire growth on a sandwich composite structure, Journal of Fire Sciences. 31 (2012) 3–34. doi:10.1177/0734904112453010.

[78] H. Olsen, J. Sjöström, R. Jansson, J. Anderson, Thermal properties of heated insulation materials, in: Interflam 2013, 2013: pp. 1049–1060.

[79] J. Sjöström, R. Jansson, Measuring thermal material properties for structural fire engineering, in: 15th International Conference on Experimental Mechanics, Porto, 2012.

[80] A. Rinta-Paavola, Master's thesis, Numerical simulation of passive fire protection

systems, Aalto University, 2017.

[81] ASTM D7309 - 11, Standard test method for determining flammability characteristics of plastics and other solid materials using microscale combustion, West Conshohocken, PA, 2011. doi:10.1520/D7309-11.

[82] R.E. Lyon, R. Walters, A microscale combustion calorimeter, Washington D.C., 2002.

[83] R.E. Lyon, R.N. Walters, S.I. Stoliarov, N. Safronava, Principles and practice of microscale combustion calorimetry, New Jersey, 2013.

[84] ISO 1716:2010, Reaction to fire tests for products - Determination of the gross heat of combustion (calorific value), (n.d.).

[85] M. Janssens, Calorimetry, in: M. Hurley, D. Gottuk, J.R. Hall, K. Harada, E. Kuligowski, M. Puchovsky, J.L. Torero, J.M.J. Watts, C. Wieczorek (Eds.), The SFPE Handbook of Fire Protection Engineering, 5th Edition, Springer, 2016. doi:10.1007/978-1-4939-2565-0.

[86] K. McGrattan, S. Hostikka, R. McDermott, J. Floyd, M. Vanella, Fire Dynamics Simulator User's Guide, Sixth Edit, 2018. doi:10.6028/NIST.SP.1019.

[87] K. McGrattan, S. Hostikka, R. McDermott, J. Floyd, M. Vanella, Fire Dynamics Simulator Technical Reference Guide Volume 1:Mathematical Model, Sixth Edit, 2018. doi:10.6028/NIST.SP.1018.

[88] J. Zhang, M. Delichatsios, M. Colobert, Assessment of fire dynamics simulator for heat flux and flame heights predictions from fires in SBI tests, Fire Technology. 46 (2010) 291–306. doi:10.1007/s10694-008-0072-6.

[89] T.G. Ma, J.G. Quintiere, Numerical simulation of axi-symmetric fire plumes: Accuracy and limitations, Fire Safety Journal. 38 (2003) 467–492. doi:10.1016/S0379-7112(02)00082-6.

[90] R.D. Peacock, P.A. Reneke, W.D. Davis, W.W. Jones, Quantifying fire model evaluation using functional analysis, Fire Safety Journal. 33 (1999) 167–184. doi:PII: S0379-7112(99)00029-6.

[91] N. Johansson, S. Svensson, P. van Hees, A study of reproducibility of a full-scale multi-room compartment fire experiment, Fire Technology. 51 (2015) 645–665. doi:10.1007/s10694-014-0408-3.

[92] E. Ronchi, P.A. Reneke, R.D. Peacock, A method for the analysis of behavioural uncertainty in evacuation modelling, Fire Technology. 50 (2014) 1545–1571. doi:10.1007/s10694-013-0352-7.

[93] L. Audouin, L. Chandra, J.L. Consalvi, L. Gay, E. Gorza, V. Hohm, S. Hostikka, T. Ito, W. Klein-Hessling, C. Lallemand, T. Magnusson, N. Noterman, J.S. Park, J. Peco, L. Rigollet, S. Suard, P. Van-Hees, Quantifying differences between computational results and measurements in the case of a large-scale well-confined fire scenario, Nuclear Engineering and Design. 241 (2011) 18–31. doi:10.1016/j.nucengdes.2010.10.027.

[94]   V.K.R. Kodur, T.Z. Harmathy, Properties of building materials, in: M.J. Hurley (Ed.), SFPE Handbook of Fire Protection Engineering, 5th editio, Springer, 2016: pp. 277–324. doi:10.1007/978-1-4939-2565-0.

[95]   European Insulation Manufacturers Association Website, (n.d.). https://www.eurima.org/about-mineral-wool.html (accessed March 18, 2018).

[96]   L. Chapelle, Y. Kusano, M.R. Foldschack, Microstructural characterization of stone wool, (2014) 22–26.

[97]   S. Dyrbøl, Heat transfer in rockwool modelling and method of measurement, Technical University of Denmark, 1998.

[98]   P. van Hees, J. Wellekens, Brandweerstand van met minerale wol geïsoleerde fluidumverdeelnetten. Algemeen toepasbare berekeningsmethode, Rijksuniversitet Gent, 1986.

[99]   DS/EN 1363-1 Fire resistance tests - Part 1: General Requirements, (2012).

[100]   P. Keerthan, M. Mahendran, Thermal performance of composite panels under fire conditions using numerical studies: plasterboards, rockwool, glass fibre and cellulose insulations, Fire Technology. 49 (2012) 329–356. doi:10.1007/s10694-012-0269-6.

[101]   P. Hartlieb, M. Toifl, F. Kuchar, R. Meisels, T. Antretter, Thermo-physical properties of selected hard rocks and their relation to microwave-assisted comminution, Minerals Engineering. 91 (2016) 34–41. doi:10.1016/j.mineng.2015.11.008.

[102]   N. Bénichou, M.A. Sultan, Thermal properties of lightweight-framed construction components at elevated temperatures, Fire and Materials. 29 (2005) 165–179. doi:10.1002/fam.880.

[103]   S.E. Magnusson, S. Thelandersson, A discussion of compartment fires, Fire Technology. 10 (1974) 228–246. doi:10.1007/BF02588848.

[104]   Q. Xu, C. Jin, G. Griffin, Y. Jiang, Fire safety evaluation of expanded polystyrene foam by multi-scale methods, Journal of Thermal Analysis and Calorimetry. 115 (2014) 1651–1660. doi:10.1007/s10973-013-3431-6.

[105]   Q. Xu, C. Jin, J. Hristov, G. Griffin, Y. Jiang, The melt/shrink effect of low density thermoplastics insulates cone calorimeter tests, Thermal Science. 21 (2017) 2177–2187. doi:10.2298/TSCI150304058X.

[106]   J.P. Hidalgo-Medina, Performance based methodology for the fire safe design of insulation materials in energy efficient buildings, The University of Edinburgh, 2015.

[107]   D. Hopkin, T. Lennon, V. Silberschmidt, A laboratory study into the fire resistance performance of structural insulated panels (SIPs), Proceedings of the 6th International Conference Structures in Fire. (2010) 611–619.

[108]   J. Troitzsch, Plastics flammability handbook, 3rd editio, Hanser Publishers,

Munich, 2004.

[109] K. Prasad, R. Kramer, N. Marsh, M. Nyden, Numerical simulation of fire spread on polyurethane foam slabs, Proceedings of the 11th International Conference Fire and Materials. (2009).

[110] R.H. Krämer, M. Zammarano, G.T. Linteris, U.W. Gedde, J.W. Gilman, Heat release and structural collapse of flexible polyurethane foam, Polymer Degradation and Stability. 95 (2010) 1115–1122. doi:10.1016/j.polymdegradstab.2010.02.019.

[111] W. Parker, A procedure for predicting the heat release rate of furniture composites from measurements on their components, Proceedings of the 5th International Symposium Fire Safety Science. (1997) 129–140.

[112] M. McLaggan, M. Meinert, A. Dragsted, P. van Hees, Development tool for ETICS facade fire testing, in: A. Dederichs (Ed.), Book of Abstracts Nordic Fire and Safety Days, Copenhagen, 2017: p. 9.

[113] D. Hopkin, V. Silberschmidt, J. El-Rimawi, T. Lennon, Modelling the fire resistance of structural insulated panels : Heat transfer, Proceedings of The12th International Fire Science and Engineering Conference INTERFLAM. (2010).

[114] R. Hadden, A. Alkatib, G. Rein, J.L. Torero, Radiant ignition of polyurethane foam: the effect of sample size, Fire Technology. 50 (2012) 673–691. doi:10.1007/s10694-012-0257-x.

[115] ISO 5660-1, Reaction-to-fire tests -- Heat release, smoke production and mass loss rate -- Part 1: Heat release rate (cone calorimeter method), (2015).

[116] R. Vanspeybroeck, P. van Hees, P. Vandevelde, Combustion behaviour of polyurethane flexible foams under cone calorimetry test conditions, 17 (1993) 155–166.

[117] B. Schartel, M. Bartholmai, U. Knoll, Some comments on the use of cone calorimeter data, Polymer Degradation and Stability. 88 (2005) 540–547. doi:10.1016/j.polymdegradstab.2004.12.016.

[118] K.T. Paul, Cone calorimeter: Initial experiences of calibration and use, Fire Safety Journal. 22 (1994) 67–87. doi:10.1016/0379-7112(94)90052-3.

[119] E. Onate, R. Rossi, S.R. Idelsohn, K.M. Butler, Melting and spread of polymers in fire with the particle finite element method, (2010) 1046–1072.

[120] K.M. Butler, A model of melting and dripping thermoplastic objects in fire, Proceedings of the 11th International Conference Fire and Materials. (2009).

[121] ISO 5657. Reaction to fire tests - ignitability of building products using a radiant heat source, (1997).

[122] N. Johansson, Fire dynamics of multi-room compartment fires, PhD Thesis, Lund University, 2015.

[123] J. Hietaniemi, J. Vaari, T. Hakkarainen, J. Huhta, U.-M. Jumppanen, T. Korhonen, I. Kouhia, J. Siiskonen, H. Weckman, Fire safety of cavity spaces: characteristics of

fires in building voids, their structural prevension and extinguishing. VTT research notes 2249, Helsinki, 2004.

[124] J. Hietaniemi, T. Hakkarainen, J. Huhta, U.M. Jumppanen, I. Kouhia, J. Vaari, H. Weckman, Fire safety of cavity spaces: prevention of fire spread in building voids. VTT research notes 2202, Helsinki, 2003.

[125] J. Hietaniemi, T. Hakkarainen, J. Huhta, T. Korhonen, J. Siiskonen, J. Vaari, Fire safety of cavity spaces. Experimental and simulation study of fires in cavities. VTT Tiedotteita - Research Notes 2128, Espoo, 2002.

[126] H. Ingason, U. Wickström, Measuring incident radiant heat flux using the plate thermometer, Fire Safety Journal. 42 (2007) 161–166. doi:10.1016/j.firesaf.2006.08.008.

[127] B.J. McCaffrey, G. Heskestad, A robust bidirectional low-velocity probe for flame and fire application, Combustion and Flame. 26 (1976) 125–127. doi:10.1016/0010-2180(76)90062-6.

[128] D. Baroudi, A. Ferrantelli, K.Y. Li, S. Hostikka, A thermomechanical explanation for the topology of crack patterns observed on the surface of charred wood and particle fibreboard, Combustion and Flame. 182 (2017) 206–215. doi:10.1016/j.combustflame.2017.04.017.

[129] M. Matzen, J.M. Marti, E. Onate, S. Idelsohn, B. Schartel, Particle finite element modelling and advanced experiments on dripping V-0 polypropylene, in: Proceedings of 15h International Conference Fire and Materials, Interscience Communications Limited, San Francisco, 2017: pp. 57–62.

[130] M. Bruns, Burn: a 3D model of burning materials, in: Proceedings of the 14th International Interflam Conference, Interscience Communications Limited, 2016: pp. 83–94.

[131] D. Kontogeorgos, M. Founti, Numerical investigation of simultaneous heat and mass transfer mechanisms occurring in a gypsum board exposed to fire conditions, Applied Thermal Engineering. 30 (2010) 1461–1469. doi:10.1016/j.applthermaleng.2010.03.006.

[132] N. Bal, Uncertainty and complexity in pyrolysis modelling, PhD thesis, University of Edinburgh, 2012.

[133] K. Mcgrattan, S. Miles, Modeling fires using computational fluid dynamics (CFD), in: M. Hurley, D. Gottuk, J.R. Hall, K. Harada, E. Kuligowski, M. Puchovsky, J. Torero, J.M. Watts, C. Wieczorek (Eds.), SFPE Handbook of Fire Protection Engineering, 5th Edition, Springer, New York, 2016.

ANNEX A

30 second averaged visual flame heights from the experimental programme presented in paper IV

Target HRR (kW)	Actual HRR (kW)	Cavity width (m)	Flame height L (m)
6.5	6.1	0.10	0.34
6.5	7.1	0.06	0.41
6.5	6.8	0.05	0.39
6.5	6.2	0.03	0.52
6.5	6.3	0.10	0.32
6.5	6.3	0.06	0.41
6.5	6.5	0.05	0.40
6.5	6.5	0.03	0.55
6.5	6.7	0.02	0.68
6.5	6.5	0.10	0.35
6.5	6.5	0.06	0.39
6.5	6.5	0.03	0.60
6.5	6.6	0.05	0.44
6.5	6.5	0.02	0.65
6.5	6.5	0.04	0.45
6.5	6.5	0.04	0.44
6.5	6.5	0.04	0.46
6.5	6.3	0.04	0.45
6.5	6.1	one wall	0.40

9.7	9.5	one wall	0.47
9.7	No data available	0.10	0.50
9.7	No data available	0.04	0.74
9.7	No data available	0.06	0.59
9.7	No data available	0.03	0.90
9.7	No data available	0.05	0.62
9.7	No data available	0.02	0.86
9.7	No data available	0.04	0.76
9.7	No data available	0.04	0.75
9.7	No data available	0.04	0.73
9.7	No data available	0.04	0.73
9.7	No data available	0.04	0.70
9.7	No data available	0.04	0.69
9.7	No data available	0.02	0.80
9.7	No data available	0.02	0.79
9.7	No data available	0.10	0.47
9.7	No data available	0.06	0.55
9.7	9.9	0.05	0.64
9.7	9.6	0.03	0.96
9.7	No data available	0.10	0.49
9.7	9.7	0.06	0.55
9.7	9.7	0.05	0.55
9.7	9.7	0.03	0.91
12.6	12.8	one wall	0.61
12.6	12.5	0.04	0.97
12.6	12.6	0.04	0.92
12.6	12.4	0.04	1.07

12.6	12.7	0.10	0.60
12.6	12.8	0.06	0.71
12.6	12.7	0.05	0.75
12.6	12.5	0.03	1.31
12.6	12.6	0.10	0.67
12.6	12.7	0.06	0.70
12.6	12.6	0.05	0.75
12.6	12.6	0.03	1.39
12.6	12.7	0.10	0.68
12.6	12.6	0.06	0.69
12.6	12.5	0.05	0.77
12.6	12.5	0.03	1.31
15.8	No data available	0.10	0.76
15.8	No data available	0.10	0.74
15.8	No data available	0.10	0.70
15.8	No data available	0.10	0.72
15.8	No data available	0.10	0.66
15.8	No data available	0.10	0.69
15.8	No data available	one wall	0.65
15.8	15.9	0.06	0.79
15.8	15.9	0.05	0.86
15.8	15.6	0.04	1.00
15.8	No data available	0.10	0.71
15.8	No data available	0.05	0.85

ANNEX B

Appended scientific Papers I to V:

Paper I   Livkiss K, Andres B, Johansson N, van Hees P. Uncertainties in modelling heat transfer in fire resistance tests: A case study of stone wool sandwich panels. Fire and Materials. 2017; 41:799–807. DOI: 10.1002/fam.2419

Paper II   Livkiss K, Andres B, Bhargava A, van Hees P. Characterization of Stone Wool Properties for Fire Safety Engineering Calculations. Journal of Fire Sciences. 2018 DOI: 10.1177/0734904118761818

Paper III   Livkiss K, van Hees P. Development of a dynamic shrinkage/collapse measurement method for cellular polymer foams, Interflam - Nr Windsor, June 2016, pp. 991-1002

Paper IV   Livkiss K., Svensson S, Husted B, van Hees P. Flame Heights and Heat Transfer in Façade System Ventilation Cavities. Fire Technology. 2018; 1-25. DOI: 10.1007/s10694-018-0706-2

Paper V   Livkiss K., Husted B, Beji T, van Hees P, Numerical study of a fire-driven flow in a narrow cavity, Fire Safety Journal. 2019, 108: 102834 DOI: 10.1016/j.firesaf.2019.102834

Fire Safety Engineering
Lund University